The Role of Formins in Endothelial Adherens Junction Regulation

Iqra Mumal

A thesis submitted to the
Faculty of Graduate and Postdoctoral Studies
In partial fulfillments of the requirements for the
M.Sc. degree in Cellular and Molecular Medicine

Cellular and Molecular Medicine
Faculty of Medicine
University of Ottawa

Abstract

Adherens junctions are cadherin-dependent structures that mediate intercellular signaling and structural integrity of the endothelial barrier. Formins are a highly conserved family of cytoskeletal remodeling proteins whose activity has been implicated in regulating adherens junction formation in other cell-types. Therefore, we tested the hypothesis that formin activity is essential for adherens junction assembly in endothelial cells. A small-molecule formin inhibitor (smiFH2) was used to determine the effect of formin inhibition on junction formation using an *in vitro* vascular permeability assay. We determined that smiFH2 treatment caused a dose-dependent inhibition of junction formation. We used siRNAs to knockdown expression of the seven formins shown to be expressed in TIME cells and determined that individual knockdown of FHOD1, FHOD3 and Dia1 significantly increased the permeability of the endothelial monolayer. Interestingly, FMNL2 knockdown actually potentiated barrier function. Knockdown of the remaining formins had little or no effect on junction formation. Knockdown of FHOD3 had the greatest inhibitory effect on junction assembly; VE-cadherin protein levels were decreased in FHOD3-depleted cells. The FHOD3 knockdown cells were also elongated in comparison to controls and formed thin linear adherens junctions and few focal adherens junctions. In contrast, the morphology of FMNL2-depleted cells did not appear obviously different from controls. In conclusion, our results suggest that multiple formins play diverse roles in adherens junction formation and maintenance in endothelial cells.

Table of Contents

List of Tables

Chapter 2: Material and Methods

List of Figures

Chapter 1: Introduction

Chapter 2: Material and Methods

Chapter 3: Results

Chapter 4: Discussion

Appendix 1

List of Abbreviations

ADP.....Adenosine diphosphate
ATP .....Adenosine triphosphate
AJ…….Adherens Junction
BirA……Bifunctional ligase/repressor
cAMP……...Cyclic adenosine monophosphate
CME…….Clathrin-Mediated Endocytosis
Co-IP……..Co-immunoprecipitation
DAPI……4',6-diamidino-2-phenylindole
Dia.....Diaphanous
DID……..diaphanous autoinhibitory domain
DAD……diaphanous autoregulation domain
DMSO……Dimethyl Sulfoxide
DRF……...Diaphanous Related Formin
E-cadherin……...Epithelial Cadherin
EC…….....Endothelial Cell
ECM……...Extracellular matrix
EDTA……..Ethylenediaminetetraacetic acid
EGF…….Endothelial Growth Factor
EGTA……..Ethyleneglycol-*bis*(β-aminoethyl)-N,N,N′,N′-tetraacetic Acid
ERK……..Extracellular Signal Related Kinase
FBS……....Fetal Bovine Serum
FGF……Fibroblast Growth Factor
FH1 .....Formin Homology 1
FH2 .....Formin Homology 2
FH2 .....Formin Homology 3
FHOD…….Formin Homology Domain-Containing Protein
FITC……Fluorescein Isothiocyanate
FMN .....Formin
FMNL1 .....Formin-like-1
FMNL2 .....Formin-like-2
FMNL3 .....Formin-like-3
FA…….....Focal Adhesions
FAJ…….Focal Adherens Junction
GAP……GTPase activating proteins
GBD……GTPase binding domain
GEF……..Guanine Nucleotide Exchange Factors
GFP……..Green Fluorescent Protein
GTP……..Guanosine triphosphate
HCl…….....Hydrochloric Acid
HUVEC……Human Umbilical Vein Endothelial Cells
IGF……..Insulin-like Growth Factor
INF .....Inverted Formin
LAMP-1……...Lysosomal-Associated Membrane Protein 1
MAPK…….Mitogen-Activated Protein Kinase

MLC……..Myosin Light Chain
MRTF……Myocardin Related Transcription Factor
MTOC…….Microtubule Organizing Center
ROCK .....Rho-associated coiled-coil-forming kinases
RT-PCR.....Reverse transcription polymerase chain reaction
PECAM-1……Platelet Endothelial Cell Adhesion Molecule-1
PBS……..Phosphate Buffered Saline
PCR……Polymerase Chain Reaction
PFA……...Paraformaldehyde
PI-3K…….Phosphatidylinositol 3-Kinase
SDS…….....Sodium Dodecyl Sulfate
SH3 .....Src homology 3
siRNA……Small Interfering Ribonucleic Acid
smiFH2……...Small-Molecule Inhibitor of the Formin Homology Domain
SRF…….....Serum Response Factor
TIME……...Telomerase-Immortalized Microvascular Endothelial Cells
TNF…….....Tumor Necrosis Factor
TfR……Transferrin Receptor
VE-cadherin…….Vascular-Endothelial Cadherin
VASP……...Vasodilator-Simulated Phosphoprotein
VEGF……...Vascular Endothelial Growth Factor
VEGFR2……Vascular Endothelial Growth Factor Receptor 2
ZO……..…….....Zona Occuldens

Acknowledgments

I would like to thank everyone who supported me throughout my Masters. First, I would like to thank Dr. John Copeland for his mentorship and guidance. His enthusiasm always kept me motivated and excited to discover more. I would also like to thank the members of my advisory committee, Dr. Jonathan Lee and Dr. Christina Addison for their advice and suggestions for my project.

I would also like to thank Sarah Copeland and Allan Heibein for training me and always helping me when I needed it the most. A special thanks to Sarah Copeland for answering my countless questions and to Kim Wong for the microscopy training and assistance throughout my two years. Finally, thanks to the rest of the lab, and the summer students, for always being there for me. I would also like to thank the Trinkle-Mulcahy and Jasmin lab for their generosity with their equipment, other materials and their advice.

Finally I would like to thank my family for their endless support. Thanks to my mom and my dad who always pushed me to do my best. Finally, a special thanks to my brother, who always reminds me to relax when life gets too stressful.

Chapter 1

Introduction

1 Introduction

1.1 Types of Junctions in Endothelial cells

Endothelial cells form three main structures that play major roles in maintaining vascular permeability: Focal Adhesions (FAs) (fig. 1.1), Focal Adherens junctions (FAJs) (fig. 1.2) and Adherens Junctions (AJs). Endothelial cells start to reorganize their junctions when they are exposed to shear stress (i.e. laminar flow of blood) (Dejana and Orsenigo 2013; Malek and Izumo 1996). Focal adhesions, the first structures to rearrange, appear as quickly as 20 seconds after the application of shear stress *in vitro*. The role of focal adhesions is to tether the cytoskeleton to the extracellular matrix via cytoplasmic linker proteins (Tan *et al.* 2010). The proteins that compose a focal adhesion include vinculin, paxillin, talin, integrins and focal adhesion kinase among others. Soon after focal adhesions re-arrange, another type of junction starts to form, the focal adherens junction. The role of focal adherens junctions is to link adjacent endothelial cells through homotypic interactions. Similar to focal adhesions, FAJs serve as stress fiber insertion sites at the cell periphery. Some of the proteins present at FAJs are Vascular Endothelial (VE)-cadherin, p120-catenin, β-catenin, α-catenin and the focal adhesion protein vinculin. Phenotypically, FAJs take on a patchy, zipper-like appearance while mature AJs exhibit a linear appearance (Huveneers *et al.* 2012; Millan *et al.* 2010). As cellular remodeling approaches equilibrium, increased vinculin and VE-cadherin expression promotes the resolution of FAJs into mature adherens junctions. The final structure, the adherens junction, has a crucial role in maintaining endothelial integrity and modulation of permeability (Dejana and Orsenigo 2013; Tzima *et al.* 2005).

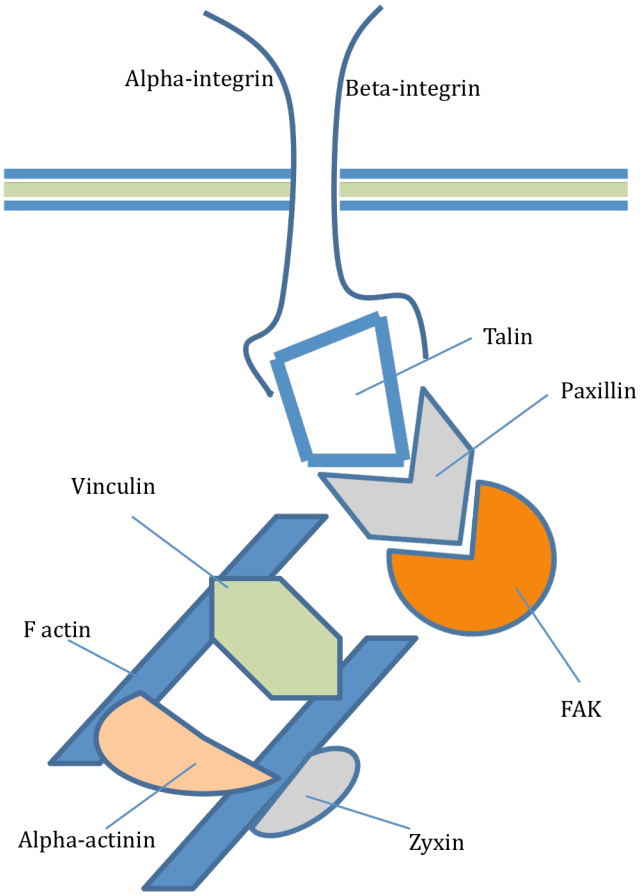

Fig. 1.1. Structure of a focal adhesion. A focal adhesion functions to tether the extracellular matrix to the actin cytoskeleton. Focal adhesions are large complexes, which consist of integrins and scaffold proteins. Focal adhesions are sites where integrins link actin-associated cytoskeletal proteins (talin, vinculin, α-actinin) and signaling molecules such as FAK and paxillin to the structural macromolecules of the extracellular matrix. Source: Kal Van Tam *et al.* 2012.

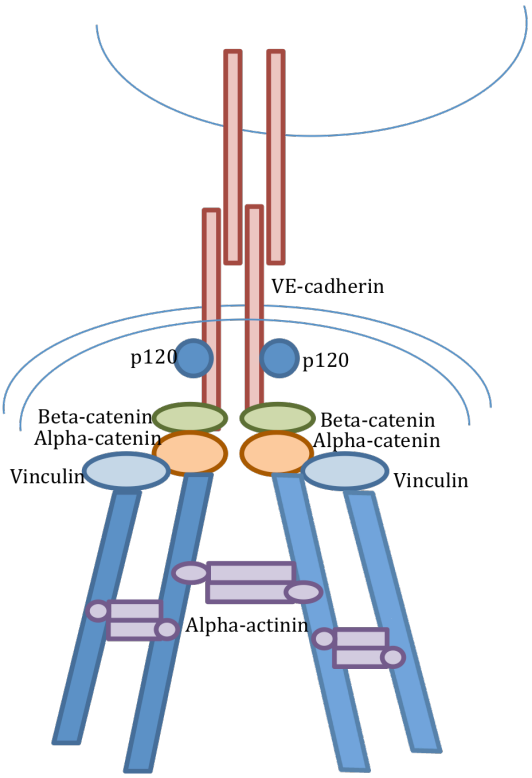

Fig. 1.2. Structure of a focal adherens junction. FAJs function as sites of attachment of radial F-actin bundles to the junctions. They appear as part of junction remodeling, stimulated by agents such as thrombin, VEGF and TNFα. Through interactions between VE-cadherin on neighbouring cells, opposing cadherin dimers can integrate the actin cytoskeletons. β-catenin binds α-catenin, which is central in recruiting a number of cytoskeletal proteins, including the actin-binding protein vinculin and α-actinin. p120 catenin, which is related to β-catenin, binds to VE-cadherin and functions in cadherin turnover, perhaps by regulating cadherin trafficking. Source: Kobielak *et al.* 2004.

1.2 Adherens Junctions

1.2.1 Adherens Junction Structure

Adherens junctions (fig. 1.3) are present in every endothelial cell type and are the main vascular permeability regulators. The prominent protein that composes an adherens junction is VE-cadherin. This is a calcium-dependent cadherin that is composed of a conserved cytoplasmic tail and five extracellular cadherin repeats. The main function of VE-cadherin is to allow neighbouring cells to adhere in a homophilic manner; other functions include modulation of vascular permeability and contact inhibition (Dejana and Orsenigo, 2013). VE-cadherin indirectly couples the cytoskeleton of neighbouring cells, thereby creating an intercellular scaffold that allows the endothelial monolayer to withstand stress (Halbleib *et al.* 2006).

VE-cadherin abundance at junctions is regulated through the action of the cytokine Vascular Endothelial Growth Factor (VEGF). VEGF binds to the VEGF-receptor (VEGFR2), which is present on the membrane of every endothelial cell. Upon binding of VEGF, Src kinase, which normally associates with VEGFR2, phosphorylates VE-cadherin. This leads to VE-cadherin endocytosis through a clathrin-mediated pathway. Eventually, this will cause a decrease in cell-cell association with a concomitant increase in vascular permeability (Gavard and Gutkin, 2006).

VE-cadherin is located at junctions between endothelial cells and contains binding sites for p120 catenin, β-catenin and plakoglobin. p120-catenin controls VE-cadherin abundance at both focal and mature adherens junctions by regulating cadherin degradation through a clathrin-dependent pathway. A decrease in p120-catenin levels causes a dramatic decrease in VE-cadherin protein levels and an increase in vascular

permeability (Xiao *et al.* 2005). Also bound to VE-cadherin is the protein β-catenin, which functions to connect VE-cadherin to α-catenin. α-catenin binds the cadherin-catenin complex to the actin cytoskeleton in two ways. First, α-catenin itself can bind to filamentous actin, connecting the two structures. Secondly, α-catenin can bind directly with actin binding proteins such as vinculin and α-actinin, thus connecting the complex to the cytoskeleton. Vinculin is only present at FAJs while α-actinin is present at FAJs and AJs (Huveneers *et al.* 2012; van Bull *et al.* 2009).

1.2.2 Adherens Junction: Function, Recycling and Degradation

Focal and mature adherens junctions in endothelial cells are not static structures, but are, in fact, regularly remodeled. Each time there is a rearrangement in junctions, there is a change in the abundance of VE-cadherin. The movement of VE-cadherin is crucial to the remodeling of these junctions in response to signaling stimuli such as VEGF or mechanical stresses such as shear stress (Nanes *et al.* 2012; Wilson and Ye, 2014). Therefore, during remodeling, VE-cadherin undergoes endocytosis, degradation and general recycling. Both clathrin-dependent and clathrin-independent pathways have been shown to be involved in VE-cadherin recycling (fig. 1.4) (Zhang *et al.* 2014).

VE-cadherin has mostly been linked to recycling through Clathrin-Mediated Endocytosis (CME). CME works through the use of adaptor protein complexes that can bind to both clathrin and the transmembrane protein targeted for internalization, thereby directing the protein into a clathrin-coated vesicle. In the case of VE-cadherin, CME begins with stimulation by VEGF. Adaptor protein complexes bind VE-cadherin, recruit the endocytic machinery and then cluster into clathrin-coated pits. The protein dynamin helps the clathrin-coated pits bud off from the plasma membrane and form endocytic

vesicles. Internalized proteins such as VE-cadherin can be recycled back to the plasma membrane or sent to the lysosome for degradation. Most of the internalized VE-cadherin in the clathrin-coated vesicular pathway results in lysosomal degradation (Zhang *et al.* 2014; Xiao *et al.* 2005; Chiasson *et al.* 2009).

The strength of the cell junctions is dependent, largely, on the amount of VE-cadherin that is present at junctions. Therefore, while a significant amount of internalized VE-cadherin is targeted to the lysosomes, there is also a considerable amount that is recycled back to the plasma membrane. Hence, by choosing to recycle some and degrade other VE-cadherin, recycling pathways can help adjust the amount of VE-cadherin at junctions (Giannotta *et al.* 2013). One of the ways that VE-cadherin is recycled back to the junctions is through the action of Rab GTPases. The Rab family of small GTPases is localized to the cytoplasmic face of specific intracellular membranes. Their main function is to regulate distinct steps in membrane trafficking pathways. The Rab GTPases, when GTP-bound, recruit specific sets of effector proteins onto the membranes. Through these effectors, Rab GTPases regulate vesicle formation, actin- and tubulin-dependent vesicle movement, and membrane fusion (Stenmark and Olkonnen 2001).

Rab GTPases play a role in recycling and degrading membrane components such as E-cadherin, the epithelial homolog of VE-cadherin. Rab5 and Rab7 GTPases are necessary for the lysosomal degradation of E-cadherin (Palacios *et al.* 2005). Rab4 and Rab11a GTPases are involved in recycling proteins back to the membrane. E-cadherin is known to associate with Rab11a-positive vesicles when being recycled back to plasma membrane. Rab11a-positive vesicles also help transport newly synthesized E-cadherin

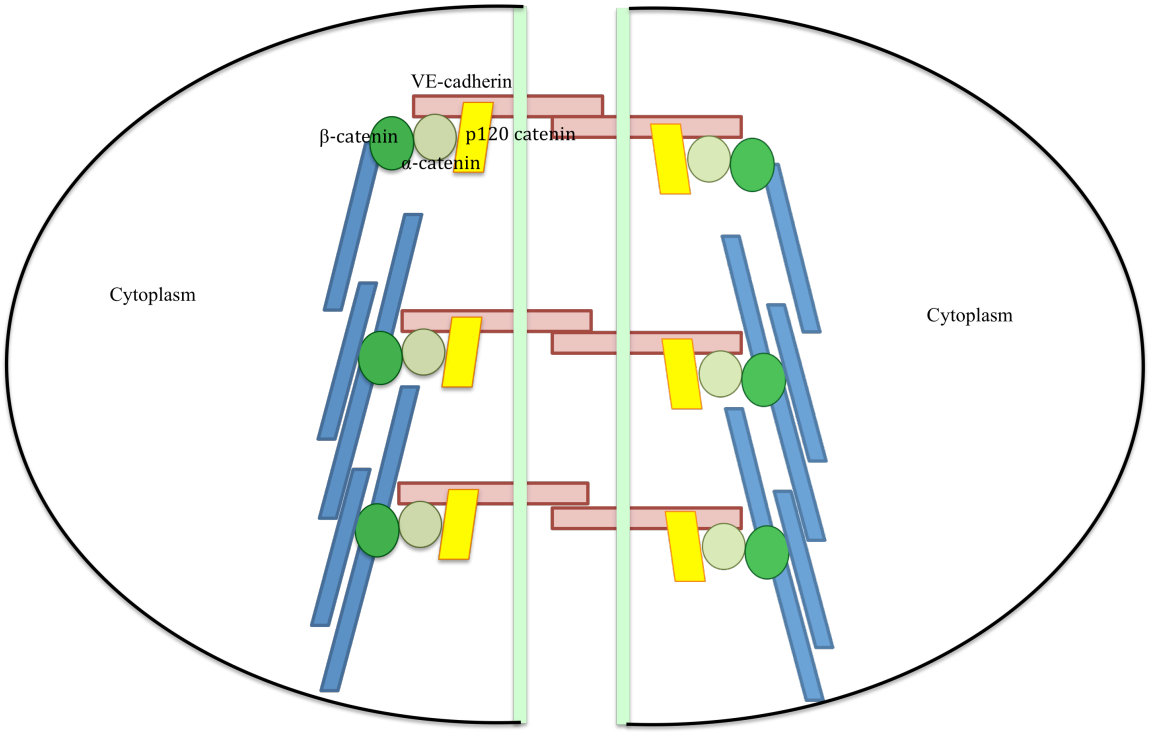

Fig. 1.3. Structure of a mature adherens junction. Adherens junctions perform multiple functions including initiation and stabilization of cell-cell adhesion, regulation of the actin cytoskeleton, intracellular signaling and transcriptional regulation. The major protein characterizing the adherens junction is VE-cadherin. The cytoplasmic component of VE-cadherin interacts with members of the catenin family including p120-catenin, β-catenin, and α-catenin. Together, these proteins control the formation, maintenance and function of adherens junctions. Source: Mikelis *et al.* 2014.

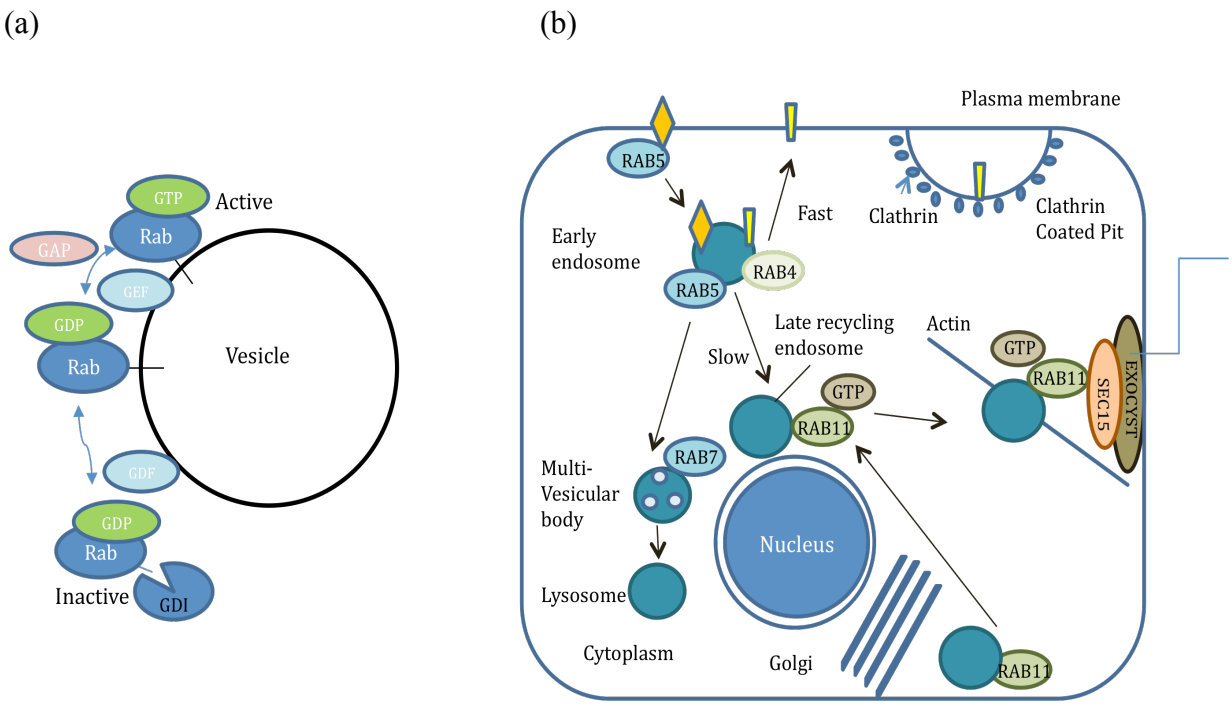

Fig. 1.4. Rab GTPases and E-cadherin Recycling. (a) Rab GTPases are regulated by guanine nucleotide exchange factors (GEFs) that exchange GDP for GTP to generate the active Rab-GTP form and GTPase activating proteins (GAPs) that generate the inactive Rab-GDP form (b) Membrane proteins are endocytosed into early endosomes, which is mediated by Rab5. Proteins from the early endosome can be recycled back to the cell surface by a fast Rab4-mediated pathway and a slow Rab11a-mediated process. Early endosomes can also traffic proteins through Rab5 to the multivesicular body, and then through Rab7 to the lysosome. Late recycling endosomes can also acquire E-cadherin via Rab11a from the Golgi complex. Rab11a-positive late recycling endosomes are delivered to the cell surface along actin filaments, where Rab11a binding to the exocyst component SEC15 tethers these vesicles to the plasma membrane. CME works through the use of adaptor protein complexes that can bind to both clathrin and E-cadherin, thereby directing E-cadherin into a clathrin-coated vesicle. Source: Guichard *et al.* 2014.

from the golgi apparatus to the plasma membrane (Lock and Stow, 2005). Therefore, Rab GTPases play a major role in fine-tuning the amount of E-cadherin present at junctions.

1.3 The Endothelial Actin Cytoskeleton

1.3.1 Actin: Structure and Function

The actin cytoskeleton is an integral component of the endothelial barrier function. The actin cytoskeleton provides a strong, dynamic intracellular scaffold that is essential in organizing the cell shape, cell size and intracellular adhesion. The cytoskeleton has three different, but related structures that together fulfill all its functions. These structures include the membrane cytoskeleton, the cortical actin rim and actomyosin-based stress fibers (fig. 1.5). Endothelial actin reorganization is essential in the response to inflammation (Prasain and Stevens 2009).

5-15% of the total protein in endothelial cells is actin, which exists as both globular actin (G-actin) and filamentous actin (F-actin). G-actin subunits polymerize in order to form the double stranded F-actin. They polymerize and depolymerize depending on the cells needs (Patterson and Lum, 2001). Actin polymerization, first of all, requires nucleation, which takes place when three actin monomers bind together. G-actin monomers spontaneously collide and nucleate to form a dimer, and then a trimer. The nucleation process is assisted by proteins like formins that associate with the monomers, stabilize the dimer and facilitate the assembly of the trimer. Then, elongation involves the binding of ATP bound G-actin to existing F-actin. The fast growing end (barbed end) of F-actin is where actin monomers quickly bind and elongate the filament. The slow growing end (pointed end) has actin monomers binding, but at a much slower rate, which makes F-actin polar. Depolymerization occurs when there is hydrolysis of

bound ATP to ADP, which causes adjacent monomers to lose affinity for each other (Lodish *et al.* 2000; Prasain and Stevens 2009).

Actin polymerization, F-actin bundling and filament depolymerization is regulated by many actin-binding proteins, such as formins, profilin, cofilin and Ena/VASP. Formins protect the barbed end of an actin filament from capping proteins throughout the elongation process, thereby facilitating actin polymerization. Profilin binds G-actin and facilitates the exchange of ADP-actin for ATP-actin. In addition, profilin binds monomeric actin and forms a complex, which is then added to the growing end of actin polymers by proteins such as formins, VASP and WASP. Another actin binding protein, cofilin, helps depolymerize actin filaments by inducing dissociation of ADP-actin from the pointed end of F-actin. Lastly, Ena/VASP takes G-actin monomers to the barbed end and has the ability to bundle actin filaments (Pollard and Borisy, 2003).

1.3.2 Cortical Actin Rim

When endothelial cells divide and form a monolayer, they reach a stage of quiescence where they cease to divide. In quiescent endothelial cells, a cortical actin rim forms around the cell that associates with cell-cell and cell-matrix adhesion complexes. It serves to tether adhesion complexes, such as tight junctions, adherens junctions and PECAM-1 associated junctions, to cellular organelles. This function of the cortical actin rim is extremely important in maintaining a solid endothelial cell barrier (Dudek and Garcia, 2001).

The cortical actin rim is organized and stabilized right underneath the spectrin-based membrane skeleton. This is done with the help of spectrin, which cross-links F-actin to inter-endothelial junction proteins such as ZO-1, α-catenin, connexin-43 and

VASP. The Arp 2/3 complex plays a role in this process by nucleating new actin branches from pre-existing F-actin, which helps stabilize cortical actin cytosketal networks (Dudek and Garcia 2001; Prasain and Stevens 2009).

Substances that disturb the cortical actin rim cause an increase in endothelial permeability. For example, permeability increasing agents such as thrombin restructure the cortical actin resulting in intercellular gaps. Often, these agonists will work to increase cytosolic calcium, decrease cAMP and activate RhoA/Rho kinase; all of these result in the increased formation of stress fibers. Thus, these various events will initiate actin reorganization and conclude in the redistribution of cortical actin into stress fibers (Maekawa *et al.* 1999; Dudek and Garcia, 2001; Prasain and Stevens, 2009). In contrast, substances that make the cortical actin rim more stable cause a decrease in permeability by preventing inflammatory agonists from disrupting the endothelial barrier (Phillips *et al.* 1989).

1.3.3 Stress Fibers

Stress fibers are actomyosin bundles that are made of F-actin filaments with alternating polarity that are cross-linked with actin binding proteins. Stress fibers are essential for inducing cell contraction (Cramer *et al.* 1997). Stress fibers extend through the cells, while the cytoskeleton and cortical actin rim are close to the membrane. The size and degree of inter-endothelial cell gaps are influenced by stress fibers. Stress fibers cause an increase in permeability because they increase centripetal tension, reorganize adhesion complex structures and cause cell-cell borders to form gaps. As stress fibers form, cells retract from their borders. Stress fibers and cortical actin rim generate

opposing centripetal and centrifugal forces, to keep a basal level of tension in the cell (Prasain and Stevens, 2009).

Rho GTPases such as RhoA, Rac and Cdc42 can control organization of the actin cytoskeleton by regulating extracellular signals (Wojciak-Stothard and Ridley 2002). In particular, RhoA plays a major role in stress fiber formation in a number of ways. RhoA activates Rho kinase, which functions to phosphorylate and thus inactivate a number of actin-regulating proteins. One of the proteins that Rho kinase phosphorylates is the myosin light chain (MLC) phosphatase. Inhibition of this phosphatase leads to increased phosphorylation of MLC. Increased MLC phosphorylation increases actomyosin interaction, which causes F-actin to bundle into stress fibers. Another way through which RhoA works to increase stress fibers is by inhibiting the actin binding protein cofilin. Since activated cofilin depolymerizes F-actin and decreases stress fiber formation, inhibition of this protein has the effect of preserving stress fiber formation. Finally, GTP-bound RhoA activates mDia, a formin which nucleates and polymerizes stress fibers. Thus, Rho GTPases, especially RhoA, work together to increase stress fiber formation and consequently, increase barrier disruption (Birukova *et al.* 2004; Essler *et al.* 1998; Sealer *et al.* 1999; Verin *et al.* 2001).

1.3.4 The Membrane Skeleton

The membrane skeleton is formed with the actin-binding protein spectrin. Together with short actin filaments, spectrin forms a tetrameric complex, and through that, a cytoskeletal network on the cytosolic surface of endothelial cells. While the membrane skeleton plays a crucial role in organizing and maintaining adherens junctions in non-endothelial cells, it plays a particularly important role in the regulation of

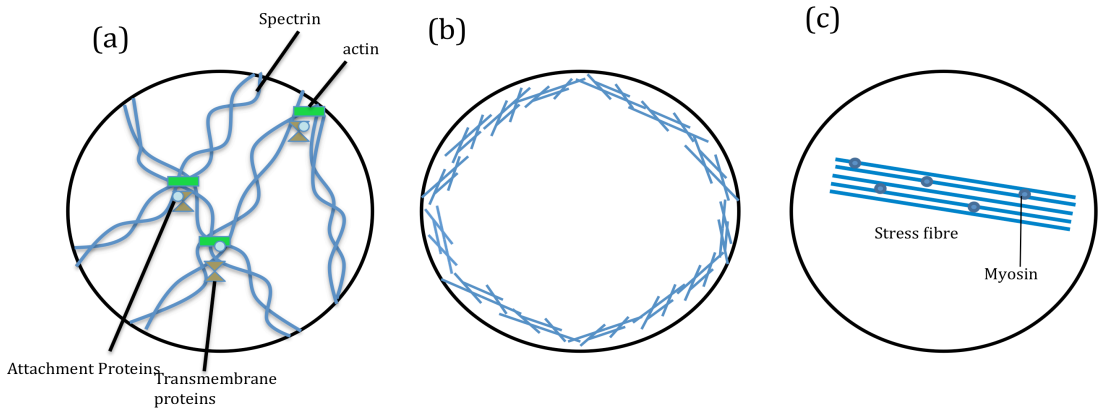

Fig. 1.5. Types of actin structures in endothelial cells. The actin cytoskeleton is comprised of three distinct, but interrelated structures, including (a) actin cross-linking of spectrin within the membrane skeleton, (b) the cortical actin rim, and (c) actomyosin-based stress fibers. Endothelial barrier function is reliant on cell-cell and cell-matrix adhesions that define the limits of cell borders. The cytoskeleton helps provide a strong and dynamic intracellular scaffold that helps respond to stimuli and remodel the cell to withstand changes in response to environmental cues.

endothelial barrier function. It helps localize actin-binding proteins such as α-actinin, vinculin and formins close to AJs, which allows the F-actin to be linked with α-catenin. This link helps in the formation and stabilization of adherens junctions. Another way through which the membrane skeleton contributes to maintaining barrier integrity is by linking to integrins in focal adhesions and thus, to the extra-cellular matrix (Machnicka *et al.* 2012; Prasain and Stevens, 2009).

1.3.5 Microtubules: Structure and Function

Microtubules are formed by alternating α- and β-tubulin heterodimers that assemble head-to-tail to form a hollow, polarized tubule. α-tubulin monomers are always exposed at the minus end (slow-growing end) while β-tubulin monomers are exposed at the plus end (fast-growing end). Both α- and β-subunits bind GTP, which allows them to assemble on to the plus end of the microtubule. The molecule of GTP bound to the β-tubulin subunit can be hydrolyzed into GDP, which influences the stability of the heterodimer in the microtubule. Dimers bound to GTP usually assemble into microtubules while dimers bound to GDP tend to fall apart. Microtubules are attached to the microtubule-organizing centre (MTOC) through their minus end and it is the positive end that orients itself towards the leading edge of the cell during migration (Petrache *et al.* 2003, Bogatcheva and Verin, 2008).

Microtubules constantly undergo assembly and disassembly, and combined with the actin cytoskeleton, determine cell shape and barrier integrity. A majority of microtubules in endothelial cells are dynamic, and remodeling of these microtubules can play a major role in regulating endothelial permeability. Dysfunction in barrier formation is usually accompanied by change in the entire microtubule system network. This is characterized

by a disappearance of peripheral microtubules and shorter microtubules growing out of the centrosome (Petrache *et al.* 2003, Alieva *et al.* 2010).

Microtubule stabilization strengthens barrier function while microtubule disruption impairs barrier function. When an edemagenic agent, such as thrombin, is applied to endothelial cells, microtubules reorganization is apparent just 5 minutes after. In contrast, the actin cytoskeleton takes 30 minutes to remodel in response to thrombin (Alieva *et al.* 2014). Since microtubules react faster than the actin filament system, they are most likely responsible for the initial changes in cell morphology during barrier dysfunction. Microtubules are the first target in the circuit of reactions leading to barrier disruption, and it is most likely this change in microtubules that leads to change in the actin filament network. One of the ways that microtubule disruption affects the actin cytoskeleton is through restructuring the cortical actin rim into stress fibers. This exhibits the important role that microtubule-actin cross talk plays in the establishment and maintenance of endothelial permeability (Birukova *et al.* 2004).

1.4 Formins

There are 15 formins found in all vertebrates, which can be divided into seven subgroups: DAAM1,2; Dia1-3; FHOD1,3; FMNL1-3; INF1,2; FMN1,2; and Delphilin (Higgs 2005) (fig. 1.6). Formins are involved in regulating many actin-based processes such as cell motility, cell invasion, cell-cell junction assembly, cell division, cell polarity and cell shape (Goode and Eck 2007). Mainly, formins play a major role in the formation of cellular structures such as stress fibers, unbranched actin filaments and plasma membrane protrusions. Formins nucleate actin filaments through the activity of two

conserved formin homology domains: FH1 and FH2. The conserved domain FH1 is a ligand for proteins that contain the SH3 domain and the small actin-binding protein profilin. The FH2 domain can bind the actin filament barbed end throughout the elongation process while protecting it from capping proteins. In many fungal and metazoan formins, another domain known as formin homology 3 (FH3) is present. The FH3 domain often overlaps with the GTPase binding domain (GBD) and is involved in targeting.

Formins exist in an autoinhibited state through the intramolecular interaction between diaphanous autoinhibitory domain (DID) and diaphanous autoregulatory domain (DAD). Formins are activated through the binding of a small GTPase, such as Rac1 or Rho, to the GBD/FH3 domain. The binding of a small GTPase releases the intramolecular inhibitory interaction between the GBD and DAD and renders the protein active. The protein composition of some formins, outside of the FH1 and FH2 domain, are diverse, which suggests that the formin family members may have different functions from each other (Kühn *et al.* 2014; Schönichen and Geyer 2010).

Both epithelial and endothelial cell junctions are stabilized by cortical actin cables that are polymerized at and extend from the junctions. Junctions can bind to pre-existing actin filaments, but because they are dynamic and constantly being remodeled, they need to also regulate actin assembly themselves. Therefore, cadherin-mediated cell-cell adhesions require actin nucleators such as formins and the Arp 2/3 complex (Kovacs *et al.* 2002; Kobielak *et al.* 2004; Carramusa *et al.*, 2007). In fact, the Arp 2/3 complex, which acts to promote the formation of a branched actin filament network, has not only been shown to localize to AJs, but also shown to physically associate with AJ

components (Kovaks *et al.* 2002). Formins have been implicated in a variety of processes regulating cell junctions in epithelial and endothelial cells (fig. 1.7).

1.4.1 Formin1

One major example of a formin that has been implicated in adherens junction maintenance is the formin Formin1 (Fmn1). Isoform IV of formin1 localizes to the cell junctions and binds α-catenin through its coiled-coil domain. At the junctions, it acts to provide a means of *de novo* actin polymerization at junctions. When a mutant construct of isoform IV Fmn1 that could not nucleate actin polymerization was over-expressed, actin cables were not formed at junctions and the junctions were misaligned. Therefore, Fmn1, specifically isoform IV, plays a major role in maintaining cell-cell junctions (Dettenhofer *et al.* 2008; Kobielak *et al.* 2004).

1.4.2 Diaphanous-related formin-1

The diaphanous-related formins (DRFs) have come to light as a group of proteins that can bridge the divide between G-protein signals and the cytoskeleton through their ability to bind small GTPases of the Rho family and consequently remodel the cytoskeleton. In many cell types, including endothelial and epithelial, Rho is necessary for and activated by cell-cell adhesion complexes. RhoA binding to Diaphanous-related formin 1 (Dia1), causes the latter protein to go from an inactive conformation to an active one (Li and Higg, 2003). Disruption in adherens junction formation caused by inhibition of RhoA is rescued by the expression of constitutively active Dia1. These findings suggest that Dia1 participates in the Rho-dependent regulation of adherens junctions (Carramussa *et al*. 2007).

Apart from participating in RhoA-mediated junction formation, Dia1 also helps form α-catenin-β-catenin complexes and localizes AJ components, such as E-cadherin, to cell-cell junctions. Dia1 achieves this through its ability to regulate the actin network at cell-cell contact sites (Sahai and Marshall 2002). Finally, Dia1 plays a role in endothelial adherens junction regulation by binding and sequestering Src kinase, which would otherwise phosphorylate VE-cadherin. Phosphorylation of VE-cadherin leads to its endocytosis and consequently, barrier disruption (Gavard *et al.* 2008).

1.4.3 Formin-like proteins

The human genome encodes three Formin-like (FMNL) proteins, FMNL1, FMNL2 and FMNL3. FMNL1 is mainly expressed in leukocytes. FMNL2 and FMNL3 are widely expressed in multiple human tissues.

1.4.3.1 Formin like-2

Formin Like-2, FMNL2, is another member of the formin family. The FH1 and FH2 domain, like in other formins, binds and nucleates actin. FMNL2 also contains a GTPase-binding domain and an autoregulatory domain. The DAD domain regulates activation via an autoinhibitory interaction with the GBD/FH3 domain. Active Rho GTPases bind to the N-terminal GBD to relieve autoinhibition. There are multiple splice variants that are predicted for this gene (Block *et al.* 2012).

FMNL2 is a downstream effector of the Rho GTPase family, which affects cell morphology and movement by activating effectors in different cellular compartments. One of the ways FMNL2 is involved in this process is through regulating cortical actin filament dynamics. FMNL2 also plays a major role in actin-based processes such as cell movement and invasion and promotes the formation of protrusive actin structures, such

as lamellipodia and filopodia, at the leading edge of migrating cells (Kühn *et al.* 2015; Block *et al.* 2012).

Recently, a bigger role of FMNL2 in junction assembly and turnover has come to light. Rac1 binds to the FMNL2 GTPase binding domain and activates the formin by relieving its autoinhibition. This helps FMNL2 localize to cell junctions, associate with E-cadherin-catenin complexes and form AJs. Furthermore, once FMNL2 is activated, it works to promote junctional actin assembly. It is still unclear how FMNL2 is recruited to adherens junctions, however, without FMNL2, adherens junctions between neighbouring cells fail to form (Griksheit *et al.* 2015).

1.4.3.2 Formin like-3

Formin like-3 (FMNL3) also plays a role in cell-cell adhesion. FMNL3 localizes to the plasma membrane in a punctate manner and gathers mostly at filopodia, ruffles and cell-cell adhesions. There is a smaller amount of dynamic cytoplasmic FMNL3, which enriches near cell-cell junctions and fuses with the plasma membrane. These FMNL3 proteins appear to originate from internal membranes such as endocytic vesicles. siRNA mediated suppression of FMNL3 caused a decrease in filopodia and also a decrease in cell-cell adhesion in cells migrating as a sheet. FMNL3, thus, appears to play a role in cell-cell adhesion (Hetheridge *et al.* 2012; Gauvin *et al.* 2015).

FMNL3 localizes to endothelial cell junctions where F-actin cables assemble. FMNL3 helps maintain the stable F-actin content at the junctions by continuously polymerizing F-actin cables. Thus, a reduction in FMNL3 would lead to decreased actin polymerization, which in turn would cause destabilized endothelial junctions. FMNL3

also plays a role in blood vessel morphogenesis as a depletion of FMNL3 caused a failure in blood vessel lumenization and lumen instability (Gauvin *et al.* 2015).

1.4.4 Formin Homology Domain-Containing Proteins

FHOD, or formin homology domain-containing proteins, are different from the other DRFs. The N- and C- terminal portions of FHOD proteins differ considerably in both composition and length of domains. Most of the current research done on FHOD proteins comes from studies done in Drosophila and *C. elegans* (Bechtold *et al.* 2014). FHOD proteins play major roles in the formation of contractile actin bundles, regulation of cell migration and sarcomeric actin filament organization (Ono *et al.* 2010).

1.4.4.1 Formin Homology Domain-Containing Protein 1

Formin Homology Domain-Containing Protein 1 (FHOD1) plays a role in integrin-based adhesions (focal adhesions), actin polymerization, cell spreading and migration. FHOD1 assembles actin filaments at focal adhesions and that stabilizes and leads to focal adhesion maturation. FHOD1 is recruited to focal adhesions through direct interaction with Src kinases. Upon recruitment, the correct localization of FHOD1 leads to the activation of Rho kinase and starts the Rho-ROCK cascade. Thus, FHOD1 is required for focal adhesion maturation but also works upstream of Rho kinase, which is involved in maintaining cell-cell junction integrity (Gasteier *et al.* 2003; Iskratsch *et al*. 2013).

1.4.4.2 Formin Homology Domain-Containing Protein 3

Formin homology 2 domain containing 3, FHOD3, is another member of the formin family. The FHOD3 structure contains a central FH1 domain, a C-terminal FH2 domain, an N-terminal GTPase binding domain (GBD), a diaphanous autoinhibitory

domain (DID) and a C-terminal diaphanous autoregulation domain (DAD). FHOD3 exists in an autoinhibited state that is relieved by the binding of a small GTPase such as Rac1 or Rho. Once activated, FHOD3 stimulates actin filament synthesis. FHOD3 can also be directly activated by ROCK1 phosphorylation of three amino acids in the C-terminal region of the formin (Iskratsch *et al.* 2013).

FHOD3 has mostly been characterized as a sarcomeric protein. FHOD3 mainly localizes to actin fibers and the remaining protein displays filamentous staining. FHOD3 is an actin-organizing protein that aids in stress fiber formation and elongation. The muscle-specific isoform of FHOD3 plays a major role in sarcomeric and myrofibril organization during myofibrillogenesis. Non-muscle FHOD3 is expressed at high levels in the embryonic atrium (Iskratsch *et al.* 2010; Kan-O *et al*. 2012; Iskratsch *et al.* 2013). Currently, a role for FHOD3 in regulating endothelial cell junction formation has not been investigated.

1.5 Hypothesis

Studies in epithelial cells have suggested that formins are likely to play key roles in adherens junction formation and maintenance. A similar role for formins in endothelial cells has not been investigated. We hypothesize that formin activity is essential for adherens junction formation in endothelial cells.

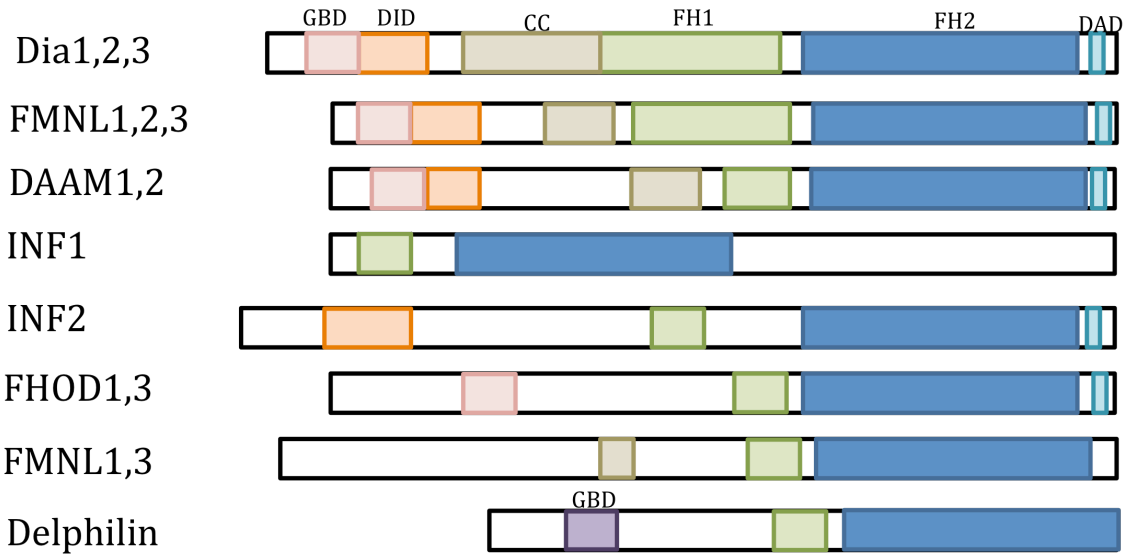

Fig. 1.6. Schematic of the fifteen Human Formin Homology Proteins. Formins can be divided into seven sub-families: Diaphanous (Dia), Formin-like (FMNL2), Dishevelled-associated activator of morphogenesis (DAAM), Inverted formin (INF), Formin homology domain-containing protein (FHOD), Formin (FMN), and Delphilin. Each formin contains the functional domains: Formin Homology 1 and Formin Homology 2. Some of the formins also have the regulatory domains: Diaphanous Inhibitory Domain (DID), coiled-coiled Domain (CC) and Diaphanous Autoregulatory Domain (DAD). Certain formins also have a GTPase-binding domain or PDZ domain at the N-terminus. The DRF subgroup comprise of the Dias, FMNLs and DAAMs proteins.

Fig. 1.7. The potential roles of formins in junction remodeling and cellular morphological changes. Isoform IV of formin1 has been shown to localize to the cell junctions and bind α-catenin through its coiled-coil domain. At the junctions, it acts to provide a means of *de novo* actin polymerization at junctions. RhoA binding causes Dia1 activation, which plays an essential role in forming α-catenin-β-catenin complexes and localizing E-cadherin to cell-cell junctions. Upon activation, Dia1 also sequesters Src-kinase, which inhibits VE-cadherin endocytosis. FMNL2 was found to be required for actin assembly and turnover at newly formulated cell junctions by helping Rac1-induced actin assembly at the junctions. FMNL3 localizes to the cell membrane and helps maintain the stable F-actin content at the junctions by continuously polymerizing F-actin cables. Rac1-bound FHOD1 associates with F-actin and leads to the formation of thick actin fibers, leading to cytoskeletal changes. FHOD1 also assembles actin filaments at focal adhesions and that stabilizes and leads to focal adhesion maturation.

‘

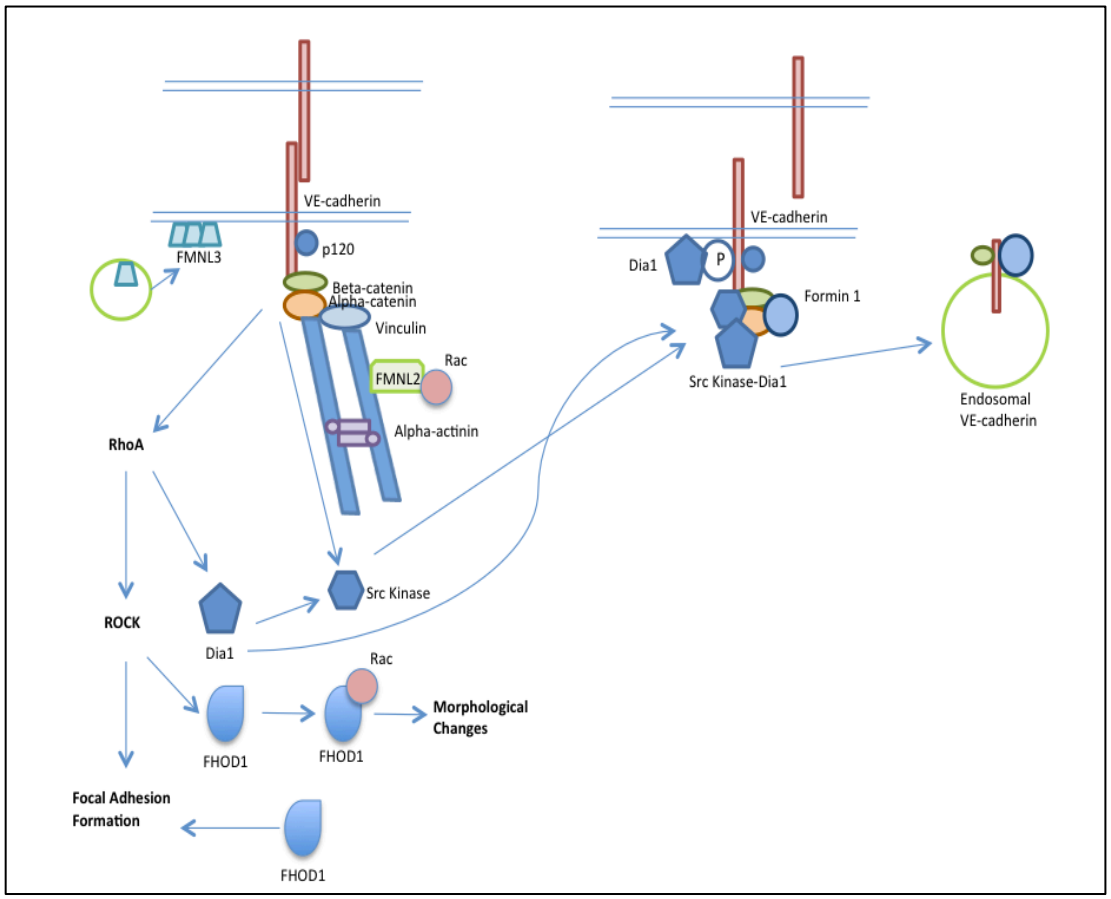
VE-cadherin
FMNL3
p120
Beta-catenin
Alpha-catenin
Vinculin
Rac
FMNL2
Alpha-actinin
RhoA
ROCK
Dia1
Src Kinase
Rac
FHOD1
FHOD1
Morphological Changes
Focal Adhesion Formation
FHOD1
VE-cadherin
Dia1
P
Formin 1
Src Kinase-Dia1
Endosomal VE-cadherin

Chapter 2

Material and Methods

2.1 Cell Culture

Table 2.1: Cell lines used in this thesis

Cell Line	Supplier	Cell type	Organism	Medium	Conditions
NIH3T3	ATCC	Fibroblast	*Mus musculus*	10% DBS (ATCC) in DMEM (ATCC)	37°C, 5% CO_2
TIME	ATCC	Microvascular Endothelial Cells	*Homo sapiens*	Endothelial Basal Medium + growth factors (ATCC)	37°C, 5% CO_2

Telomerase-Immortalized Microvascular Endothelial cells were cryopreserved in liquid nitrogen vapour phase in media + 10% DMSO (Sigma). They were thawed and cultured in Endothelial Basal Media (ATCC) supplemented with Microvascular Endothelial Cell Growth Factor Kit- VEGF (ATCC PCS-110-041). The growth media kit contained 5 ng/mL VEGF, 5 ng/mL EGF, 5 ng/mL FGF, 15 ng/mL IGF-1, 10mM L-Glutamine, 50 μg/mL Ascorbic Acid, 0.75 Units/mL Heparin Sulfate, 1 μg/mL Hydrocortisone and 5% FBS. Cell cultures were maintained in a humidified 95% air/5% CO_2 incubator.

TIME cells were washed with 1XPBS and then trypsinized with 0.05% Trypsin and 0.02% EDTA (ATCC) at 37°C until cells had detached from the dish. Once cells had lifted, the trypsin was neutralized with TIME media and transferred to a sterile centrifuge tube. The cell suspension was spun down at 250 x g for 10 minutes. The supernatant was removed and the cells were suspended in 6-8 mL of complete media. 10 μL of the cell suspension was used to count cells in the hemocytometer. TIME cells were seeded at a density of 5000-8000 cells/cm^2 and used between passages 25- 35.

NIH3T3 cells were passaged as follows. Cells were washed with 1XPBS and trypsinized in 0.25% Trypsin-0.53 mM EDTA until cells had lifted. Growth media was added to the cells in order to neutralize the trypsin. Cells were counted using a hemocytometer and transferred to a new culture dish at a density of 3000-5000 cells per cm^2.

2.2 Immunofluorescence

Coverslips used for immunofluorescence were treated for 5 hours with a solution of 40% HCl and 60% ethanol. After extensive washing with distilled water, the coverslips were left to soak in 70% ethanol overnight, and then stored in fresh 70% ethanol for further use. These coverslips were flamed before use.

TIME cells were seeded onto collagen-coated coverslips prepared as follows. A 0.01 N HCl solution was made by adding 41.6 µL concentrated HCl (stock 12 M) to 50 mL of sterile water. 50 µL of 3 mg/mL collagen (Advanced Biomatrix) was added to 10 mL of the 0.01 N HCl solution and 1 mL of this solution was put on each coverslip for 1-2 hours. The coverslips were then washed with 2 mL of sterile water 5 times, followed by washing with 2 mL of 1XPBS 5 times.

Cells were fixed for immunofluorescence in 4% paraformaldehyde (PFA) in 1XPBS for 10 minutes. After fixation, they were washed twice with 1XPBS and permeabilized with 0.3% Triton X-100 plus 10% donkey serum in 1xPBS for 20 minutes. Cells were then incubated with the primary antibody in a solution of 5% donkey serum and 0.03% Triton X-100 in 1XPBS at room temperature for 1 hour. Cells were then washed 3 times in 1X PBS. Cells were then incubated with secondary antibody in the same solution of 5% donkey serum and 0.03% Triton X-100 in 1XPBS at room temperature for 1 hour.

Cells were then washed 3 times for 5 minutes in 1X PBS, 1 time in distilled H_2O and mounted using VectaShield mounting media with DAPI (Vector Labs). Images were captured on a Zeiss Axio Imager Z1 microscope equipped with an AxioCamHRm camera and using a 63X oil objective (ECPlan-NeoFluor, 0.75 NA). Images were processed with Axiovision 4.5.

Table 2.2. Antibodies used for immunofluorescence

Antibody	Dilution	Species	Supplier (Catalog #)
VE-Cadherin	1/100	Goat	Santa Cruz Biotechnology (sc-6458)
Vinculin	1/400	Mouse	Sigma-Aldrich (V9131)
α-catenin	1/100	Rabbit	Abcam (ab51032)
β-catenin	1/200	Rabbit	EMD Millipore (05-665)
α-actinin	1/200	Rabbit	Abcam (ab59468)
Paxillin	1/300	Mouse	Abcam (ab3127)
Actin (Phalloidin)	1/40	Toxin	Molecular Probes (F432)
Acetylated Tubulin	1/100	Rabbit	Sigma-Aldrich (T 6793)
Focal Adhesion Kinase	1/200	Mouse	BD Transduction Laboratories (610088)
α-Tubulin	1/500	Mouse	Santa Cruz Biotechnology (sc-58667)
p120-Catenin	1/100	Rabbit	BD Transduction Laboratories (610133)
FHOD3	1/100	Rabbit	Biorbyt (orb156871)
Transferrin Receptor	1/200	Rabbit	Abcam (ab84036)
γ-Tubulin	1/5000	Mouse	Sigma-Aldrich (T 6557)
Pericentrin	1/1000	Rabbit	Abcam (ab4448)
LAMP-1	1/50	Rat	Santa Cruz Biotechnology (sc-19992)

2.3 Western Blotting

For western blotting, TIME cells were washed twice with cold 1XPBS and scraped in 1X laemmli loading buffer (SDS). Samples were then boiled for 10 minutes and stored at -20°C. For larger proteins, an 8% acrylamide gel was prepared and samples were boiled for 5 minutes prior to loading. After loading, the gel was run for 1hr at 185 V and transferred onto a nitrocellulose membrane at 100 V for 1hr and 6 minutes. After transferring, the membrane was blocked in 5% skimmed milk powder prepared in 1xPBS (blotto) for 1hr. The membrane was incubated overnight at 4°C with the appropriate antibody diluted in blotto. The membrane was then washed 3 times with blotto for 10 minutes each and then incubated with the appropriate secondary antibody conjugated to horseradish peroxidase diluted in blotto for 1hr. After the final incubation, the membrane was washed with blotto 3 times 10 minutes each and then washed 2 times for 5 minutes each with 0.2% Tween-20 in 1XPBS. Immunoreactive proteins were visualized by chemiluminesence (Western Lighting Plus reagent, Perkin Elmer). Blots were exposed on autoradiographic film (Kodak) or on the GE Image Quant LAS4010 Imaging System. Where anti-tubulin antibody was used as a loading control the same blot was stripped in a solution of 0.1M Glycine and 0.5% SDS, at pH 2.5 for 40 minutes, blocked in blotto for 1hr and re-probed for 30 minutes at room temperature with a mouse anti-tubulin antibody. The blot was further probed with donkey-anti-mouse secondary antibody conjugated to horseradish peroxidase for 30 minutes, washed and then visualized as above.

Table 2.3. Dilution and supplier of antibodies for western blotting

	Primary	Secondary	Supplier
Dia1	1/1000	1/50000	Santa Cruz Biotechnology (sc-10885)
Dia3	1/500	1/50000	Abcam (ab129668)
Daam1	1/2000	1/50000	Dunn Lab
Daam2	1/1000	1/50000	Copeland Lab
INF1	1/10000	1/50000	Copeland Lab
INF2	1/1000	1/50000	Higgs Lab
FMNL2	1/5000	1/100000	Copeland Lab
FMNL3	1/2000	1/50000	Copeland Lab
Dia2	1/1000	1/50000	Santa Cruz Biotechnology (sc-10889)
Formin1	1/1000	1/50000	Santa Cruz Biotechnology (sc-22724)
FHOD-1	1/500	1/50000	Santa Cruz Biotechnology (sc-365437)
FMNL1	1/500	1/50000	Santa Cruz Biotechnology (sc-390466)
FHOD-3	1/500	1/50000	Santa Cruz Biotechnology (sc-374601)
VE-cadherin	1/200	1/50000	Santa Cruz Biotechnology (sc-6458)
β-catenin	1/1000	1/50000	EMD Millipore (05-665)
α-catenin	1/1000	1/50000	Abcam (ab51032)
p120-catenin	1/1000	1/50000	BD Transduction Laboratories (610133)
α-actinin	1/1000	1/50000	Abcam (ab59468)

Focal Adhesion Kinase	1/200	1/50000	BD Transduction Laboratories (610088)
Paxillin	1/40000	1/50000	Abcam (ab3127)
Vinculin (mouse)	1/2000	1/50000	Sigma-Aldrich (V9131)
Vinculin (Rabbit)	1/200	1/50000	Life Technologies (700062)
α-Tubulin	1/50000	1/50000	Santa Cruz Biotechnology (sc-58667)
Transferrin Receptor	1/5000	1/50000	Abcam (ab84036)
Rab7	1/1000	1/50000	Abcam (ab50533)
Rab11a	1/1000	1/50000	Abcam (ab3612)

2.4 siRNA Transfection

DICER substrate duplexes (Integrated DNA Technologies) targeting the gene of interest along with a scrambled universal negative control were tested according to the supplier's guidelines.

siRNA duplexes were reconstituted to 20μM using RNase free buffer. These duplexes were further diluted 1/10 to generate a 2 μM siRNA working solution. The RNA duplex as well as the negative control duplex was transfected into 1.25 x 10^5 cells (1 well of a 6-well plate) at concentrations of 0.1, 1 and 10 nM. Cells were harvested at 24, 48 and 72 hours post-transfection. The concentration and timing for siRNA transfection were optimized for each formin to achieve highest knockdown without affecting cell viability (Table 2.4). The RNA duplex, among the three provided, that showed the best knockdown result as determined by western blotting was used for subsequent experiments.

Table 2.4: Optimal knockdown concentration for formins present in TIME cells

Formin	Duplex	Concentration	6 cm dish
FMNL3	D2	1 nM	2 µL
FMNL2	D1	1 nM	2µL
FHOD1	D2	1 nM	2µL
Dia1	D2	1 nM	2µL
FHOD3	D3	4 nM	8µL
Daam1	D1	1 nM	2µL
Daam2	D2	1 nM	2µL

For 1 well of a 6 well plate, 1-4 nM of siRNA duplex were added to 200µl Opti-MEM in one centrifuge tube. In another centrifuge tube, 2µl DharmaFECT 1 transfection reagent (Dharmacon) was added to 200 µl Opti-MEM . The two tubes were incubated for 5 minutes at room temperature. The contents of tubes 1 and 2 were then combined and incubated for 20 minutes at room temperature. Culture media was removed from the dishes and replaced by 1.6 mL of antibiotic and heparin-free complete TIME media. Antibiotics and heparin sulfate inhibit transfection complex formation and therefore should be excluded from the complex formation step. siRNA transfection complexes were then added dropwise onto the cells. Experiments were performed 72 hours post transfection.

2.5 *In Vitro* Vascular Permeability Assay

In vitro vascular permeability assay kits were obtained from EMD Millipore (ECM644). Before cells were seeded onto the inserts, the inserts needed to be hydrated with 250 µL complete media for 15 minutes at room temperature. The media was

removed and TIME cells were seeded at a density of 2 x 10^5 cells/insert in 200 μL onto collagen-coated inserts that were placed in wells with 500 μL full growth media. Once seeded, the cells were allowed to grow to a confluent monolayer for 72 hours. After 72 hours, media in the insert was removed and replaced with a 150 μL of 1/40 dilution of FITC-dextran (ECM644, EMD Millipore) in complete media and left in darkness for 20 minutes. After this time, the inserts containing the FITC-dextran solution were removed and 500 μL of media in the lower chamber was collected in an eppendorf tube. A 100 μL of this 500 μL solution was used to measure the concentration of FITC-dextran by using an opaque black 96-well plate. A fluorescence-multi well plate reader was used with filters for 485 nm excitation and 535 nm emission. Defects in barrier formation were detected by passage of FITC-dextran across the endothelial cell layer and into the underlying well (Fig. 2.1).

When testing the effects of smiFH2 on barrier formation, 15 μM smiFH2 was added to the insert 2 hours before FITC-dextran. When treating the cells with TNF-α as a control for the smiFH2 experiment, the drug was added to media 48 hours after seeding and 24 hours before adding FITC-dextran. In order to test the effects of knockdowns, siRNA-transfected cells were first grown on a 6cm dish for 24 hours post transfection. Then, cells were trypsinized, counted and seeded onto the inserts at a density of 2 x 10^5 cells/insert. These cells were allowed to grow for 48 hours before the application of FITC-dextran.

After the assay was complete, the inserts were stained with a cell stain (provided) and the monolayer visualized on a microscope. This was done by first removing all the media in both the well and the insert and then adding 100 μL of cell stain (provided). This cell

stain remained on the insert, protected from light for 20 minutes. After 20 minutes, the cell stain was removed and the inserts were washed with 500 µL of 1XPBS twice. Before imaging, 500 µL of 1XPBS was added to the insert and then viewed under the brightfield setting on a microscope.

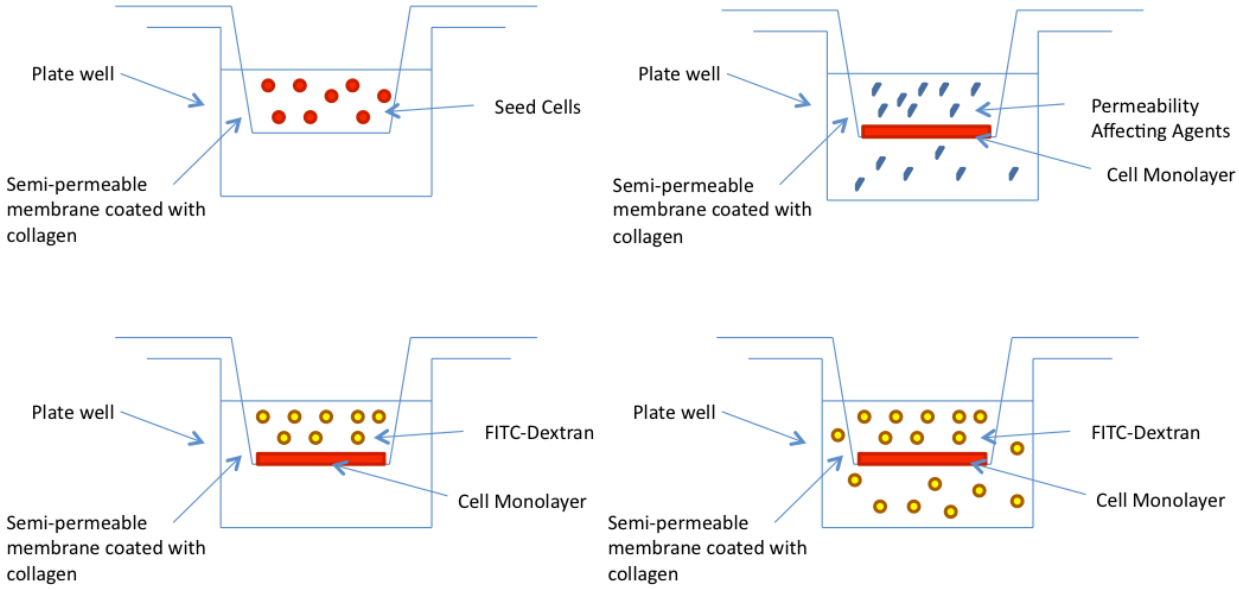

Adapted from EMD Millipore

Fig. 2.1. Protocol for the *In vitro* vascular permeability assay. Endothelial cells are seeded on inserts and grown to a confluent monolayer. The monolayer is treated with junction disrupting compounds after which FITC-dextran is added to the insert. FITC-dextran permeates the monolayer and goes into the bottom well. The media in the well is then read through a fluorescence-multi well plate reader.

2.6 smiFH2 treatment

10 mg smiFH2 (EMD Millipore) was suspended in 200 μL of DMSO (50 mg/mL) and then stored at -20°C. TIME cells were seeded onto coverslips and grown for 72 hours in order to form a confluent monolayer. At 72 hours, 5, 10 and 15 μM smiFH2 were added to the cells for 2 hours. DMSO was added to one of the coverslips as vehicle-control. After two hours, the coverslips were fixed in 4% PFA and then stained to look at various proteins. In the case of the permeability assay, after 2 hours, media with smiFH2 was taken out of the inserts and media with FITC-dextran was added. The media underneath the well was tested for the amounts of FITC-dextran in the solution.

2.7 TIME cell transfection

TIME cells were seeded on coverslips at a density of 125,000 cells/well of a 6-well plate. 24 hours after seeding, the cells were transfected with 0.3 μg of plasmid. Plasmid DNA was added to 200 μL Opti-MEM . 4 μL of Transfex (ATCC) was added to the plasmid-Opti-MEM tube and incubated at room temperature for 15 minutes. Culture media was removed from the wells and replaced with 1.8 mL of antibiotic and heparin-free complete TIME media. Transfected cells were either fixed or harvested 24 hours post-transfection.

When transfecting siRNA, TIME cells were seeded at a density of 125,000 cells/coverslip. 24 hours later, siRNA duplexes were added to 200 μL Opti-MEM in one tube. 2 μL of DharmaFECT 1 was added to 200 μL of Opti-MEM (1/100 dilution) in a different tube. Both tubes were kept at room temperature for 5 minutes. The DharmaFECT-Opti-MEM tube was added to the siRNA- Opti-MEM tube and left to incubate for 20 minutes. Culture media was removed from the wells and replaced by 1.6

mL of antibiotic and heparin-free complete TIME media. After 20 minutes, 400 μL of the Opti-MEM-siRNA-plasmid mix was added dropwise to each well. The cells were either fixed or harvested at 72 hours.

Double transfection of siRNA and plasmid DNA was preformed as follows. 0.3 μg of a plasmid was added to 200 μL Opti-MEM along with the siRNA duplex. 2 μL of DharmaFECT duo (Dharmacon) was added to a separate tube of 200 μL Opti-MEM (1/100 dilution) and both tubes were left to incubate at room temperature for 5 minutes. 200 μL of the DharmaFECT-Opti-MEM mixture was added to siRNA and plasmid tube. This tube was left to incubate at room temperature for 20 minutes. Meanwhile, culture media was removed from the wells and 1.6 mL of antibiotic and heparin-free complete TIME media was added. After 20 minutes, 400 μL of the siRNA-plasmid-DharmaFECT duo mix was added dropwise to each well. The cells were fixed at 72 hours.

2.8 RNA Extraction

TIME cells were grown to 70-80% confluence in a 10cm petri dish. Total RNA was harvest using an RNeasy mini kit from Qiagen. First, media was aspirated and the cells were washed 3 times with room temperature 1XPBS. The cells were then scraped using 600 μL of buffer RLT with 1% β-mercaptoethanol and sheared using a 20-gauge needle 5 times. Then, 600 μL of 70% ethanol were added to the mixture. The lysate was mixed well by pipetting up and down and then 700 μL of it was transferred to a column where the RNA binds the membrane. The lysate was centrifuged for 15 seconds at 8000 x g. The fluid beneath the column was discarded and the membrane was washed with 350 μL of buffer RW1 and centrifuged for 30 seconds at 8000 x g. The membrane was washed again, twice, with 500 μL buffer RPE. The column was then transferred to a new

collection tube and spun for 2 minutes at full speed. The column was put into an eppendorf tube and RNA was eluted by adding 50 µL RNase free water to the column and spun at 8000 x g for 1 minute. The RNA was stored at -80°C. The total RNA concentration was determined with a BioTek microplate spectrophotometer using a Take3 Trio micro-volume plate and the computer program Gen5. The $OD_{260/280}$ ratio provides an estimate of the purity of RNA and A_{260} x 40 determines single-stranded RNA quantity in µg/µL.

2.9 cDNA Preparation

The preparation of cDNA from RNA was performed using the Transcriptor High Fidelity cDNA synthesis kit (Roche). 2 ng RNA was added to 2.5 µM Anchored-oligo(dt) primer in water. This mixture was then heated to 65°C for 10 minutes in a Biometra Thermocycler and then immediately cooled on ice. 1 x (8mM $MgCl_2$) Transcriptor High Fidelity Reverse Transcriptase Reaction buffer, 20 U Protector RNase inhibitor, 1 mM dNTP mix, 5 mM DTT and 22 U Transcriptor High Fidelity Reverse transcriptase were added to the previous mixture of template-primer. This mixture was incubated for 30 minutes on the thermocycler at 55°C. Finally, the reverse transcriptase was inhibited by heating the mixture to 85°C for 5 minutes. The cDNA was stored at -20°C.

2.10 RT-PCR Analysis

In order to identify the FHOD3 isoform present in TIME cells, we performed reverse transcription polymerase chain reaction (RT-PCR) using TIME cell cDNA. Due the large size of the FHOD3 gene, primers were designed in a way that FHOD3 would be amplified in three distinct fragments. The primers were designed to incorporate restriction digest sites in order to later clone the fragments into vectors. (fig. 2.2). The

PCR was performed using Phusion High-Fidelity DNA polymerase kit from NEB. 10.8 µl Nuclease free water, 4 µl high fidelity (HF) buffer, 2 µl 10 mM dNTPs, 2 µl 10 µM forward and reverse primer (IDT, see table 2.5), 2 µl cDNA and 0.2 µl Phusion DNA polymerase were all mixed gently together to make a 20 µl reaction. This was done in three separate tubes for the three different sets of primers corresponding to the 5' end fragment (1 kb), middle fragment (1.8 kb) and the 3' end fragment (1.5 kb). The PCR reactions were performed in a Biometra Thermocycler (see the GeneAmp RNA PCR kit protocol for full PCR details and for the thermocycler conditions). Conditions of each PCR program vary depending on the Tm of the primers and the length of the fragment to be amplified. Conditions of each program are listed in table 2.6.

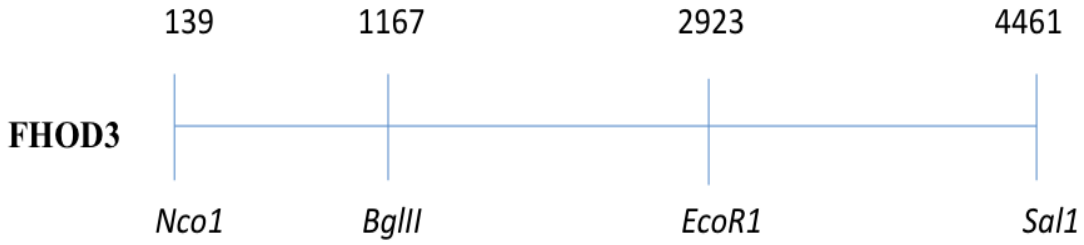

Fig. 2.2. Full length FHOD3 isoform cloning. In order to amplify the entire gene, FHOD3 was divided into three fragments, which were individually amplified through RT-PCR. The primers were designed to incorporate restriction digest sites so that each of the fragments could collectively eventually be cloned into vectors. Nco1 and BglII were the restriction sites incorporated into the 5' end fragment, BglII and EcoRI were incorporated into the middle fragment and EcoRI and SalI were incorporated into the 3' end fragment.

Table 2.5: Primer sequences for the cloning of FHOD3 from TIME cell cDNA

Name	Primer Direction	Primer Sequence	Primer Position
Nco1	Forward	5' GGCCATGGCCACGCTGGCTTGCCGGGTGC 3'	139
BglII	Forward	5' CCCAACCAAGTGCGAGATCTGCGTG 3'	1167
BglII	Reverse	5' CACGCAGATCTCGCACTTGGTTGGG 3'	1190
EcoRI	Forward	5' CCGACGCTGCAGAGAATTCCTGTGGTC 3'	2923
EcoRI	Reverse	5' GACCACAGGAATTCTCTGCAGCGTCGG 3'	2953
Sal1	Reverse	5' CCCGTCGACTCACAGCTGCAACTCCGAGGTGCC 3'	4461

Table 2.6: PCR Program Details for each set of Reactions

Fragments	**Nco1-BglII (1 kb)**	**BglII-EcoR1 (1.8 kb)**	**EcoR1-Sal1 (1.5 kb)**
Initial Denaturation	98˚C for 30 seconds	98˚C for 30 seconds	98˚C for 30 seconds
35 Cyles	1. 98˚C for 10 Seconds 2. 72˚C for 30 seconds 3. 72˚C for 27 seconds	1. 98˚C for 10 Seconds 2. 72˚C for 30 seconds 3. 72˚C for 54 seconds	1. 98˚C for 10 Seconds 2. 72˚C for 30 seconds3. 3. 72˚C for 45 seconds
Final Extension	72˚C for 10 seconds	72˚C for 10 seconds	72˚C for 10 seconds
Hold	4˚C	4˚C	4˚C

Once these programs had run and each fragment had been amplified, the mixtures were run on a 0.8% agarose gel. Bands were visualized with ethidium bromide, excised and extracted (Qiaquick gel extraction kit). Only two of the three fragments, the 5' end and the 3' end fragments, were able to be amplified through PCR. We sequenced the PCR products of the two fragments in order to identify the FHOD3 isoform present in TIME cells. While the 5' end sequence of most FHOD3 isoforms are identical, sequencing the 3' end narrowed down the choices to 4 isoforms (isoform 1, 2, 3 and X10). In further attempts to obtain the last fragment, we amplified a portion of FHOD3 extending from the beginning of the middle fragment to the end of the 3' end fragment. This resulted in a band that matched the fragment size. Upon sequencing of this fragment,

we were able to narrow down the FHOD3 isoform present in TIME cells as being isoform 1. The cDNA for isoform 1 was ordered through GeneCopoeia (Z4905).

2.11 Cell Area Measurements

The area, length and width of a cell were measured using Northern Eclipse (Version 7.0, Empix Imaging Inc.). The cell images were taken on Zeiss Axio Images Z1 microscope and then converted into a tiff file. The image was opened in Northern Eclipse and calibrated to the correct magnification. Using the measuring tool, individual cells were outlined and the program calculated the area, length and width of the cell. Cell measurements were taken from 3 different experiments and each time, 100 cells were counted.

2.12 Colocalization Measurements

Colocalization between two proteins was measured using the colocalization plug-in for Axiovision (Version 4.8, Zeiss). The software allows the user to draw a line around the transfected cell and measure colocalization by calculating the Pearson Coefficient for the two proteins. The Pearson Coefficient is a type of correlation coefficient that represents the relationship between two variables that are measured on the same interval or ratio scale. The results are between -1 and 1. A coefficient of 1 means that there is total positive correlation between the two variables, 0 means that there is no correlation and a coefficient of -1 means that there is total negative correlation (Dunn *et al.* 2011). Colocalization measurements were taken from 3 different experiments and each time, 25-30 cells were counted.

2.12 Statistical Significance

All statistical analyses were performed with Microsoft Excel and represented as averages. Error bars in graphs represent the SEM and n = number of cells. P value of <0.05 was used to determine significance. The statistical tests performed were two-tailed t-test of two sample equal variance. This specific t-test is used to compare two groups in cases where subjects are randomly assigned to two groups and then given the first group treatment A and the second group treatment B. This test was judged as appropriate. Variance and normality were tested to make sure that a suitable statistical test was chosen.

Chapter 3

Results

3.1 smiFH2 treatment increased endothelial permeability in an *in vitro* vascular permeability assay

In order to determine if formins were involved in maintaining or regulating endothelial permeability, TIME cells were treated with a small molecule inhibitor of FH2 domain (smiFH2) on an *in vitro* vascular permeability assay (fig.3.1) (Rizvi *et al.* 2009). TIME cells were treated with three different concentrations of smiFH2 (5,10 and 15 μM) for 2 hours. Cells were also treated with TNF-α as positive control and DMSO as vehicle control. TNF-α is an adipokine that is involved in systemic inflammation and is known to increase monolayer permeability (Hoffman *et al*. 2002).

There was a dose-dependent increase in permeability in cells treated with smiFH2. Cells treated with the 5 μM smiFH2 showed little change in permeability from untreated cells while cells treated with 15 μM smiFH2 ($p<0.05$) produced the highest change in permeability. As a control for cell death or detachment, giemsa cell stain was used to visualize the cells on the insert after drug treatment. Using the brightfield setting, the cells were viewed under a microscope and there was no sign of cell death.

In parallel with the permeability assay, cells were grown on collagen-coated coverslips for three days and subjected to smiFH2 treatment. The effects of smiFH2 treatment on FA, FAJ and AJ formation were determined by immunofluorescence using available VE-cadherin and vinculin antibodies. We used fluorescently-labeled phalloidin to detect F-actin and DAPI to stain for the nucleus (fig. 3.2). Immunofluorescence results show that increasing concentrations of smiFH2 inhibit FAJ formation and present an altered morphology of AJs compared to controls. At 15 μM smiFH2, cells were depleted of stress fibers and left with a cortical actin ring around each cell. Junctional proteins like

vinculin and VE-cadherin were also depleted from 15 μM smiFH2 treated cells. In addition, the monolayer showed gaps between cells. Therefore, smiFH2-treatment results show that inhibiting formins does have an effect on endothelial permeability.

3. 2 Identifying and knocking down formins present in TIME cells

Immunoblotting was used to determine which formins are expressed in TIME cells. Antibodies against all human formins (except delphilin and formin 2) are either commercially available or have been generated in our lab. Epitope tagged derivatives of the relevant proteins were used as positive controls to assist in the identification of the correct protein (formins often show anomalous electrophoretic mobility). Our findings show that Dia1, Dia3, Daam1, Daam2, FMNL2, FMNL3, FHOD-1 and FHOD-3 are expressed in TIME cells. Ambiguous results were obtained for INF2 and FMN1 and we did not detect any evidence for expression of the remaining formin family members.

After we determined which formins were present in TIME cells, they were individually knocked down in preparation for the *in vitro* vascular permeability assay. The knockdown conditions (duplex, concentration and time) for each of these formins were established from trifecta siRNA kits (IDT) containing three duplexes each. We were able to achieve the following level of knockdown: FHOD3 (knockdown 72.79%), FHOD1 (97.96%), Dia1 (87.45%), FMNL2 (87.81%), FMNL3 (99.56%), Daam1 (99.56%) and Daam2 (96.7%) (fig. 3.3).

(a)

Sample	Relative Permeability
No cells	810
Untreated	26
DMSO	27
TNFα	100
smiFH2 5 µM	52
smiFH2 10 µM	216
smiFH2 15 µM	247

(b)

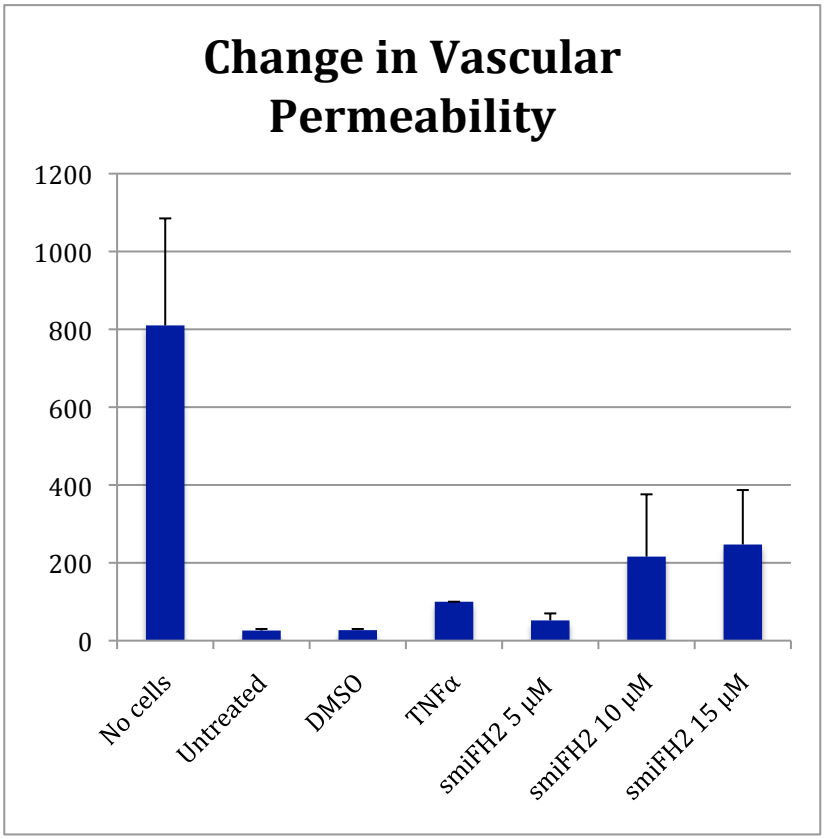

Fig. 3.1. SmiFH2 causes an increase in permeability of the endothelial monolayer. (a) FITC-dextran concentration in media after being treated by smiFH2, TNFα, DMSO or untreated. TNFα is set to 100 and other values are in relation to TNFα. (b) Bar graph depiction of FITC-dextran concentration in media after drug treatment. The amount of FITC-dextran in the media increases as the concentration of smiFH2 increases. Inhibiting formins leads to an increase in endothelial permeability. Results are a mean of three experiments. Error bars are SEM. $P < 0.05$; two-tailed T-test.

Fig. 3.2. 15 μM smiFH2-treated cells show a decrease in FAJs and an increase in detachment from neighboring cells. smiFH2 treatment was done on collagen-coated coverslips and stained for actin (green), VE-cadherin (red) and vinculin (cyan). Cells were seeded onto collagen-coated coverslips, grown for 72 hours and treated with DMSO, TNFα or smiFH2. The images correspond to untreated cells, cells treated with DMSO, TNFα-treated cells, 5 μM smiFH2-treated cells, 10 μM smiFH2-treated cells and 15 μM-treated smiFH2 cells. The loss of FAJs at 15 μM smiFH2 shows that formins are involved in junction formation. Scale bars represent 10 μM.

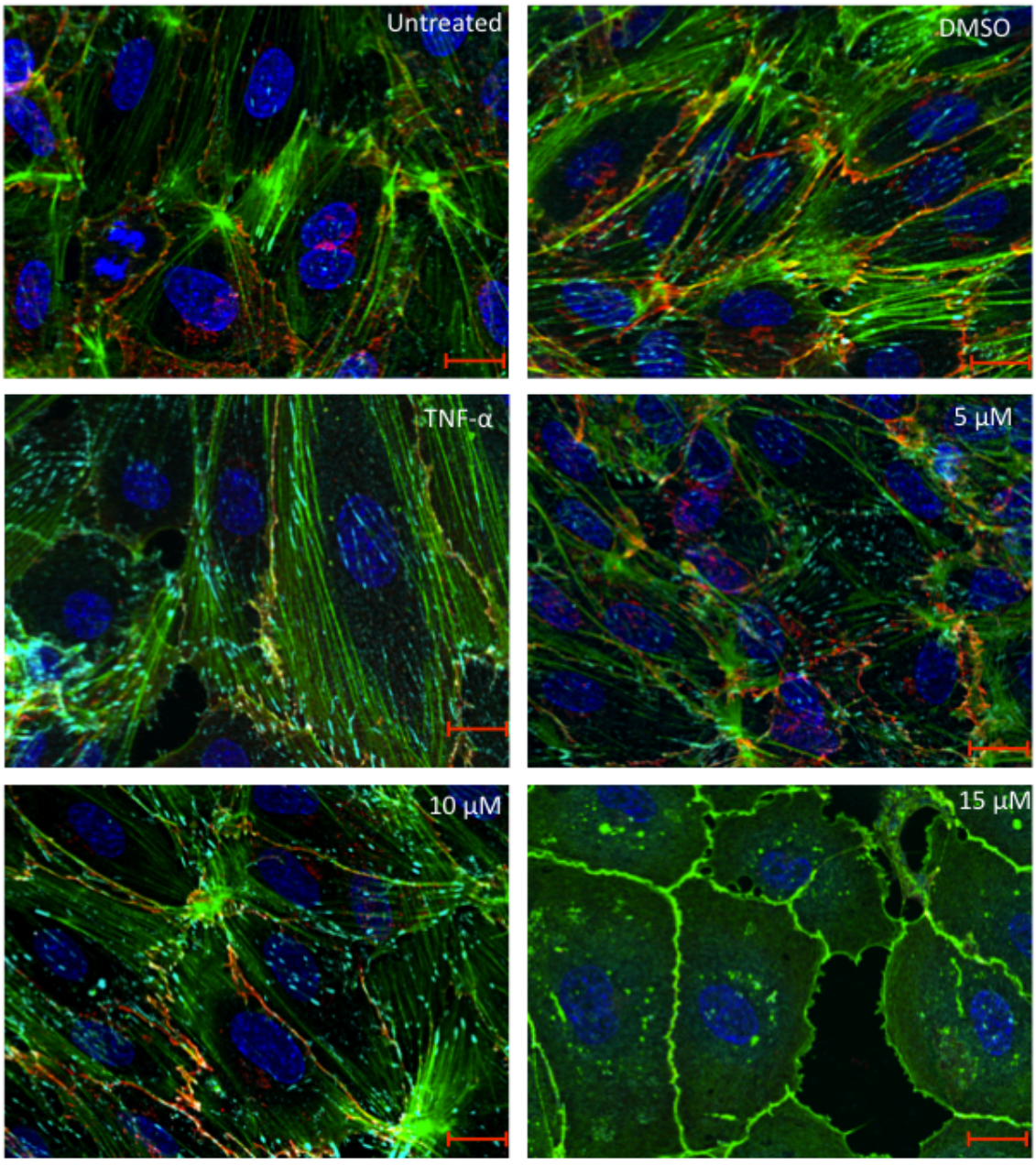
Untreated
DMSO
TNF-α
5 µM
10 µM
15 µM

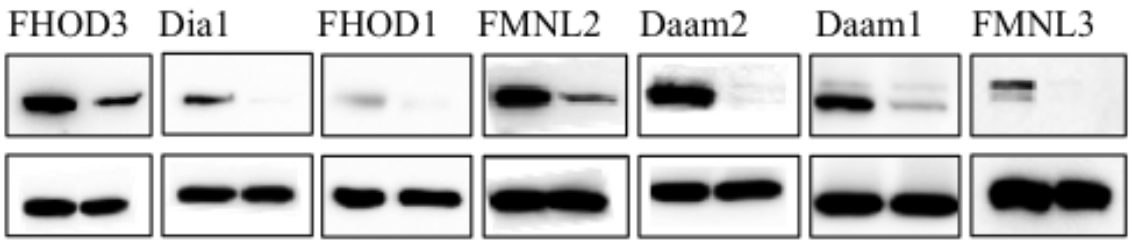

Fig. 3.3 Western blots of individual formin knockdowns. The knockdowns of FHOD3, Dia1, FHOD1, FMNL2, Daam2, Daam1 and FMNL3 are shown above from right to left. The first lane of each blot is scramble control and the second lane is the knockdown. The blots directly below each correspond to the tubulin in the knockdown cells.

3.3. Knockdown of Dia1, FHOD1, FHOD3 and FMNL2 affect vascular permeability

We repeated the *in vitro* vascular permeability assay for cells that were individually knocked down for 7 of the 8 formins expressed in TIME cells using siRNA (fig. 3.4). We didn't knock down Dia3 because it is involved in cell division and cells transfected with Dia3 siRNA fail to proliferate. Once the siRNA conditions were established, knockdown cells, along with the appropriate controls (scramble control and TNFα treated), were tested for change in permeability. Knockdown of FHOD1, FHOD3 and Dia1 significantly increased the permeability of the barrier ($p < 0.05$). Interestingly, the knockdown of the formin FMNL2 actually had a protective effect on barrier function ($p < 0.05$). Daam1, Daam2, and FMNL3 did not have a considerable effect on permeability. The permeability assay inserts were later stained to look at the condition of the monolayer of each of these knockdowns in order to ensure that the results were not due to cell death, detachment or a failure to divide (fig. 3.5).

In parallel with the *in vitro* vascular permeability assay, knockdown cells were also seeded onto collagen-coated coverslips and stained for VE-cadherin, actin, vinculin and the nucleus (fig. 3.6). Dia1, FMNL3, FHOD1, Daam1 and Daam2 depletion did not have any obvious phenotypic effects. However, FHOD3 and FMNL2 knockdown induced differences in both junction and cell morphology when compared to the scrambled control cells. FHOD3 knockdown cells appear elongated with more linear adherens junctions and fewer focal adherens junctions as characterized by the distribution of VE-cadherin as thin and linear at the cell periphery instead of zipper-like or patchy. Vinculin appears to coat the stress fibers throughout the FHOD3 knockdown cells instead of appearing at the ends of stress fibers. This suggests that FHOD3 knockdown may be

affecting focal adhesion turnover and altering the normal transition of vinculin between FAs and FAJs. FMNL2 knockdown cells appear similar in morphology to control cells. However, the junctions of these cells appear to have broad sheets of VE-cadherin, larger than those on control cells.

We picked FHOD3 as the formins of interest in this project as it had the most notable effect on permeability. We also further investigated FMNL2 because knocking it down actually protected endothelial permeability instead of compromising it. The previous results obtained from the *in vitro* vascular permeability assay were confirmed using a second set of siRNA duplexes to control against off-target effects ($p < 0.05$) (fig. 3.7). Cell staining showed that the effect these duplexes had on barrier function did not originate from cell death or detachment (fig. 3.8). Immunofluorescence was also repeated with the second set of duplexes in order to see if FHOD3 and FMNL2 knockdown showed the same phenotypic variation as the first set of duplexes. Once again, FHOD3 knockdown cells show linear VE-cadherin staining and an increase in focal adhesions while the VE-cadherin in FMNL2 knockdown cells appear as broad sheets (fig 3.9).

3.4 FHOD3 knockdown cells display phenotypic difference in staining of junctional proteins

We looked at localization of VE-cadherin, β-catenin, p120-catenin, vinculin, paxillin and FAK in FHOD3 and FMNL2 knockdown cells because each of those proteins are present at either focal adhesions, focal adherens junctions or mature adherens junctions (Huveneers *et al.* 2012). We also did western blots on lysates of FHOD3, FMNL2 and scramble knockdown cells to determine if there was a change in levels of

Fig. 3.4. FHOD1, FHOD3 and Dia1 knockdown increase vascular permeability while the knockdown of FMNL2 decreases vascular permeability. (a) Relative FITC-dextran concentration in the media of individual formin knockdowns using an *in vitro* vascular permeability assay. Scramble control cells are set to 1. (b) Bar graph depiction of the results obtained from the *in vitro* vascular permeability assay. Knockdowns of FHOD1, FHOD3 and Dia1 show a significant increase in vascular permeability while the knockdown of FMNL2 shows a decrease in vascular permeability. Scramble control cells, untreated and TNFα treated cells were used as control. Results are a mean of four experiments. Error bars are SEM. $P < 0.05$; two-tailed T-test.

(a)

Sample	Relative Permeability
Scramble	1
Cells	0.87
TNF-α	6.45
FHOD-1	1.93
FHOD-3	3.18
Dia1	2.79
FMNL2	0.58
FMNL3	1.35
Daam1	1.00
Daam2	0.88

(b)

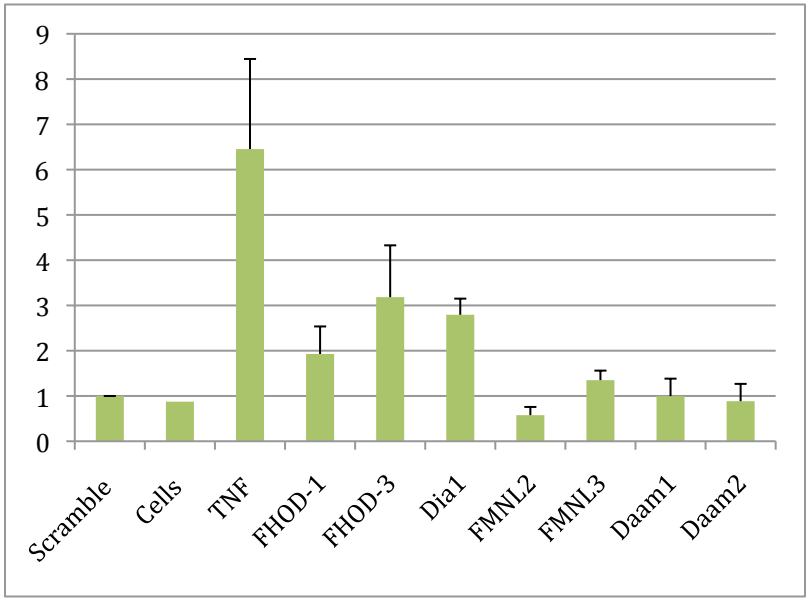

Fig. 3.5 Monolayer staining of knockdown cells confirms that results were not due to cell death. The inserts of the permeability assay were stained and then imaged under brightfield. The images are Scramble Control Cells, Untreated Cells, TNFα treated cells, Dia1, FHOD3, FHOD1, Daam1, FMNL3 and FMNL2 knockdown cells. The black regions are cells and the white regions are spaces. These images show that the permeability assay results are independent of cell death or detachment.

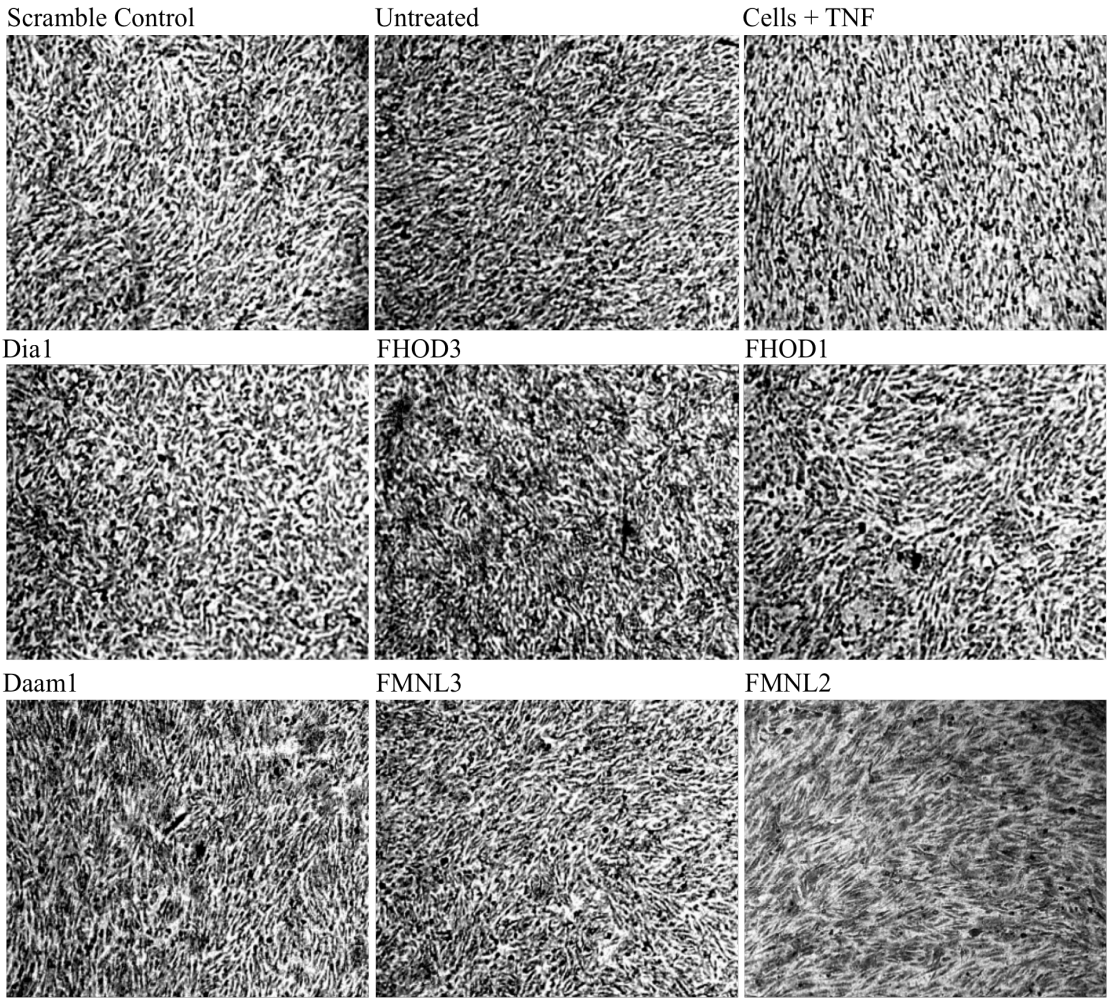
Scramble Control
Untreated
Cells + TNF
Dia1
FHOD3
FHOD1
Daam1
FMNL3
FMNL2

Fig. 3.6. Images of Dia1, FHOD1, FMNL3, Daam1 and Daam2 knockdown show no differences from scramble control cells while FHOD3 and FMNL2 knockdown cells show some phenotype variations. Knockdowns of these formins were performed on collagen-coated coverslips and stained for actin (green), VE-cadherin (red) and vinculin (cyan). Dia1, FMNL3, Daam1 and Daam2 knockdown cells did not have an obvious effect on the cells. However, FHOD3 and FMNL2 knockdown cells exhibited differences in junction formation. Scale bars are 10 μM.

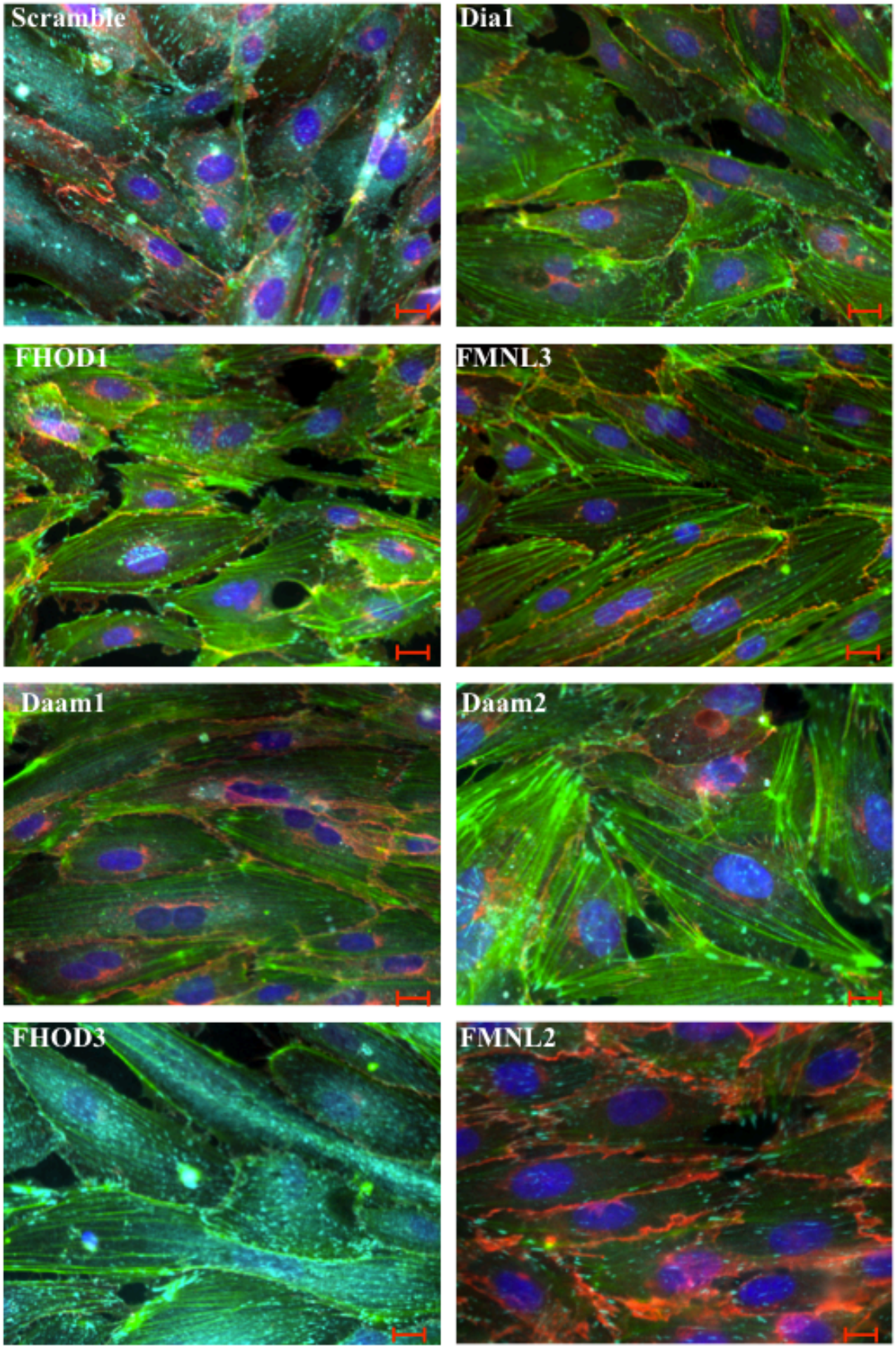
Scramble
Dia1
FHOD1
FMNL3
Daam1
Daam2
FHOD3
FMNL2

(a)

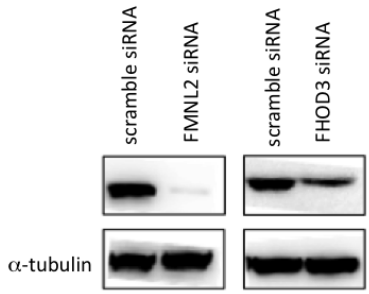

(b)

Sample	Average
Sc	1.00
TNFα	6.10
FMNL2 Duplex1	0.58
FMNL2 Duplex 2	0.56
FHOD3 Duplex 3	3.18
FHOD3 Duplex 5	3.27

(c)

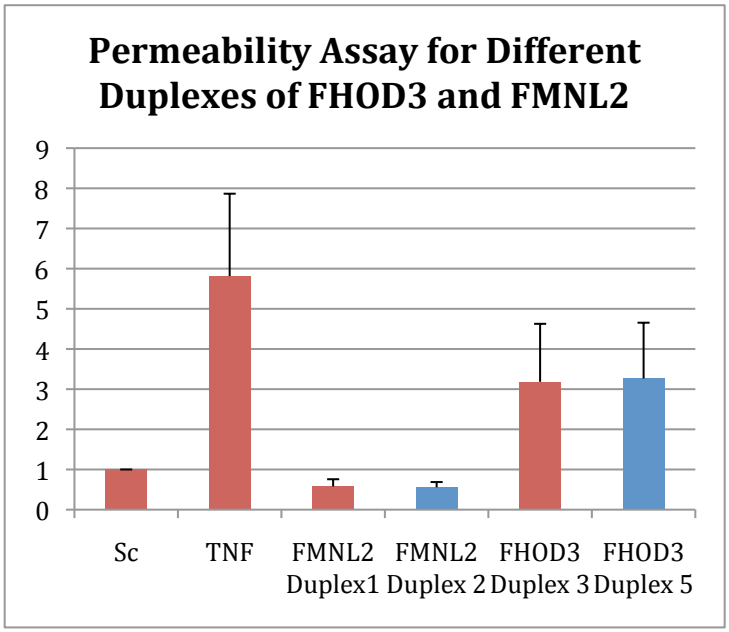

Fig. 3.7. Permeability assay results, using different duplexes, show an increase in permeability for FHOD3 knockdown cells and a decrease in permeability for FMNL2 knockdown cells. (a) Knockdown conditions set for second duplexes of FMNL2 and FHOD3. The first lane of each blot is scramble control and the second is the knockdown. The blot below each corresponds to the tubulin in the lysate above. (b) Relative FITC-dextran concentration in the media of formin knockdowns in an *in vitro* vascular permeability assay. Scramble control cells are set to 1. (c) Bar graph depiction of the results obtained from the assay done using different siRNA duplexes. Knockdowns of FHOD3 and FMNL2 using different duplexes show similar results to the knockdown of the original duplex. FMNL2 Duplex 1 and FHOD3 Duplex 3 refer to the original duplexes. FMNL2 Duplex 2 and FHOD3 Duplex 5 refer to the secondary duplexes. Scramble knockdown cells and TNFα treated cells were used as control. Results are a mean of three experiments. Error bars are SEM. $P < 0.05$; two-tailed T-test.

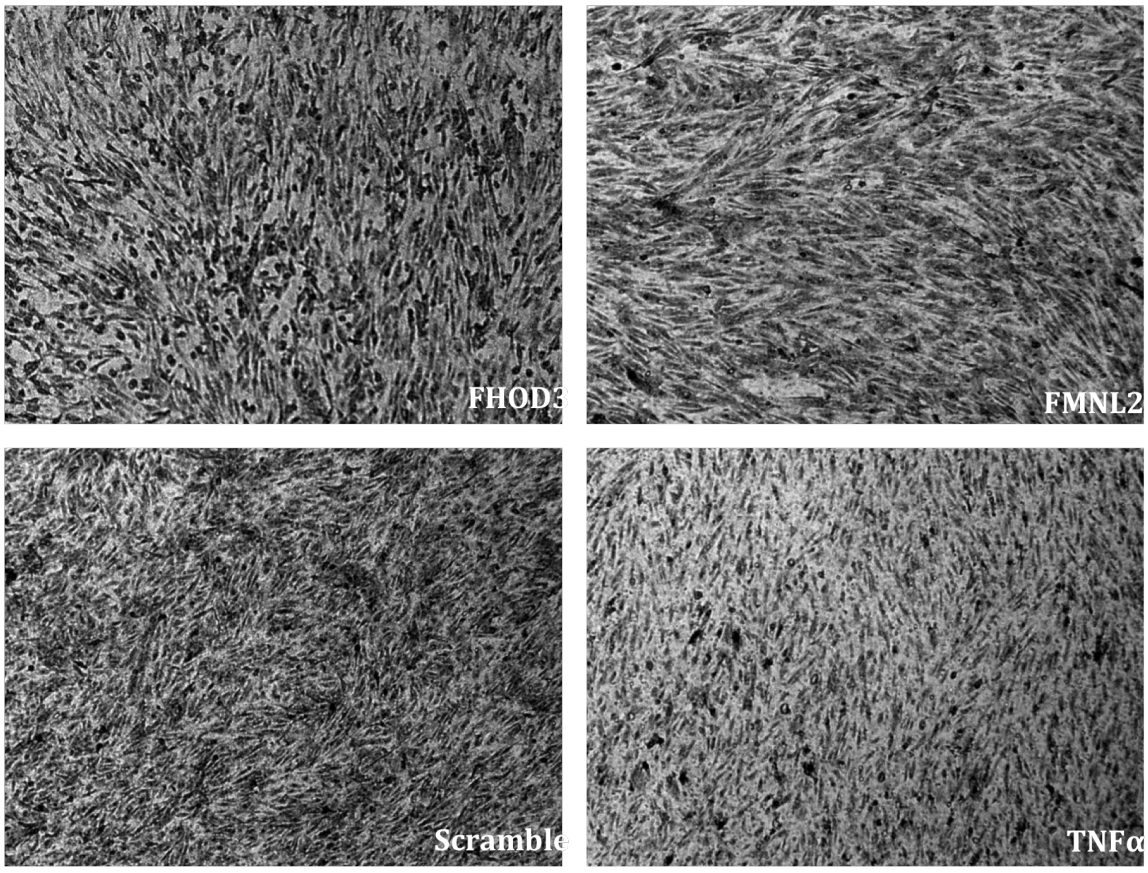

Fig. 3.8. Monolayer Staining of FHOD3 and FMNL2 knockdown cells show that change in permeability is not due to cell death. After the permeability assay was performed for the secondary duplexes of FHOD3 and FMNL2, the wells were stained and imaged under bright field. The black regions are cells and the white regions are spaces. These images show that the permeability assay results are independent of cell death or detachment.

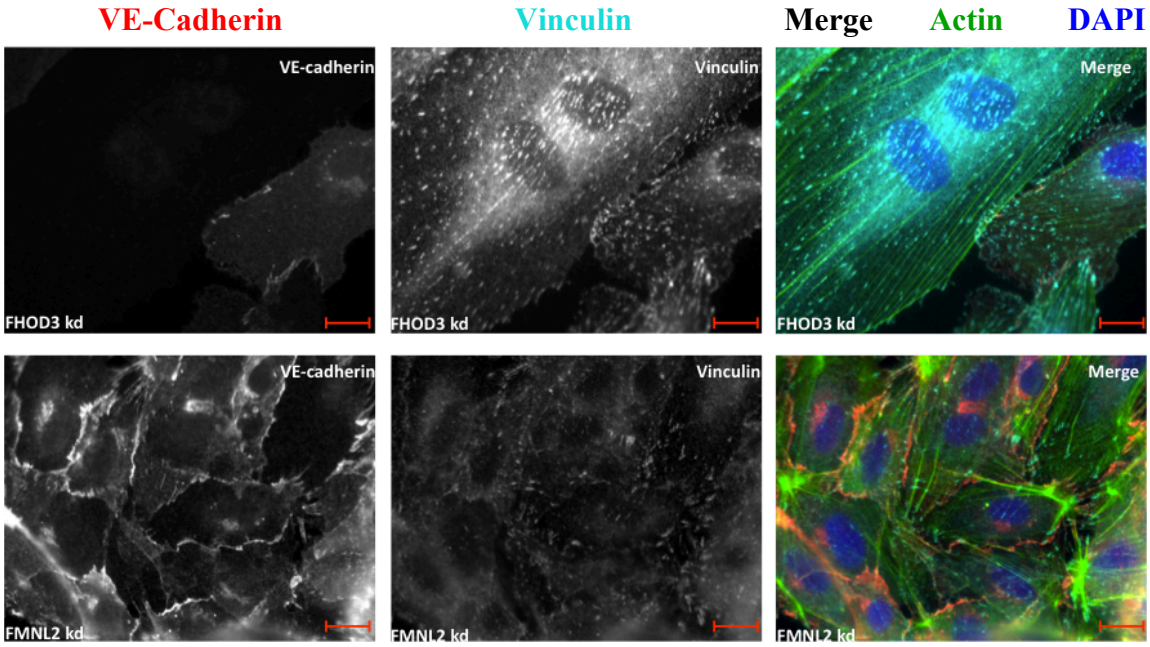

Fig. 3.9. Secondary duplexes of FHOD3 and FMNL2 siRNA show similar phenotype to the first. The staining was done for VE-cadherin (red), actin (green) and vinculin (cyan). The second duplex of FHOD3 also shows the irregular localization of vinculin and the depletion of VE-cadherin at the junctions. The second duplex of FMNL2 also shows that enlargement of VE-cadherin sheets. Scale bars at 10 μM.

proteins that were either directly involved in forming junctions or involved in recycling of junctional proteins. We were able to measure FHOD3 and FMNL2 knockdown protein levels and compare them to protein levels of scramble control cells.

VE-cadherin, β-catenin and p120-catenin appear less patchy and more linear in FHOD3 knockdown cells when compared to scramble and FMNL2 knockdown cells (fig. 3.10). The staining of vinculin and paxillin also appears different in FHOD3 knockdown cells. Instead of localizing to the ends of stress fibers, vinculin and paxillin appear along the stress fibers throughout the cell, leading to the idea that there may be an increase in focal adhesions (fig. 3.11) (Tan *et al.* 2010). In FMNL2 knockdown cells, VE-cadherin appears as large sheets instead of the zipper-like structure in control cells. In terms of protein levels, FHOD3 knockdown cells displayed a decrease in VE-cadherin expression by 80%, p120 catenin by 66%, TFR by 37%, Rab7 by 46% and Rab11a by 54% but no significant change in β-catenin, paxillin, FAK and vinculin levels. FMNL2 knockdown cells showed a decrease in TFR by 31% and an increase in Rab7 by 490% and Rab11a by 170% (fig. 3.12).

3.5. Differences in actin structures in FHOD3 and FMNL2 knockdown cells

Actin structures play a major role in maintaining vascular permeability (Prasain and Stevens, 2009). Thus, we wanted to determine if there was a change in actin structures in both FHOD3 and FMNL2 knockdown cells. First, we looked at F-actin by staining knockdown cells with phalloidin, a toxin that binds F-actin. FMNL2 knockdown cells showed a considerable increase in the formation of cortical actin and a decrease in stress fibers when compared to scramble control cells. FHOD3 knockdown cells show a

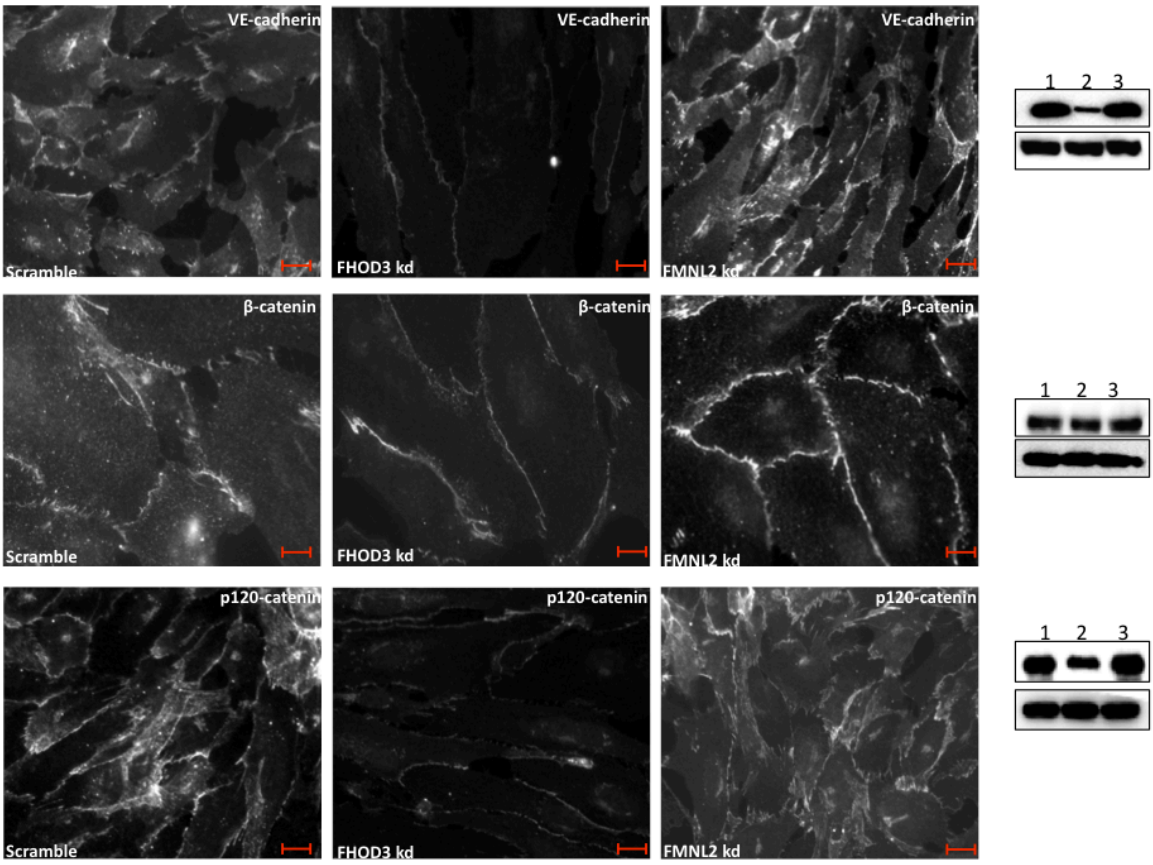

Fig. 3.10. FHOD3 and FMNL2 knockdown cells show differences in staining for junctional proteins. Cells were transfected with scramble, FHOD3 and FMNL2 siRNA, fixed with 4% PFA and stained for VE-cadherin, β-catenin and p120-catenin. VE-cadherin and p120-catenin in FHOD3 knockdown cells appear linear in structure as opposed to zipper-like formation that they exhibit in scramble control cells. Scale bars are 10 μM. The western blots beside the images correspond to the levels of the protein-of-interest in scramble control (1), FHOD3 knockdown (2) and FMNL2 knockdown cells (3). The blots directly below each correspond to the tubulin levels in the control and the knockdowns.

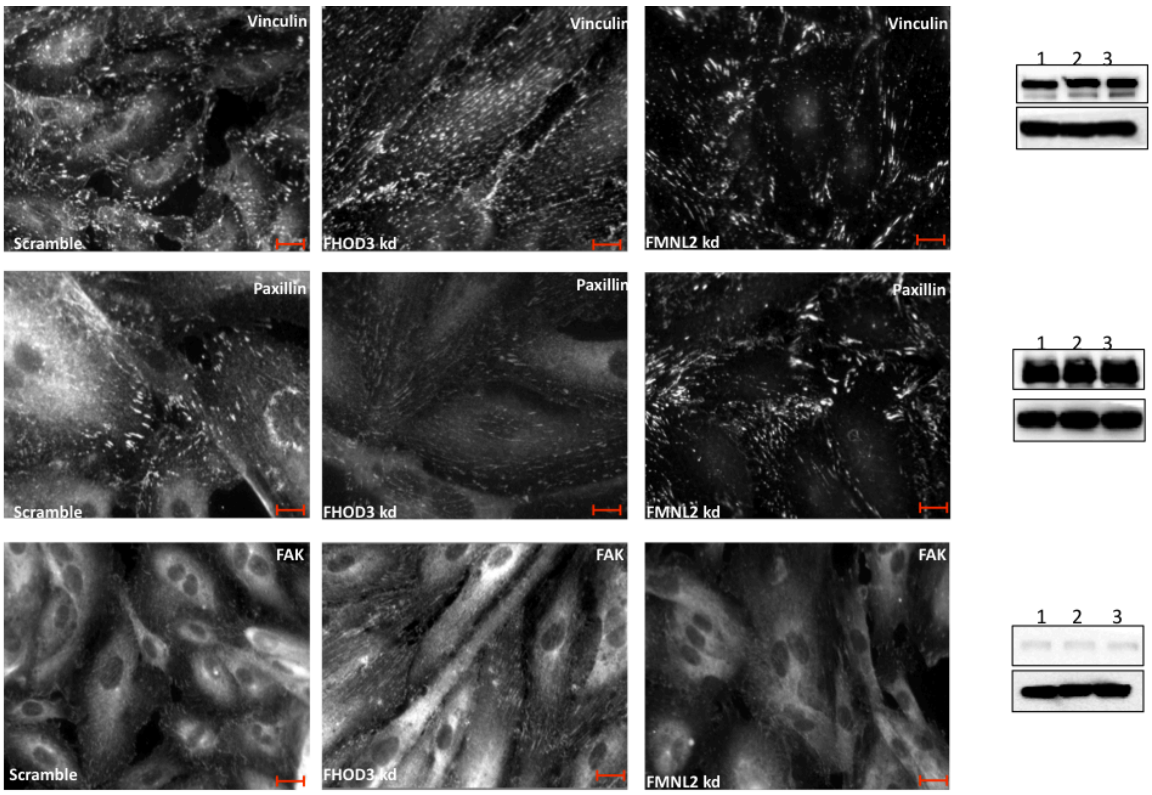

Fig. 3.11. FHOD3 and FMNL2 knockdown cells show some differences in vinculin, paxillin and FAK staining. Vinculin and paxillin in FHOD3 knockdown cells coat the stress fibers instead of appearing at the ends of stress fibers as they are in control cells. This suggests that there is an increase in the amount of focal adhesions in FHOD3 knockdown cells. There was no significant difference in FAK staining in FHOD3 knockdown or FMNL2 knockdown cells. Scale bars are 10 μM. The western blots beside the images correspond to the levels of the protein-of-interest in scramble control (1), FHOD3 knockdown (2) and FMNL2 knockdown cells (3). The blots directly below each correspond to the tubulin levels in the control and the knockdowns. There was no significant difference in level of protein in either of the knockdown cells.

Fig. 3.12. Western blots of various junctional proteins in FHOD3 and FMNL2 knockdown cells. (a) Western blots were done for vinculin, paxillin, α-actinin, transferrin receptor (TfR), p120-catenin, α-catenin, β-catenin, VE-cadherin, Rab7, Rab11a and FAK. The first lane of each blot is scramble control, the second lane is FHOD3 knockdown and the third lane is FMNL2 knockdown. The blots directly beside each correspond to the tubulin in the scramble and knockdown cells. (b) Protein levels were measured from western blots and then the proteins levels in knockdown cells were compared to levels in scramble control cells. VE-cadherin, TfR, p120-catenin, Rab7 and Rab11a were significantly downregulated in FHOD3 knockdown cells ($p < 0.05$). While none of the junctional proteins levels are affected in FMNL2 knockdown cells, there is a significant upregulation in Rab7 and Rab11a protein levels and a downregulation in TfR ($n=3$) ($p < 0.05$).

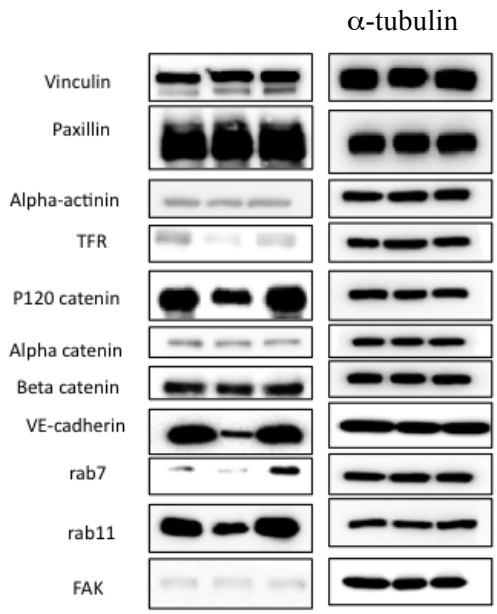
α-tubulin
Vinculin
Paxillin
Alpha-actinin
TFR
P120 catenin
Alpha catenin
Beta catenin
VE-cadherin
rab7
rab11
FAK

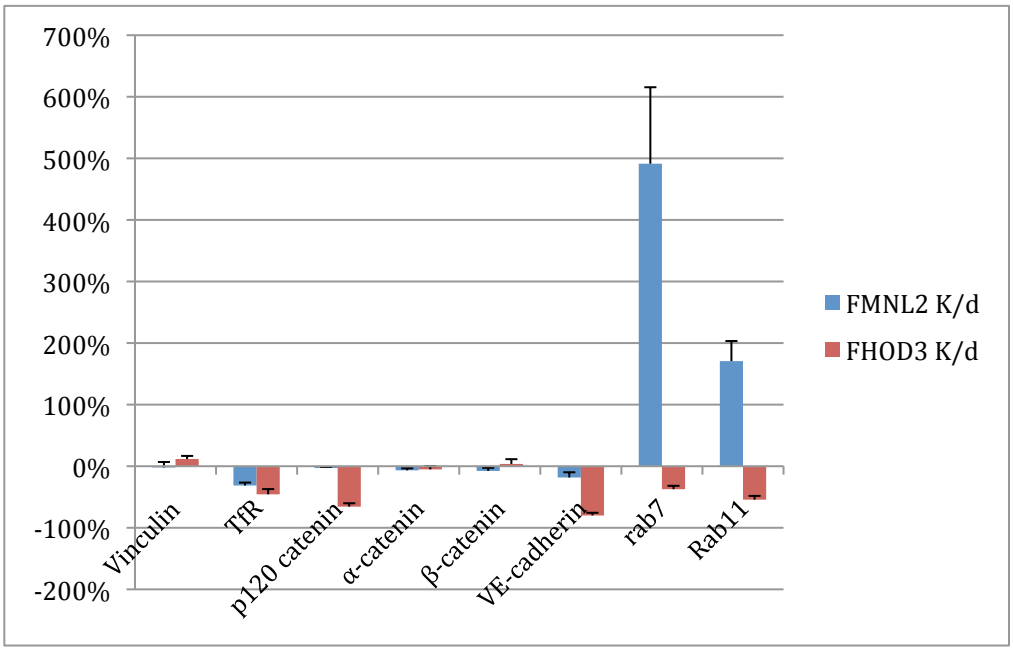
700%
600%
500%
400%
300%
200%
100%
0%
-100%
-200%
Vinculin
TFR
p120 catenin
α-catenin
β-catenin
VE-cadherin
rab7
Rab11
FMNL2 K/d
FHOD3 K/d

decrease in cortical actin and an increase in stress fiber formation when compared to scramble control cells. We also stained for α-actinin, which localizes to F-actin, and noticed similar results (fig. 3.13) (Dejana and Orsenigo 2013). After seeing the phenotypic difference in actin staining in the knockdown cells, we further investigated to see if microtubule structures were also disturbed. Therefore, we stained for acetylated microtubules and α-tubulin and found that, in FHOD3 knockdown cells, both of these structures appear more linear and bunched when compared to scramble cells (fig. 3.14). In order to make sure that the MTOC was intact in FHOD3 knockdown cells, we looked at γ-tubulin and pericentrin, which are present in the MTOC (Alieva *et al.* 2013). The staining of γ-tubulin and pericentrin appeared to be perinuclear in both scramble control and formin knockdowns, suggesting that the knockdowns don't have an effect on γ-tubulin localization, and by extension on the MTOC (fig. 3.15, fig. 3.16).

3.6. FHOD3 knockdown cells have altered morphology

The morphology of FHOD3 knockdown cells was noticeably altered, as they appeared thinner and longer when compared to scramble control cells. In order to determine if this was a significant effect, the program Northern Eclipse (Version 7.0, Empix Inc.) was used to measure the length, width and area of control, FHOD3 knockdown and FMNL2 knockdown cells. FHOD3 knockdown cells were significantly longer and had a larger cell area when compared to scramble control cells ($p < 0.05$). The width of FHOD3 knockdown cells, however, was not considerably different from that of the control cells. In addition, FMNL2 had a smaller width than the other cells as well as less cell area.

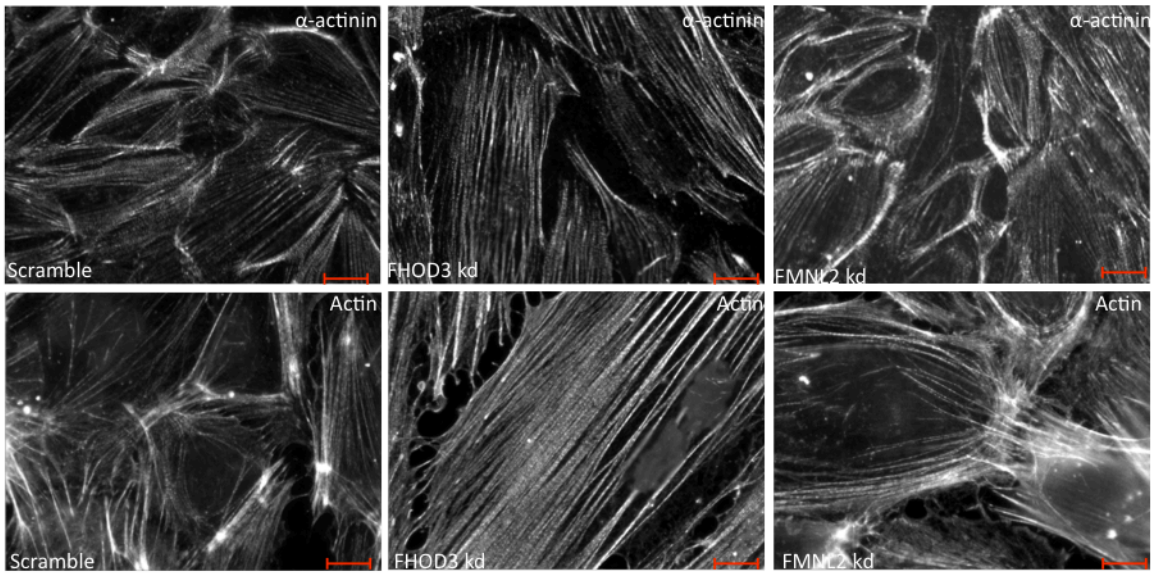

Fig. 3.13. α-actinin and phalloidin staining shows differences in actin structures of FHOD3 and FMNL2 knockdown cells. Scramble Control, FHOD3 and FMNL2 knockdown cells were fixed and stained for α-actinin and actin. The images were taken at 63x magnification to see the actin structures of these cells. FHOD3 knockdown cells, when compared to scramble knockdown cells, show an increase in stress fibers throughout the cells and depletion in cortical actin. FMNL2 knockdown cells show an increase in cortical actin structures when compared to scramble control cells. The actin staining mirrors the phenotype shown by the α-actinin staining. Scale bars are 10 μM.

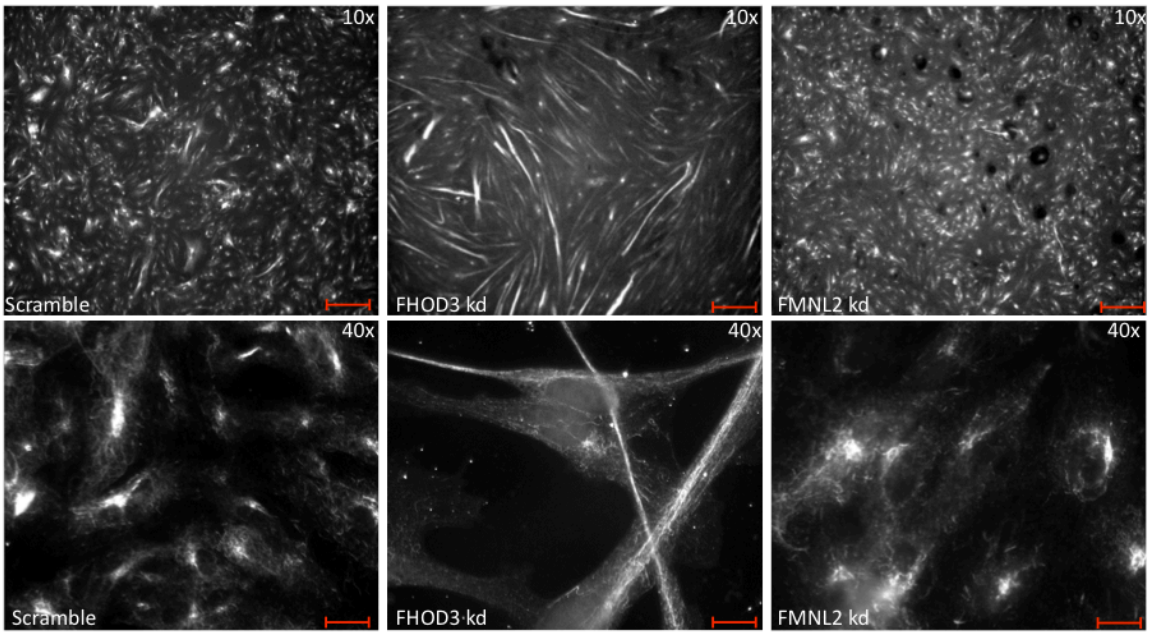

Fig. 3.14. FHOD3 knockdown cells show a change in morphology when stained with acetylated tubulin. Scramble control, FHOD3 and FMNL2 knockdown cells were fixed and stained for acetylated tubulin. The top images were taken at 10x magnification in order to show the change in morphology. FHOD3 knockdown cells showed a long, linear morphology when contrasted with scramble control cells. The bottom images are taken at 63x magnification in order to show the acetylated tubulin more clearly. This allows us to see that in FHOD3 knockdown cells, acetylated tubulin is stretched out and bunched. Scale bars are 10 μM.

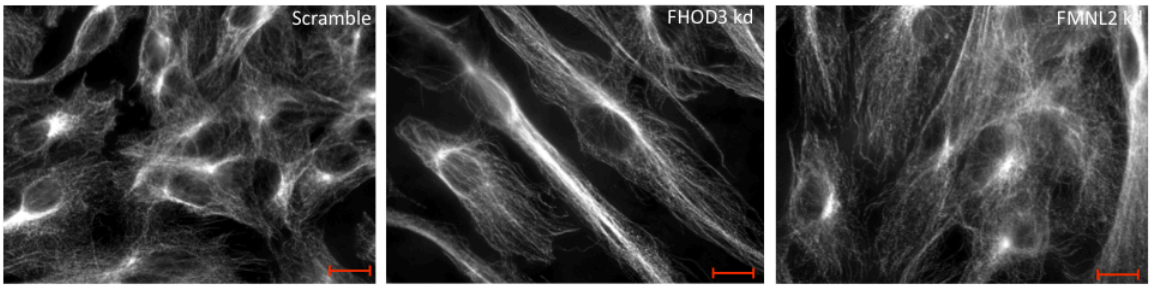

Fig. 3.15. α-tubulin structures show variation in FHOD3 knockdown cells. Scramble control, FHOD3 and FMNL2 knockdown cells were fixed and stained for α-tubulin. In FHOD3 knockdown cells, α-tubulin appears long and bunched when compared to scramble control cells. Scale bars are 10 μM.

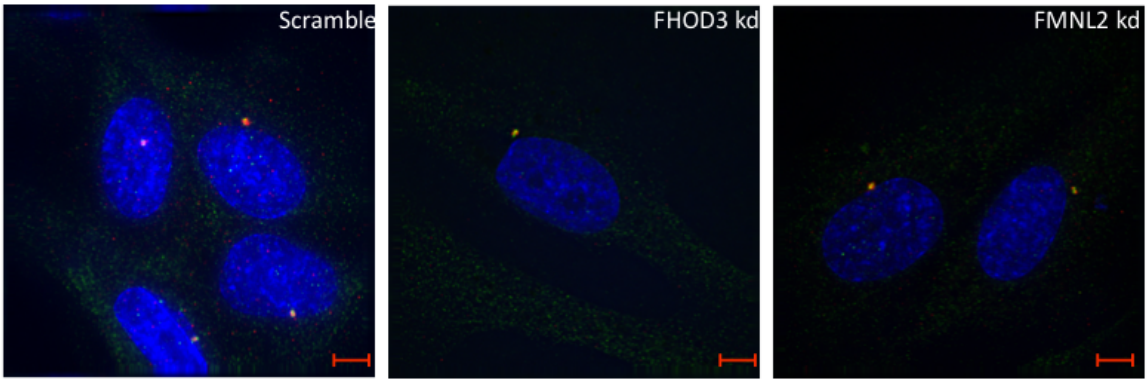

Fig. 3.16. γ-Tubulin and pericentrin structures remain intact in knockdown cells. Scramble control, FHOD3 and FMNL2 knockdown cells were fixed and stained for γ-tubulin in green and pericentrin in red. In scramble and knockdown cells, both γ-tubulin and pericentrin show perinuclear staining, suggesting that the MTOC is intact. Scale bars are 10 μM.

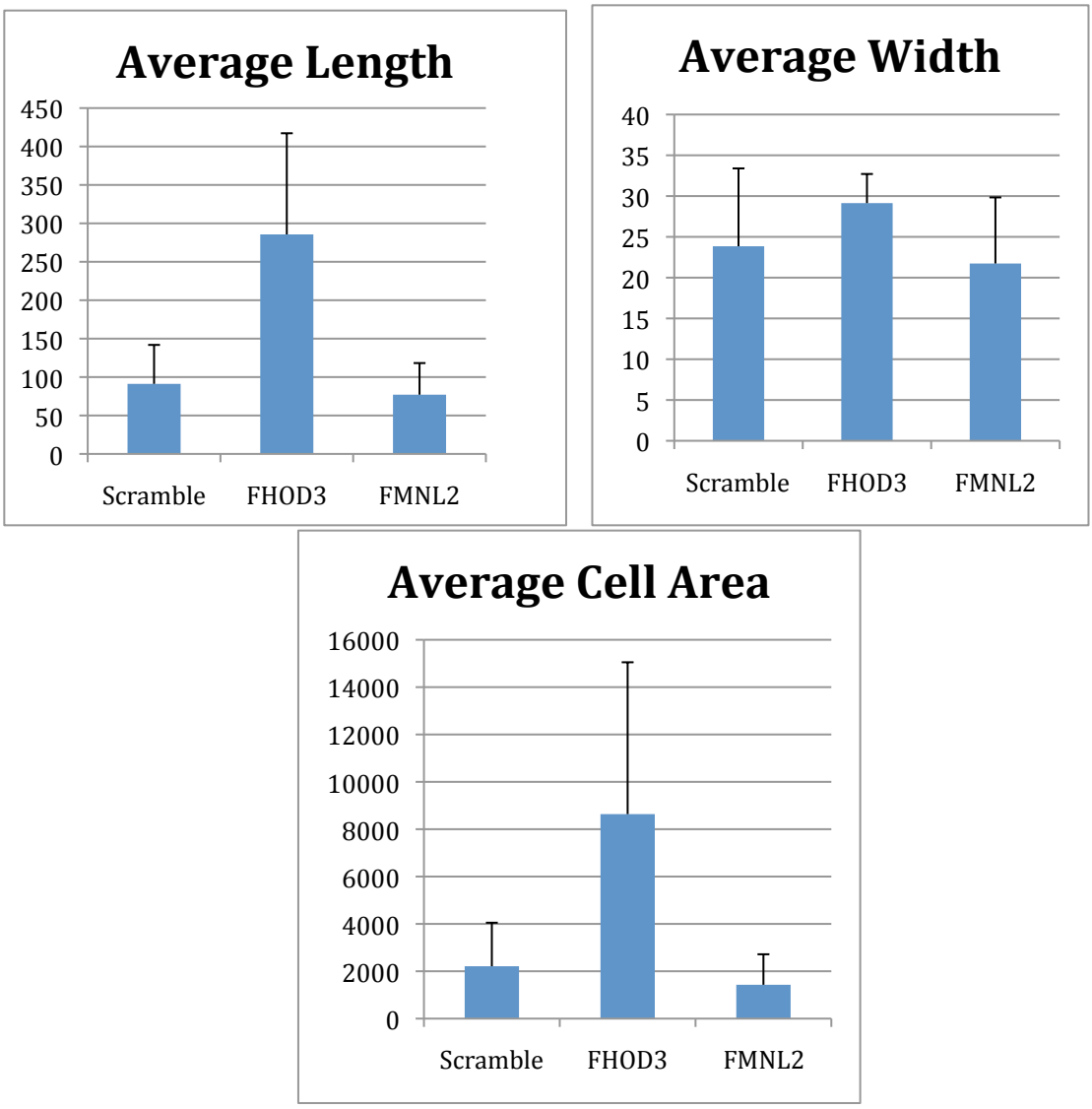

Fig. 3.17. The length, width and cell area of Scramble, FHOD3 and FMNL2 knockdown cells. Cells were transfected, fixed, stained for VE-cadherin and imaged. 100 images were acquired 3 times each on a Zeiss Axio Imager Z1 microscope. The measurements were taken using the Northern Eclipse software. FHOD3 knockdown cells had significantly higher length and more cell area when compared to both scramble control cells and FMNL2 knockdown cells ($p < 0.05$). Interestingly, the width of FHOD3 knockdown cells was not considerably different from that of the control cells. In addition, FMNL2 had a somewhat smaller width than the other cells as well as less cell area. N=3. $P < 0.05$; two-tailed T-test.

3.7. Apple-VE-Cadherin does not localize to cell junctions in FHOD3 knockdown cells

VE-cadherin was significantly depleted in FHOD3 knockdown cells and we wanted to determine if transfecting the plasmid Apple-VE-cadherin would restore VE-cadherin to junctions. TIME cells were dual-transfected with (1) Apple-VE-cadherin and FHOD3 siRNA and (2) Apple-VE-cadherin and scramble siRNA. Cells were fixed at 72 hours, stained for endogenous VE-cadherin and imaged under 63x. Over-expressed VE-cadherin did not localize to junctions in FHOD3 knockdown cells, while it did localize to junctions in scramble control cells. Instead, Apple-VE-cadherin appeared in a vesicular form, which was also recognized by the VE-cadherin antibody. This suggests that there is a defect in trafficking of VE-cadherin to the cell junctions.

A time course was conducted to see if VE-cadherin localized to junctions early on but was later taken off as the FHOD3 knockdown took hold in cells. The time course took place over 72 hours, with coverslips being fixed at 24, 48 and 72 hours post-transfection. The time course showed us that the Apple-VE-cadherin plasmid goes into scramble control cells and localizes to the junctions at each time point of 24, 48 and 72 hours. However, in FHOD3 knockdown cells, Apple-VE-cadherin localizes to cell junctions at 24h, but not at 48h and 72h. At the later times points, Apple-VE-cadherin disappears from the junctions and forms vesicle-type round structures (fig. 3.18).

3.8. VE-cadherin packages into Rab4, Rab5, Rab7 and Rab11a-positive vesicles

One of the reasons why VE-cadherin might not be localizing to junctions in FHOD3 knockdown cells could be due to issues with recycling. Since many Rab proteins have been implicated in E-cadherin recycling and there is significant homology between

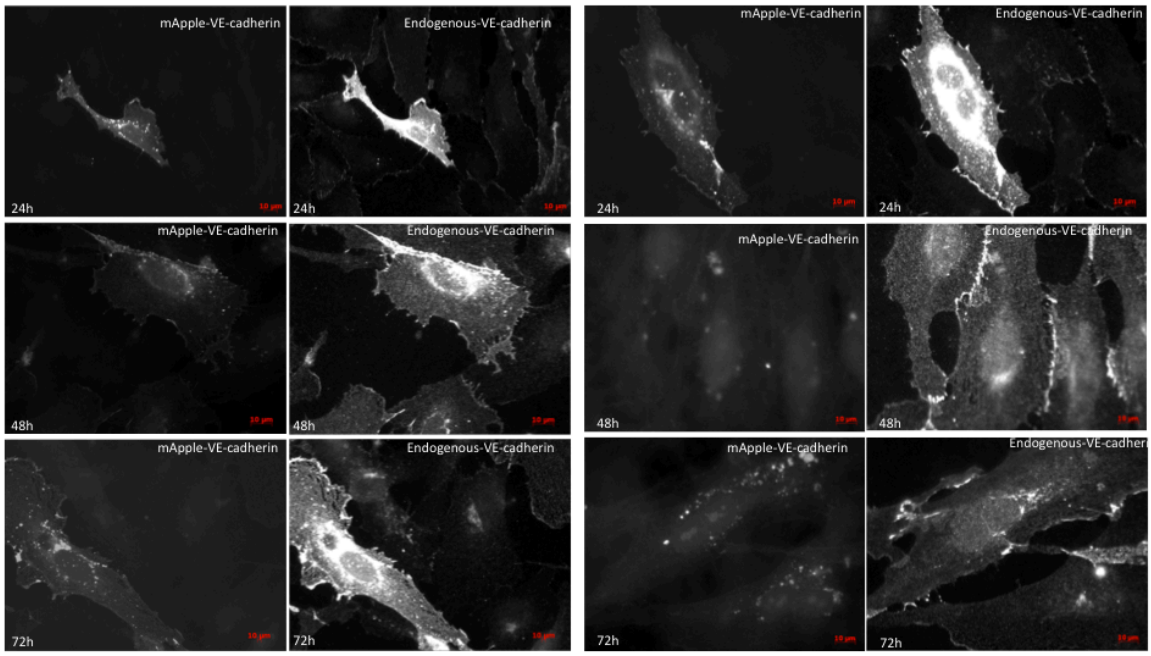

Fig. 3.18. Over-expressed VE-cadherin is removed from junctions at 48h and 72h in FHOD3 knockdown cells. Cells were transfected with either scramble control siRNA and mApple-VE-cadherin or FHOD3 siRNA and mApple-VE-cadherin and then fixed at 24, 48 and 72 hours. The fixed coverslips were stained for endogenous VE-cadherin and imaged under 63x. (a) Apple-VE-cadherin plasmid goes into scramble control cells and localizes to the junctions at each time point. (b) Apple-VE-cadherin plasmid goes into FHOD3 knockdown cells and localizes to cell junctions at 24h, but not at 48h and 72h. The Apple-VE-cadherin plasmid disappears from the junctions and forms vesicle-type round structures. Scale bars are 10 μM.

E-cadherin and VE-cadherin, it is more than likely that Rab-positive vesicles are also involved in VE-cadherin recycling (Lock and Stow 2005). We transfected in the plasmids YFP-Rab4, CFP-Rab5, YFP-Rab7 and YFP-Rab11a in TIME cells and stained for endogenous VE-cadherin. This would allow us to see which Rabs, if any, VE-cadherin was packaged in. We chose Rab4 and Rab11a since they are the recycling Rabs and we chose Rab7 because it is the Rab protein associated with degradation (Kowalczyk and Naines, 2012; Lock and Stow, 2005; Guichard *et al.* 2014). We established that VE-cadherin colocalized with all of the transfected Rabs (fig. 3.19).

Since, VE-cadherin is depleted in FHOD3 knockdown cells, the problem might originate from an inability to recycle VE-cadherin back to the membrane. In order to determine if this was the case, we transfected in FHOD3 siRNA with each of those Rabs. This would allow us to see if VE-cadherin staining showed increased or decreased association with any of the Rabs in FHOD3 knockdown cells. Cells were fixed after 72 hours and stained for VE-cadherin. Images were taken at 63x and optical sections were obtained using apotome structured illumination and processed with the colocalization plug-in for axiovision. Rab4 colocalized significantly less with VE-cadherin in FHOD3 knockdown cells than in scramble control cells ($p < 0.05$). The mean Pearson coefficient for Rab4/VE-cadherin was 0.17 in FHOD3 knockdown cells and was 0.32 in Scramble control cells (fig. 3.20). A Pearson coefficient of 1 indicates complete colocalization and a coefficient of 0 indicates no colocalization (Dunn *et al.* 2011). As Rab4 is one of the primary ways through which proteins are recycled back to the plasma membrane, a lower association with VE-cadherin would indicate that less VE-cadherin is recycled back. This may explain the appearance of VE-cadherin at junctions in FHOD3 knockdown cells as

Fig. 3.19. VE-cadherin is packaged into Rab4, Rab5, Rab7 and Rab11a-coated vesicles. Rab4, Rab5, Rab7 and Rab11a plasmids were transfected into TIME cells. The cells were stained for VE-cadherin and viewed under 63x. VE-cadherin was found to colocalize with Rab5, which indicates that it localizes to the early endosome. It is also packaged into Rab4 and Rab11a vesicles in order to be recycled back to the plasma membrane. Finally, it was also found to colocalize with Rab7 vesicles, most likely to be taken to lysosomes for destruction. Scale bars are 10 μM.

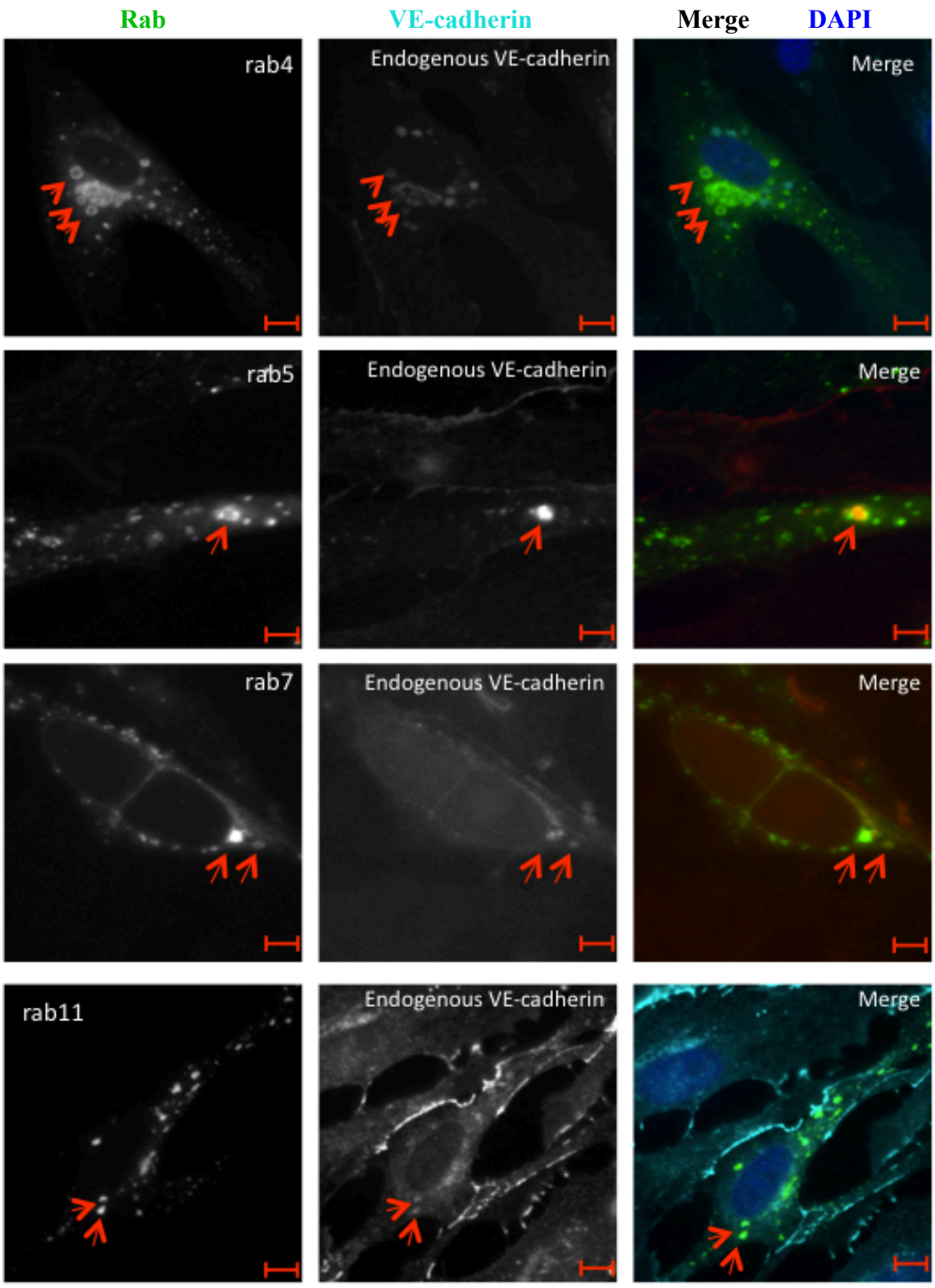
Rab
VE-cadherin
Merge
DAPI
rab4
Endogenous VE-cadherin
Merge
rab5
Endogenous VE-cadherin
Merge
rab7
Endogenous VE-cadherin
Merge
rab11
Endogenous VE-cadherin
Merge

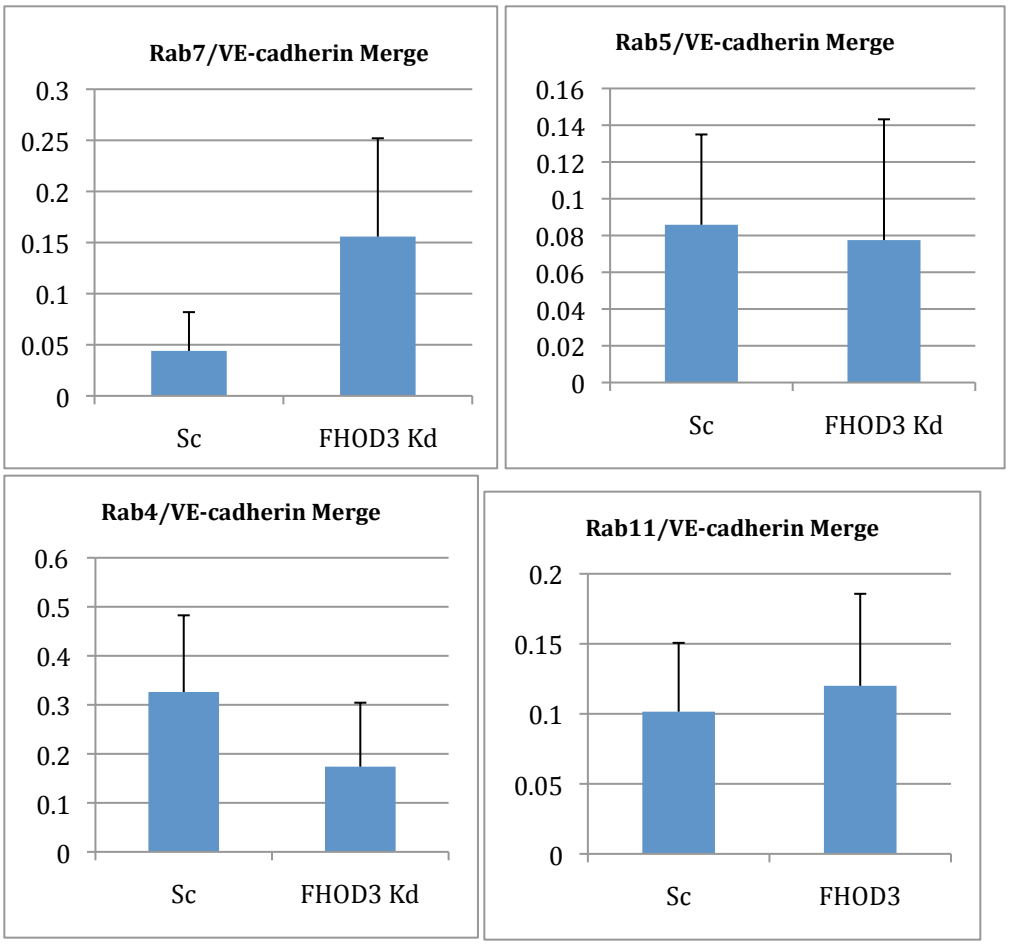

Fig. 3.20. Rab7 colocalizes more and Rab4 colocalizes less with VE-cadherin in FHOD3 knockdown cells. Cells were transfected with Rab4, Rab5, Rab7 and Rab11a as well as scramble siRNA and FHOD3 siRNA to determine a difference in colocalization. Colocalization was determined using the colocalization plug-in for Axiovision. Rab7 colocalizes more with VE-cadherin in FHOD3 knockdown cells and Rab4 colocalizes less with VE-cadherin in FHOD3 knockdown cells. This could indicate both a defect in recycling back to the plasma membrane as well as increase in degradation of VE-cadherin. N=3. Error bars are SEM. $P < 0.05$; two-tailed T-test.

thin junctions with less VE-cadherin as opposed to the larger, patchy junctions observed in control cells. A similar experiment was performed with the Rab11a plasmid, which is another recycling Rab protein. There were, however, no significant differences associated with Rab11a colocalization in FHOD3 knockdown cells. This indicates that not all recycling pathways for VE-cadherin are compromised in FHOD3 knockdown cells. Rab7 colocalized significantly more with VE-cadherin in FHOD3 knockdown cells than in scramble control cells ($p < 0.05$). The Pearson coefficient for Rab7/VE-cadherin was 0.15 in FHOD3 knockdown cells and 0.04 in scramble control cells. As Rab7 is associated with moving proteins in endosomes to the degradation compartment, this indicates that more VE-cadherin is being targeted for destruction and would explain the depletion in VE-cadherin at a protein level (Lock and Stow, 2005). As a control, the same experiment was performed for Rab5. There was no significant difference in association of VE-cadherin with Rab5 in FHOD3 knockdown cells compared to scramble control cells.

3.9. VE-cadherin localizes with LAMP-1 in FHOD3 knockdown cells

LAMP-1, lysosomal-associated membrane protein-1, is a protein associated with lysosomes, endosomes and the plasma membrane. It is mainly a lysosomal marker and works downstream of the Rab7 degradation pathway (Cella *et al.* 1996). A similar experiment as the one outlined above was performed with a LAMP-1 plasmid. TIME cells were seeded onto coverslips and then transfected with LAMP-1/FHOD3 siRNA and LAMP-1/Scramble siRNA using DharmaFECT Duo. Cells were fixed 72 hours later, stained for VE-cadherin and imaged with apotome using 63x (fig. 3.21). The colocalization software on Axiovision determined the Pearson coefficient of LAMP-1 colocalization with VE-cadherin in scramble and FHOD3 knockdown cells. The mean

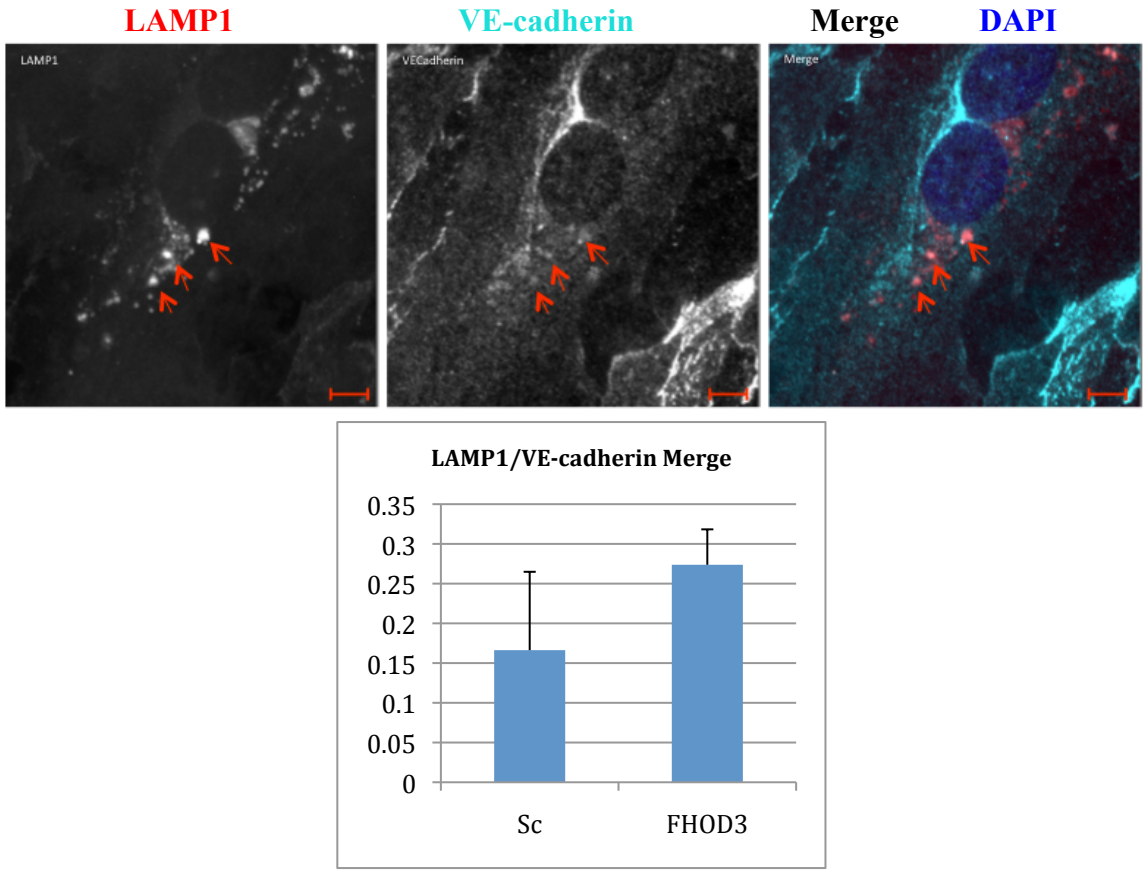

Fig. 3.21. LAMP-1 colocalization with endogenous VE-cadherin increases in FHOD3 knockdown cells. (a) Cells were transfected with LAMP-1, stained for VE-cadherin and imaged under 63x. Colocalization was observed in the images. (b) The degree of colocalization between LAMP1 and VE-cadherin was increased in FHOD3 knockdown cells when compared to scramble control cells. The Pearson coefficient was determined using the colocalization plug-in in Axiovision. N=3. Scale bars are 10 μM. $P < 0.05$; two-tailed T-test.

Pearson coefficient was 0.39 for FHOD3 knockdown and 0.21 for scramble knockdown cells ($p < 0.05$). This provides further evidence that VE-cadherin is targeted for destruction at a higher rate in FHOD3 knockdown cells than in scramble control cells.

3.10 A general recycling defect in FHOD3 knockdown cells?

We proposed that recycling may be being affected in FHOD3 knockdown cells and that is what led to the depletion of VE-cadherin at junctions and in the cell. In order to see if the phenomenon was VE-cadherin specific or applied to recycling in general, we performed a western blot to look at the levels of Transferrin Receptor (TfR) in scramble control and FHOD3 knockdown cells. Since TfR undergoes receptor-mediated endocytosis, a difference in levels of TfR could indicate a general recycling defect (Matsui and Fakuda, 2013). In FHOD3 knockdown cells, there was a decrease of 37% in levels of TfR when compared to levels in scramble control ($p < 0.05$) (fig. 3.22c). We also found that there was a decrease in Rab7 and Rab11a levels in FHOD3 knockdown cells. In order to see if there was a difference in localization, we stained cells that were FHOD3 knockdown and Rab-transfected with a TfR antibody (fig. 3.22a, fig. 3.22b). There was no significant difference in TfR colocalization with any of the Rabs in FHOD3 knockdown cells. While results indicate that general recycling/degradation pathways may be affected, the levels of VE-cadherin are down 80% in FHOD3 knockdown cells while TfR levels are only down 37%. This would indicate that even though general recycling may be disrupted, FHOD3 knockdown might affect specific VE-cadherin recycling pathways.

Fig. 3.22. Transferrin receptor is down 37% in FHOD3 knockdown cells. Cells were transfected with Rab4, Rab5, Rab7 and Rab11a and either scramble or FHOD3 siRNA. Cells were then stained with a transferrin receptor (TfR) antibody. (a) TfR colocalization in scramble control cells. (b) TfR colocalization with Rabs in FHOD3 knockdown cells. There is no significant difference in the colocalization of TfR with any of the Rabs between scramble control and FHOD3 knockdown cells. (c) There is a decrease in TfR levels in FHOD3 knockdown cells. Lane 1 corresponds to scramble control cells and lane 2 corresponds to FHOD3 knockdown cells. The volume of each band was computed using Image quant TL. Band volume is relative to tubulin. The reduction of TfR in FHOD3 knockdown cells indicates that there may be a general recycling defect. Scale bars are 10 μM. $P < 0.05$; two-tailed T-test.

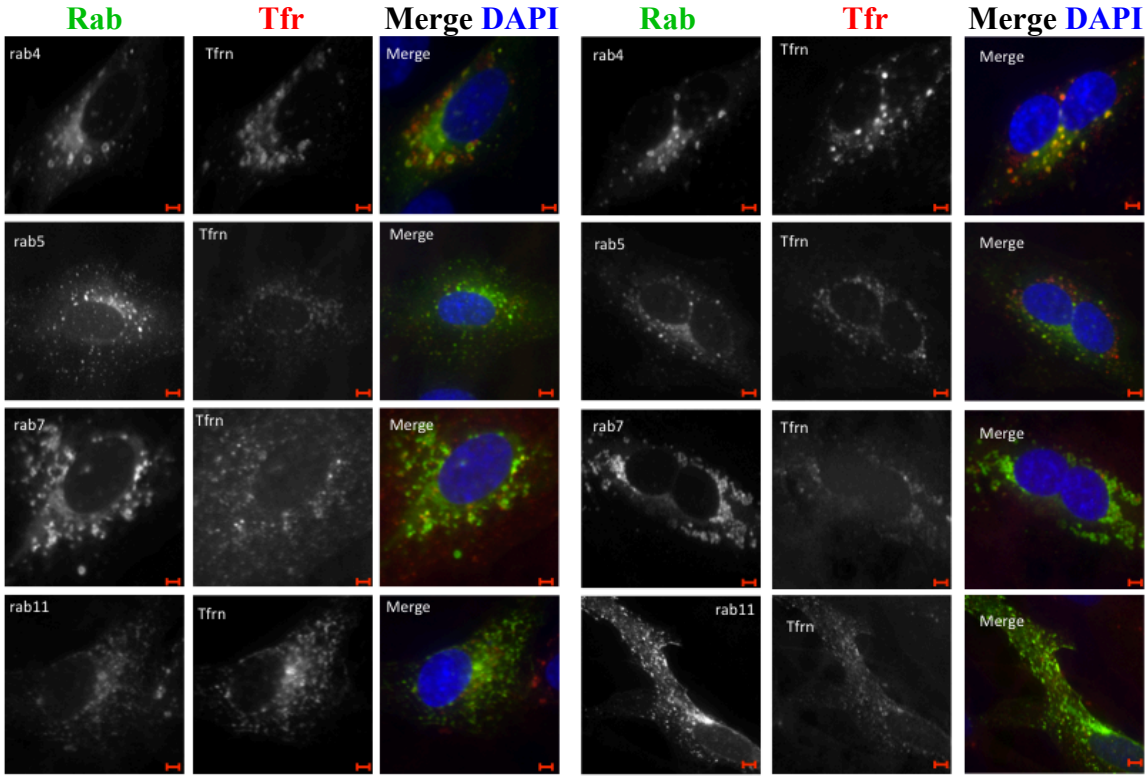
Rab
Tfr
Merge DAPI
Rab
Tfr
Merge DAPI
rab4
Tfrn
Merge
rab4
Tfrn
Merge
rab5
Tfrn
Merge
rab5
Tfrn
Merge
rab7
Tfrn
Merge
rab7
Tfrn
Merge
rab11
Tfrn
Merge
rab11
Tfrn
Merge

(c)

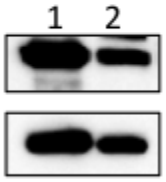
1
2

3.11 TIME cells express FHOD3 isoform 1

There are 16 FHOD3 isoforms listed in the Pubmed Gene database. To identify which FHOD3 isoform is present in TIME cells, we performed RT-PCR using TIME cell cDNA with primers specifically designed to amplify three fragments spanning the full length FHOD3 coding region. When amplified, these three fragments would be able to reconstruct the full-length cDNA. While we were able to amplify the 5' end and 3' end fragment, we were not able to obtain the middle fragment. We sequenced the fragments we were able to amplify (fig. 3.23). TIME FHOD3 mRNA, when translated, did not possess the TDEEEVE sequence in the 3' region that most of the other isoform did. Thus, through the 3' end sequence, we were able to narrow down the isoform choices to isoform 1, 2, 3 and X10. After multiple attempts, we were finally able to sequence the middle fragment, which possessed the protein sequence SRDYLDKREEQRQAREER. This allowed us to eliminate all other isoforms save for FHOD3 isoform 1.

MATLACRVQFLDDTDPFNSTNFPEPSRPPLFTFREDLALGTQLAGVHRLLQ
APHKLDDCTLQLSHNGAYLDLEATLAEQRDELEGFQDDAGRGKKHSIILRT
QLSVRVHACIEKLYNSSGRDLRRALFSLKQIFQDDKDLVHEFVVAEGLTCL
IKVGAEADQNYQNYILRALGQIMLYVDGMNGVINRNETIQWLYTLIGSKFR
LVVKTALKLLLVFVEYSESNAPLLIQAVTAVDTKRGVKPWSNIMEILEEKD
GVDTELLVYAMTLVNKTLSGLPDQDTFYDVVDCLEELGIAAVSQRHLNKKG
TDLDLVEQLNIYEVALRHEDGDETTEPPPSGCRDRRRASVCSSGGGEHRGL
DRRRSRRHSVQSIKSTLSAPTSPCSQSAPSFKPNQVRDLREKYSNFGNNSY
HSSRPSSGSSVPTTPTSSVSPPQEARLERSSPSGLLTSSFRQHQESLAAER
ERRRQEREERLQRIEREERNKFSRDYLDKREEQRQAREERYKYLEQLAAEE
HEKELRSRSVSRGRADLSLDLTSPAAPACLAPLSHSPSSSDSQEALTVSAS
SPGTPHHPQASAGDPEPESEAEPEAEAGAGQVADEAGQDIASAHEGAETEV
EQALEQEPEERASLSEKERQNEGVNERDNCSASSVSSSSSTLEREEKEDKL
SRDRTTGLWPAGVQDAGVNGQGDILTNKRFMLDMLYAHNRKSPDDEEKGDG
EAGRTQQEAEAVASLATRISTLQANSQTQDESVRRVDVGCLDNRGSVKAFA
EKFNSGDLGRGSISPDAEPNDKVPETAPVQPKTESDYIWDQLMANPRELRI
QDMDFTDLGEEDDIDVLDVDLGHREAPGPPPPPPPTFLGLPPPPPPPLLDS
IPPPPVPGNLLVPPPPVFNAPQGLGWSQVPRGQPTFTKKKKTIRLFWNEVR
PFDWPCKNNRRCREFLWSKLEPIKVDTSRLEHLFESKSKELSVSKKTAADG
KRQEIIVLDSKRSNAINIGLTVLPPPRTIKIAILNFDEYALNKEGIEKILT
MIPTDEEKQKIQEAQLANPEIPLGSAEQFLLTLSSISELSARLHLWAFKMD
YETTEKEVAEPLLDLKEGIDQLENNKTLGFILSTLLAIGNFLNGTNAKAFE
LSYLEKVPEVKDTVHKQSLLHHVCTMVVENFPDSSDLYSEIGAITRSAKVD
FDQLQDNLCQMERRCKASWDHLKAIAKHEMKPVLKQRMSEFLKDCAERIII
LKIVHRRIINRFHSFLLFMGHPPYAIREVNINKFCRIISEFALEYRTTRER
VLQQKQKRANHRERNKTRGKMITDSGKFSGSSPAPPSQPQGLSYAEDAAEH
ENMKAVLKTSSPSVEDATPALGVRTRSRASRGSTSSWTMGTDDSPNVTDDA
ADEIMDRIVKSATQVPSQRVVPRERKRSRANRKSLRRTLKSGLTPEEARAL
GLVGTSELQL

Fig. 3.23. Protein sequence of the FHOD3 isoform present in TIME cells. Through sequencing PCR fragments, we were able to narrow down the isoform present in TIME cells to isoform I. The protein sequence above corresponds to that of FHOD3 isoform I. The sequence is colour-coded to represent the conserved domains of FH1, FH2, GBD/FH3 and DAD. ⇔ FH2 domain ⇔ FH1 domain ⇔ DAD domain ⇔ GBD/FH3 domain. Source: De Castro, E *et al.* 2006.

Chapter 4

Discussion

4 Discussion

4.1 Formins play a role in adherens junction regulation

A number of studies suggest formins play an important role in regulating adherens junction formation in epithelial cells. We wished to extend these observations to see if formins play a role in maintaining endothelial permeability. One of the few papers published on the role of formins in endothelial cell adherens junctions regulation found that RhoA-activated Dia1 helps preserve junction stability by sequestering Src kinase, a known mediator of junction disassembly. This prevented endocytosis of VE-cadherin and thereby regulated endothelial permeability (Gavard *et al.* 2008). Recently, FMNL3 has been implicated in playing a role in maintaining endothelial cell junctions by helping maintain a constant and stable F-actin content in zebrafish embryos (Gauvin *et al.* 2015).

4.2 smiFH2 induces a dose-dependent increase in vascular permeability

We discovered that 15 μM smiFH2 increased vascular permeability without inducing cell death. 10 μM and 15 μM smiFH2 treatment actually caused a higher increase in permeability than TNFα. Considering that we treated our cells with TNFα for 24 hours and with smiFH2 for only 2 hours, these results suggest that inhibiting formins has a very strong effect on vascular permeability. However, there are some concerns over the validity of smiFH2 results at certain time lengths and concentrations. While smiFH2 has been used to determine formin function by many researchers, the effects induced by smiFH2 have been variable. In addition, the concentration and the duration of smiFH2 treatments are broadly ranged across various publications. Isogai *et al.* have found that smiFH2 induces cytotoxicity and a loss of p53 at high doses and at later time points. They recommend less than an hour of incubation and a concentration of less than 25 μM

in order to minimize confounding effects. While the highest concentration of smiFH2 we used was 15 μM, we treated our cells with smiFH2 for 2 hours. Thus, even though we tried to control against cytotoxicity by imaging our smiFH2-treated cells, the permeability assay results might still be due to the onset of cytotoxicity (Isogai *et al.* 2015). Due to some of the caveats presented by using smiFH2, knocking down individual formins was the best way to proceed in order to determine if formins are really involved in adherens junction regulation.

4.3 Seven formins are expressed in TIME cells

Using a variety of commercial and lab-made antibodies, we were able to detect the expression of Dia1, Dia3, Daam1, Daam2, FMNL2, FMNL3, FHOD1 and FHOD3. There are usually multiple formins present in most cell types, due to their crucial role in actin cytoskeleton remodeling, cell motility, cytokenesis and morphogensis (Dutta and Maiti, 2015). In endothelial cells, many of these formins have been implicated in a variety of other processes, such as focal adhesion formation, adherens junction regulation, cell polarity and cell shape (Prasain and Stevens, 2009; Goode and Eck, 2007). There is functional redundancy between members of the formin family, which could hamper some experiments such as siRNA-mediated formin knockdowns. Due to the redundancy, knocking down one formin might not present a phenotype as another formin continues to perform the same activity (Deward *et al.* 2010). Therefore, the presence of multiple formins indicates the importance of this family of proteins in endothelial cells. However, functional redundancy might present a limitation to individually knocking down each formin.

4.4 FMNL3, Daam1 and Daam2 don't significantly alter vascular permeability

Knockdown of Daam1 and Daam2 showed no difference in endothelial permeability. In FMNL3 knockdown cells, there was a slight increase in permeability, which may indicate a role for FMNL3 in adherens junction regulation, but the results were not significant. FMNL3 has been implicated in adherens junction stabilization by continuously polymerizing F-actin at the junctions. This was discovered by the introduction of FMNL3 siRNA and dominant-negative FMNL3 into zebrafish embryos (Gauvin *et al.* 2015). The differences between our results could be due to the change in species as prior results were found in zebrafish embryos while we conduct our experiments in human endothelial cells. In addition, it is possible that the results from this paper could not be real, but instead, an artifact of the experiment that was conducted. Kok *et al.* recently found that only a small portion of mutants that had been introduced into zebrafish lines resulted in phenotypic defects. Furthermore, the Sanger Zebrafish Mutation Project revealed that about 80% of morphant phenotypes were not observed in mutant embryos. Thus, the inconsistencies with the use of zebrafish embryos could explain the differences in the FMNL3 knockdown results (Kok *et al.* 2015; Kettleborough *et al.* 2013).

4.5 Knockdown of Dia1 shows an increase in permeability

Our results for the *in vitro* vascular permeability assay done on Dia1 knockdown cells show that Dia1 plays a role in maintaining endothelial permeability. These results confirm previously published results by Gavard *et al.*, who discovered that Dia1 inhibits VE-cadherin endocytosis by sequestering Src kinase in endothelial cells. This suggests

that our results from the permeability assay are valid and also poses an explanation for the mechanism behind the increase in permeability when Dia1 was knocked down (Gavard *et al.* 2008).

There have also been studies on the role of Dia1 in adherens junction regulation in epithelial cells. Short-hairpin RNA-mediated downregulation of Dia1 disrupted adherens junctions and displayed a dramatic decrease in E-cadherin localization to cell junctions. This phenotype was rescued by the expression of mouse Dia1. In addition, GFP-tagged Dia1 was found to localize to cell junctions, which was accompanied by an increase in the width of the adhesion zone as well as an increase in E-cadherin and β-catenin at the junctions (Carramusa *et al.* 2007). Dia1 has also been discovered to regulate E-cadherin localization and help form α-catenin-β-catenin complexes in epithelial cells through its ability to regulate the actin network at adherens junction sites (Sahai and Marshall 2002). Since epithelial cells reflect a similar role for Dia1 as endothelial cells, this lends confidence to not only our Dia1 knockdown results but to the vascular permeability results at large. The fact that our Dia1 knockdown results reflect extensive research done on the role of Dia1 shows that our system is working well.

4.6 FHOD1 knockdown causes an increase in permeability

Knockdown of FHOD1 also caused a significant increase in permeability. While there are no previous reports linking FHOD1 to adherens junctions, there is evidence that FHOD1 is recruited to focal adhesions, which results in actin assembly. Since FHOD1 aids in actin assembly at FAs, it could play a similar role at adherens junctions. Less actin assembly at the adherens junctions could lead to destabilization of AJs and cause an increase in permeability (Iskratsch *et al.* 2013). Furthermore, targeting of FHOD1 to the

integrin sites depends on a direct interaction with Src family kinases. Src kinases, as mentioned before, are sequestered by Dia1 to prevent VE-cadherin endocytosis. Since FHOD1 interacts with Src kinase, it could act similar to Dia1 and play a role in preventing VE-cadherin endocytosis (Gavard *et al.* 2008). This could explain the increase in vascular permeability when FHOD1 is knocked down. Finally, FHOD1 has been found to mediate thrombin-induced stress fiber formation in endothelial cells. Since vasoactive mediators such as thrombin participate in regulation of barrier function, depletion in FHOD1 would halt thrombin-induced stress fiber formation and interfere with proper regulation of barrier function. Unfortunately, imaging FHOD1 knockdown cells provided few clues, as there were no obvious phenotypic differences between FHOD1 knockdown cells and scramble control. There are many ways that FHOD1 could be involved in regulating permeability and further research needs to be done to discover its role in barrier function.

4.7 Knockdown of FMNL2 provides a protective effect on vascular permeability

FMNL2 knockdown actually decreased permeability in the vascular permeability assay. FMNL2 has mostly been reported as playing a major role in lamellipodia/filopodia formation. Only recently has it been linked to adherens junctions through Rac1, a small GTPase that is known to play a role in forming stress fibers (Guo *et al.* 2006). Rac1-induced actin assembly at adherens junctions is dependent on FMNL2, which mostly likely means that FMNL2 plays a role in stress fiber formation (Grikscheit *et al.* 2015; Kühn *et al.* 2015). Thus, a knockdown of FMNL2 would decrease stress fiber formation. We confirmed this result by looking at actin structures in FMNL2 knockdown cells and noticed that there was a definite decrease in stress fibers and an increase in cortical actin.

This could explain our FMNL2 knockdown permeability assay results as increases in stress fibers leads to an increase in permeability while a decrease in stress fibers, and a subsequent increase in cortical actin, leads to a decrease in permeability (Prasain and Stevens, 2009).

There were some phenotypic difference between FMNL2 knockdown cells and scramble control cells. The localization of junctional proteins was normal, though the width of the adhesion zone was visually larger than that of scramble control cells. FMNL2 has been shown to interact with E-cadherin and β-catenin at the junctions in epithelial cells (Grikscheit *et al.* 2015). If FMNL2 plays a role in localization of these proteins, a depletion of FMNL2 could cause VE-cadherin to not localize correctly at the cell-cell border, leading to greater plaques or sheets of VE-cadherin at junctions. A wider plaque of VE-cadherin would increase the strength of the junction and therefore lead to lower permeability.

Another feature of the FMNL2 knockdown phenotype is that the cells were smaller than scramble control cells. This could be explained by the decrease in stress fibers and the increase in cortical actin, which causes the cells to become more tightly bound and form a cobblestone network. Acetylated tubulin, α-tubulin, γ-tubulin and pericentrin staining was normal for FMNL2 knockdown cells, leading to the conclusion that it was most likely the disruption in stress fiber formation that led to an increase in cortical actin formation and thus, a decrease in permeability.

Griksheit *et al.* have recently discovered that FMNL2 localizes to cell junctions and forms AJs through a Rac1 dependent pathway in epithelial cells. These findings are contradictory to our results, which may be attributed to the differences in cell lines as

these results were discovered in breast epithelial cells. The FMNL2 isoform present in TIME cells may be different than the FMNL2 isoform present in breast epithelial cells. Since different isoforms of the same protein can have different functions, as exemplified by the fact that only isoform IV of Fmn1 localizes to cell junctions, differences in isoforms of FMNL2 could explain the contradictory results (Grikscheit *et al.* 2015; Dettenhoffer *et al.* 2008). In addition, the conflicting results could be due to the differences between epithelial and endothelial adherens junctions. The organization of endothelial AJs is more variable and their topology is less restricted than epithelial AJs. Thus, while superficially, endothelial and epithelial AJs may be seen as similar, they are structures that are both mechanistically and phenotypically different (Wallez and Huber, 2008).

4.8 Rab7 and Rab11a protein levels are significantly increased in FMNL2 knockdown cells

Immunoblotting showed that FMNL2 knockdown cells have a considerable increase in the levels of the recycling proteins Rab7 and Rab11a. Rab7 was up almost 500% and Rab11a was up 160%. FMNL2 may be involved in adherens junction formation by regulating recycling. Through its interactions with actin filaments, VE-cadherin and β-catenin, FMNL2 may keep levels of recycling at a basal level. Once FMNL2 is gone through the action of siRNAs, recycling proteins may not have the same signal from FMNL2 to stay at a certain level and they may go into overdrive. This could explain the increase in Rab levels. VE-cadherin levels stay similar to scramble control cells because while there is an increase in recycling and degradation, it is most likely that just as much is being degraded as is being sent back to the membrane. The increase in

recycling and degradation near the membrane could explain the large sheets of VE-cadherin formed in FMNL2 knockdown cells.

Since Rab7 is a degradation Rab and Rab11a is a recycling Rab, the fact that Rab7 levels are higher than Rab11a in FMNL2 knockdown cells may lead us to believe that there may be more of an increase in degradation than recycling. However, we know from our colocalization experiments that Rab4 recycles VE-cadherin at a higher rate than Rab11a. The Pearson coefficient for Rab4/VE-cadherin in control cells was 0.3, meaning that 30% of the time, Rab4 colocalizes with VE-cadherin while the Pearson coefficient for Rab11a/VE-cadherin was only 0.1. Since we never looked at Rab4 protein levels in FMNL2 knockdown cells, we don't know whether there is more of an increase in degradation or recycling. If FMNL2 is a VE-cadherin recycling regulator, a knockdown of FMNL2 could result in increased Rab expression, large sheets of VE-cadherin and a decrease in permeability (Dunn *et al.* 2011; Lock and Stow 2005).

4.9 Knockdown of FHOD3 increased permeability and presented phenotypic defects

The knockdown of FHOD3 caused the highest increase in permeability among the seven formins we knocked down in TIME cells. In preliminary results done by our lab in HUVECs, similar results were achieved with FHOD3 knockdown cells (appendix 1). However, FHOD3 has never been implicated in regulating adherens junctions. Besides its function as an actin nucleator, FHOD3 is mostly recognized as a sarcomeric protein that plays a role in myofibrillogenesis (Arimura *et al.* 2003).

FHOD3 knockdown cells appeared very different from scramble control cells. Instead of the normal, zipper-like junctions that are presented in scramble control cells, FHOD3 knockdown cells display very thin junctions. We also noticed that there was a

substantial decrease in cortical actin and an increase in stress fibers. Since cortical actin serves to tether adhesion complexes, such as adherens junction, to cellular organelles, a decrease in cortical actin could lead to insufficient tethering of AJs (Prasain and Stevens, 2009). This could lead to destabilization of AJ components and the formation of thin cell junctions. Vinculin also showed completely different localization in FHOD3 knockdown cells as it appeared all over the cell, coating the length of the stress fibers. This could be explained by one of two things: either the vinculin is not being resolved from stress fibers and unable to form FAJs or there is an increase in focal adhesions in order to deal with the loss of neighbouring cells due to an increase in permeability.

The protein quantities of junction proteins are also different in FHOD3 knockdown cells. Through conducting western blots, we were able to figure out that VE-cadherin levels are actually down 80% in FHOD3 knockdown cells. This shows that VE-cadherin is not just being mislocalized but either being degraded once its made, or affected on a transcriptional level.

FHOD3 knockdown cells are also different from scramble control cells in another major capacity: cell size and length. By measuring cells, we were able to discern that FHOD3 knockdown cells are three times longer and four times larger in cell area than scramble control cells. One explanation could be that FHOD3 plays a role in pathways that govern cell growth. Once FHOD3 is depleted, the cell growth pathways may not get the signal to stop and continue expanding. This could explain the increase in cell length and area in FHOD3 knockdown cells.

4.10 Exogenous VE-cadherin does not localize to junctions at 48h

VE-cadherin levels in FHOD3 knockdown cells were down by 80%. Recycling is a major part of regulating and maintaining adherens junctions. Since VE-cadherin was depleted at the junctions in FHOD3 knockdown cells, we wanted to determine if the phenotype could be rescued by expressing exogenous VE-cadherin in the form of Apple-VE-cadherin. A time course yielded the result that at 24 hours, Apple-VE-cadherin does localize to junctions in FHOD3 knockdown cells, but by 48 and 72 hours, it is no longer present at junctions but instead appears as circular, vesicular-type structures. These structures were not just artifact as the VE-cadherin antibody also recognized these structures. However, this effect is somewhat strange because there was still some endogenous VE-cadherin at the junctions. Perhaps as the siRNA effect takes hold, VE-cadherin comes off the junctions, but because exogenous VE-cadherin is not as stable as endogenous, it might be the first one to come off the membrane. If FHOD3 plays a role in recycling, it would make sense that as FHOD3 is knocked down, VE-cadherin gets degraded.

4.11 FHOD3 may play a role in the recycling of VE-cadherin

In order to find out if FHOD3 plays a role in VE-cadherin recycling, we first needed to map out the route through which VE-cadherin recycles. We determined that VE-cadherin associates with Rab4, Rab5, Rab7 and Rab11a in TIME cells. In order to respond to external stimuli, adherens junctions are constantly being remodeled. VE-cadherin is recycled from and back to the membrane continuously, which is why it needs many pathways through which it can be recycled and/or degraded (Li *et al.* 2008).

We found that there was both a decrease in colocalization between Rab4 and VE-cadherin and an increase between Rab7 and VE-cadherin in FHOD3 knockdown cells. A

decrease in Rab4/VE-cadherin colocalization indicates that less VE-cadherin is going back to the membrane through the slow-recycling pathway. An increase in Rab7/VE-cadherin colocalization indicates a higher than normal degradation of VE-cadherin (Palacios *et al.* 2005; Li *et al.* 2008). In addition, LAMP-1/VE-cadherin colocalization was also increased in FHOD3 knockdown cells, further lending confidence to the theory that FHOD3 may be involved in recycling. FHOD3 could be working at the early endosome, which determines whether a protein is being recycled back to the plasma membrane or being sent to the multivesicular body to be degraded with the help of Rab7.

FHOD3 may play a role in directing recycled VE-cadherin back to the plasma membrane by packaging it into Rab4-coated vesicles at the early endosome (Guichard *et al.* 2014) (fig. 4.1). A protein involved in recycling can be acting through three different mechanisms. It can help the recycled protein bud off from a membrane, it can escort the recycled protein through the cytoplasm or it can help the recycled protein fuse with the target membrane (Lodish *et al.* 2000). In FHOD3 knockdown cells, VE-cadherin may no longer be able to bud off from the early endosome, be escorted through the cytoplasm or be able to fuse with the plasma membrane. This explains the decreased localization of VE-cadherin to junctions in FHOD3 knockdown cells. While Rab4-mediated recycling is compromised in FHOD3 knockdown cells, Rab11a-mediated recycling remains intact. Since VE-cadherin is no longer being recycled back to the plasma membrane at the same level, it is being packaged into Rab7-coated vesicles for degradation. This could explain why there is both an increase in VE-cadherin degradation and a decrease in VE-cadherin recycling. In addition, increased degradation of VE-cadherin can explain the depletion of VE-cadherin at a protein level, as determined by quantitative analysis of western blots.

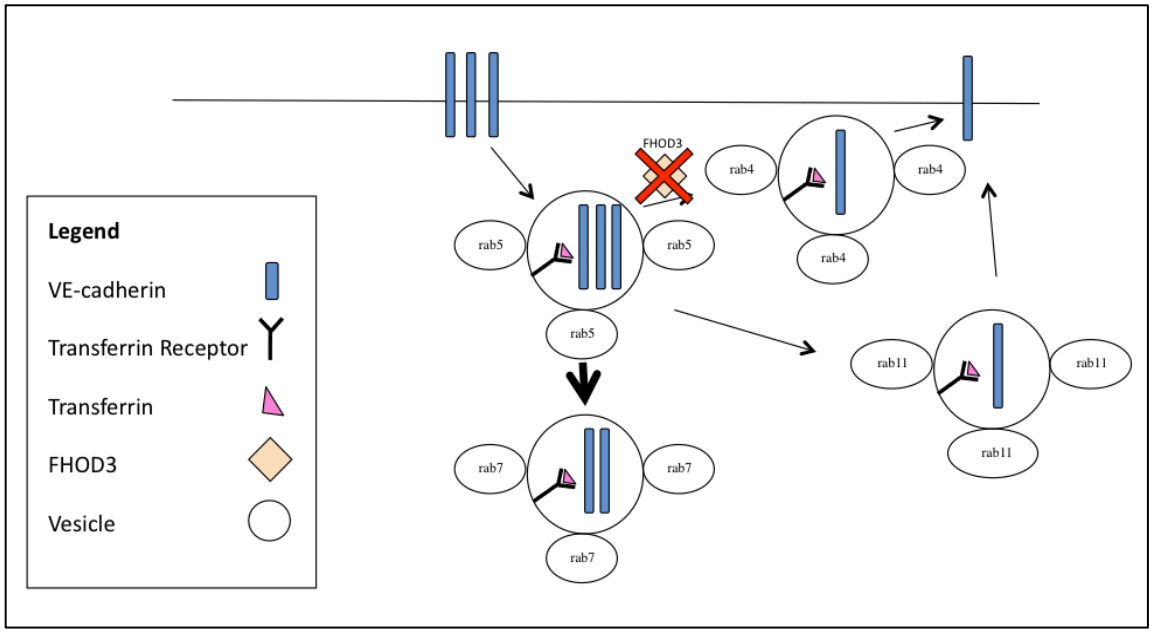

Fig. 4.1 FHOD3 may play a role in VE-cadherin recycling. FHOD3 may recycle VE-cadherin by aiding the Rab4-mediated fast recycling pathway. When FHOD3 is inhibited, Rab4 is not able to carry out VE-cadherin recycling at the same level and therefore, VE-cadherin is packaged into Rab7-coated vesicles and sent for degradation. VE-cadherin still continues to be recycled back to the plasma membrane through the Rab11-mediated slow recycling pathway.

Finally, Dia1 is involved in VE-cadherin recycling in endothelial cells and since there is some functional redundancy in formin family members, it is a possibility that FHOD3 is similarly involved in VE-cadherin recycling (Nanes *et al.* 2012).

4.12 FHOD3 may affect both general recycling and VE-cadherin-specific pathways

Since there is increased degradation of VE-cadherin in FHOD3 knockdown cells, we looked at transferrin receptor (TfR) recycling to see if this effect was VE-cadherin specific or a general recycling defect. In FHOD3 and scramble knockdown cells, we looked at TfR localization with Rab4, Rab5, Rab7 and Rab11a. We noticed that there was no significant difference between recycling of TfR with any of the Rabs. However, immunoblotting with a TfR antibody showed that TfR levels were down in FHOD3 knockdown cells by 37%. This result points to the fact that there may be a general recycling defect. TfR, like VE-cadherin, gathers at early endosomes and from there, is either recycled back to the membrane or taken to the lysosome. Since we see a decrease in both TfR and VE-cadherin, it is likely that FHOD3 acts at the early endosome to recycle these proteins back to the plasma membrane. However, due to the higher depletion of VE-cadherin, FHOD3 may also affect a pathway that is dedicated to VE-cadherin recycling or degradation. (Le *et al.* 1999; Nanes *et al.* 2014).

4.13 Future Directions

The work presented in this thesis shows that formins, particularly FHOD3 and FMNL2, are required for regulating vascular permeability. Since we discovered that isoform I is the FHOD3 isoform present in TIME cells, we would like to extend this research and express a tagged-version of isoform I to determine its localization. A GFP or a mCherry tagged version of isoform I would allow us to see the localization of FHOD3

in TIME cells. We can also perform recycling assays to measure the rates at which VE-cadherin and TfR are recycled in FHOD3 knockdown cells.

In addition to determining localization, we also want to use biotinylation as a way of detecting which proteins FHOD3 interacts with. We would like to express the construct BirA-FHOD3 in TIME cells and probe it with streptavidin. Next, we would like to perform mass spectrometry to determine which proteins FHOD3 interacts with. Once we discover the results of mass spectrometry, we can perform Co-Immunoprecipitation to confirm FHOD3 interactions with proteins involved in junction maintenance. This would help us understand how FHOD3 helps maintain endothelial permeability (Roux *et al.* 2012).

Since most of the research in this thesis was based on the role of FHOD3, the next step would be to look closer at the role of FMNL2 in the regulation of adherens junctions. First, we will have to determine which isoform of FMNL2 is expressed in TIME cells. Next, we want to express a tagged-version of FMNL2 to see where it localizes to in TIME cells. Based on those results, we will pursue further research to determine the role of FMNL2 in endothelial permeability.

Ultimately, the goal of these studies is to help ameliorate the condition of atherosclerosis by making the endothelial barrier stronger. An isoform specific FMNL2 inhibitor could achieve such a goal by decreasing endothelial permeability.

4.14 Conclusion

In this work, we identified four formins, FHOD1, FHOD3, Dia1 and FMNL2 that play a role in maintaining endothelial permeability. We discovered that FHOD1, FHOD3 and Dia1 play a protective role in maintaining vascular permeability while FMNL2

disrupts vascular permeability. We discerned that FHOD3 knockdown cells lose VE-cadherin and these cells show a distinct phenotype of thin, linear junctions as opposed to the zipper-like, patchy junctions in control cells. Our data suggests that FHOD3 may play a role in adherens junction maintenance by regulating VE-cadherin recycling and/or degradation. FMNL2, on the other hand, may play a role in regulating vascular permeability by inducing stress fiber formation, which leads to an increase in permeability. These findings may help provide a basis for further research into the roles of formins in maintaining endothelial vascular permeability.

Appendix 1

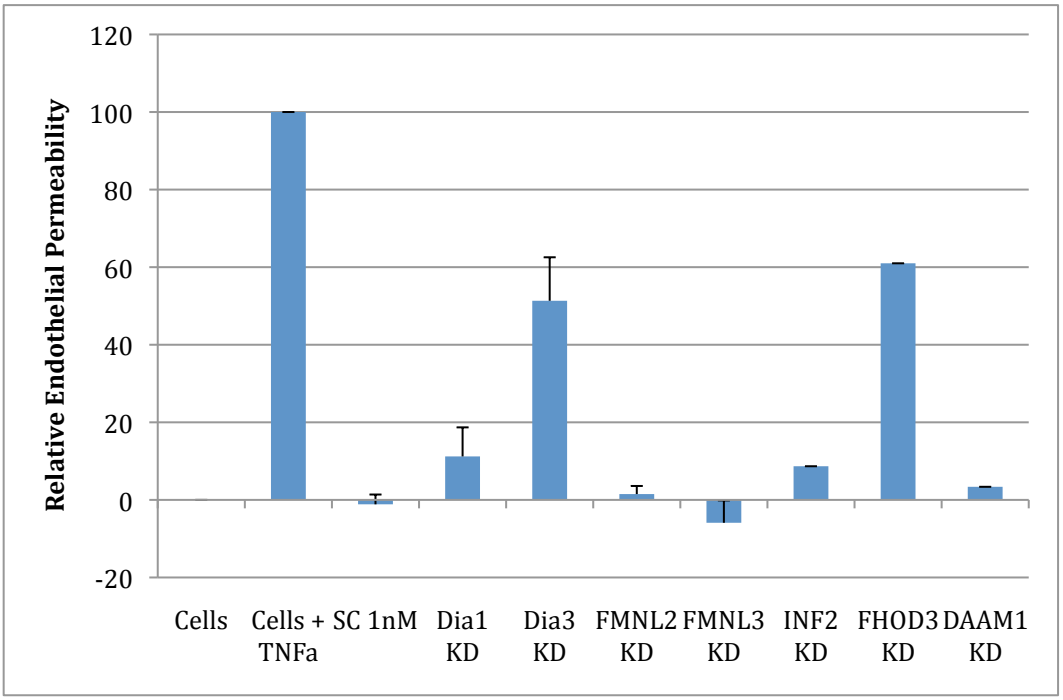

Fig. 5.1 Barrier formation in HUVECs requires Dia3. (A) HUVECs were transfected with siRNAs against FMNL2, FMNL3, Dia1, or Dia3 and plated on collagen-coated transwells. The permeability assay measures the passage of fluorescent dextran across a porous substrate; this passage is blocked when endothelial cells plated on this substrate form a confluent monolayer. Cells treated with 100ng/mL TNFα for 20h serve as a negative control for barrier function; untreated cells serve as a positive control. Results are the mean of three experiments. Error bars are SEM. **(B)** Representative western blots confirming knockdown. Lanes 1, 4, 7, 10 were untransfected cells; lanes 2, 5, 8, 11 were cells transfected with a scrambled control; and lanes 3, 6, 9, 12 were transfected with siRNA duplexes specific to Dia1, FMNL2, Dia3, and FMNL3, respectively.

References

Alieva, Irina B., *et al.* "Microtubules growth rate alteration in human endothelial cells." *BioMed Research International* 2010 (2010).

Alieva IB, *et al.* The Leading Role of Microtubules in Endothelial Barrier Dysfunction: Disassembly of Peripheral Microtubules Leaves Behind the Cytoskeletal Reorganization. *Journal of cellular biochemistry*. 2013;114(10):2258-2272.

Arimura, Takuro, *et al.* "Dilated cardiomyopathy-associated FHOD3 variant impairs the ability to induce activation of transcription factor serum response factor." *Circulation Journal* 77.12 (2013): 2990-2996.

Bechtold, Meike, *et al.* "FHOD proteins in actin dynamics—a formin'class of its own." *Small GTPases* 5.2 (2014): 1-6.

Block, Jennifer, *et al.* "FMNL2 drives actin-based protrusion and migration downstream of Cdc42." *Current Biology* 22.11 (2012): 1005-1012.

Bogatcheva, Natalia V., and Alexander D. Verin. "The role of cytoskeleton in the regulation of vascular endothelial barrier function." *Microvascular research* 76.3 (2008): 202-207.

Birukova, Anna A., *et al.* "Protein kinase A attenuates endothelial cell barrier dysfunction induced by microtubule disassembly." *American Journal of Physiology-Lung Cellular and Molecular Physiology* 287.1 (2004): L86-L93.

Carramusa L, *et al.* Mammalian diaphanous-related formin Dia1 controls the organization of E-cadherin-mediated cell-cell junctions. J Cell Sci. 2007;120:3870–3882

Cella, Nathalie, *et al.* "The lysosomal‐associated membrane protein LAMP‐1 is a novel differentiation marker for HC11 mouse mammary epithelial cells."*Differentiation* 61.2 (1996): 113-120.

Chiasson, Christine M., *et al.* "p120-catenin inhibits VE-cadherin internalization through a Rho-independent mechanism." *Molecular biology of the cell* 20.7 (2009): 1970-1980.

De Castro, Edouard, *et al*. "ScanProsite: detection of PROSITE signature matches and ProRule-associated functional and structural residues in proteins."*Nucleic acids research* 34.suppl 2 (2006): W362-W365.

Dejana, Elisabetta, and Fabrizio Orsenigo. "Endothelial adherens junctions at a glance." Journal of cell science 126 (2013): 2545-2549.

Dettenhofer, Markus, *et al.* "Formin 1-isoform IV deficient cells exhibit defects in cell spreading and focal adhesion formation." *PLoS One*3.6 (2008): e2497-e2497.

Dudek SM and Garcia JG. Cytoskeletal regulation of pulmonary vascular permeability. J Appl Physiol. 2001;91:1487–1500.

Dunn, Kenneth W., Malgorzata M. Kamocka, and John H. McDonald. "A practical guide to evaluating colocalization in biological microscopy." *American Journal of Physiology-Cell Physiology* 300.4 (2011): C723-C742.

Dutta, Priyanka, and Sankar Maiti. "Expression of multiple formins in adult tissues and during developmental stages of mouse brain." *Gene Expression Patterns* (2015).

Gasteier, Judith E., *et al.* "Activation of the Rac-binding partner FHOD1 induces actin stress fibers via a ROCK-dependent mechanism." *Journal of Biological Chemistry* 278.40 (2003): 38902-38912.

Gavard, Julie, Vyomesh Patel, and J. Silvio Gutkind. "Angiopoietin-1 prevents VEGF-induced endothelial permeability by sequestering Src through mDia."*Developmental cell* 14.1 (2008): 25-36.

Gavard, Julie, and J. Silvio Gutkind. "VEGF controls endothelial-cell permeability by promoting the β-arrestin-dependent endocytosis of VE-cadherin." *Nature cell biology* 8.11 (2006): 1223-1234.

Gauvin, Timothy J., *et al.* "The formin FMNL3 assembles plasma membrane protrusions that participate in cell–cell adhesion."*Molecular biology of the cell* 26.3 (2015): 467-477.

Giannotta, Monica, *et al.* "VE-cadherin and endothelial adherens junctions: active guardians of vascular integrity."*Developmental cell* 26.5 (2013): 441-454.

Guichard, Annabel, Victor Nizet, and Ethan Bier. "RAB11-mediated trafficking in host-pathogen interactions." *Nature Reviews Microbiology* 12.9 (2014): 624-634.

Halbleib, Jennifer M., and W. James Nelson. "Cadherins in development: cell adhesion, sorting, and tissue morphogenesis." Genes & development 20.23 (2006): 3199-3214.

Hetheridge, Clare, *et al.* "The formin FMNL3 is a cytoskeletal regulator of angiogenesis." *Journal of cell science* 125.6 (2012): 1420-1428.

Hofmann, S., *et al.* "The tumour necrosis factor-alpha induced vascular permeability is associated with a reduction of VE-cadherin expression."*European journal of medical research* 7.4 (2002): 171-176.

Huveneers, S. *et al.* Vinculin associates with endothelial VE-cadherin junctions to control force-dependent remodeling. J Cell Biol 196, 641-52 (2012).

Iskratsch, Thomas, *et al.* "FHOD1 is needed for directed forces and adhesion maturation during cell spreading and migration." *Developmental cell* 27.5 (2013): 545-559.

Iskratsch, Thomas, *et al.* "Two distinct phosphorylation events govern the function of muscle FHOD3." *Cellular and Molecular Life Sciences* 70.5 (2013): 893-908.

Isogai, Tadamoto, Rob van der Kammen, and Metello Innocenti. "SMIFH2 has effects on Formins and p53 that perturb the cell cytoskeleton." *Scientific reports*5 (2015).

Kan-o, Meikun, *et al.* "Mammalian formin Fhod3 plays an essential role in cardiogenesis by organizing myofibrillogenesis." *Biology open* 1.9 (2012): 889-896.

Kettleborough, Ross NW, *et al.* "A systematic genome-wide analysis of zebrafish protein-coding gene function." *Nature* 496.7446 (2013): 494-497.

Kobielak A, Pasolli HA, Fuchs E. Mammalian formin-1 participates in adherens junctions and polymerization of linear actin cables. Nat Cell Biol. 2004;6:21–30

Kok, Fatma O., *et al.* "Reverse genetic screening reveals poor correlation between morpholino-induced and mutant phenotypes in zebrafish."*Developmental cell* 32.1 (2015): 97-108.

Kovacs EM, Goodwin M, Ali RG, Paterson AD, Yap AS Curr Biol. 2002 Mar 5; 12(5):379-82.

Kühn, Sonja, and Matthias Geyer. "Formins as effector proteins of Rho GTPases." *Small GTPases* 5.3 (2014): 1-15.

Lodish, Harvey, *et al.* "Receptor-Mediated Endocytosis and the Sorting of Internalized Proteins." (2000).

Malek, Adel M., and Seigo Izumo. "Mechanism of endothelial cell shape change and cytoskeletal remodeling in response to fluid shear stress." *Journal of Cell Science* 109.4 (1996): 713-726.

Marshall, Wallace F., *et al.* "What determines cell size?." *BMC biology* 10.1 (2012): 101.

Matsui, Takahide, and Mitsunori Fukuda. "Methods of Analysis of the Membrane Trafficking Pathway from Recycling Endosomes to Lysosomes."*Methods in enzymology* 534 (2013): 195-206.

Millan, J. *et al.* Adherens junctions connect stress fibres between adjacent endothelial cells. BMC Biol 8, 11 (2010).

Mikelis, Constantinos M., *et al.* "RhoA and ROCK mediate histamine-induced vascular leakage and anaphylactic shock." *Nature communications* 6 (2015).

Nanes, Benjamin A., *et al.* "p120-catenin binding masks an endocytic signal conserved in classical cadherins." *The Journal of cell biology* 199.2 (2012): 365-380.

Ono, Shoichiro. "Dynamic regulation of sarcomeric actin filaments in striated muscle." *Cytoskeleton* 67.11 (2010): 677-692.

Kowalczyk, Andrew P., and Benjamin A. Nanes. "Adherens junction turnover: regulating adhesion through cadherin endocytosis, degradation, and recycling."*Adherens Junctions: from Molecular Mechanisms to Tissue Development and Disease*. Springer Netherlands, 2012. 197-222.

Lock, John G., and Jennifer L. Stow. "Rab11 in recycling endosomes regulates the sorting and basolateral transport of E-cadherin." *Molecular biology of the cell* 16.4 (2005): 1744-1755.

Machnicka, B., *et al.* "Spectrin-based skeleton as an actor in cell signaling."*Cellular and Molecular Life Sciences* 69.2 (2012): 191-201.

Palacios, Felipe, *et al.* "Lysosomal targeting of E-cadherin: a unique mechanism for the down-regulation of cell-cell adhesion during epithelial to mesenchymal transitions." *Molecular and cellular biology* 25.1 (2005): 389-402.

Petrache, Irina, *et al.* "The role of the microtubules in tumor necrosis factor-α–induced endothelial cell permeability." *American Journal of Respiratory Cell and Molecular Biology* 28.5 (2003): 574-581.

Phillips PG, *et al.* Phallacidin prevents thrombin-induced increases in endothelial permeability to albumin. Am J Physiol. 1989;257:C562–567.

Pollard, Thomas D., and Gary G. Borisy. "Cellular motility driven by assembly and disassembly of actin filaments." *Cell* 112.4 (2003): 453-465.

Prasain, Nutan, and Troy Stevens. "The actin cytoskeleton in endothelial cell phenotypes." *Microvascular research* 77.1 (2009): 53-63.

Rizvi, Syed A., *et al.* "Identification and characterization of a small molecule inhibitor of formin-mediated actin assembly." *Chemistry & biology* 16.11 (2009): 1158-1168.

Schönichen, André, and Matthias Geyer. "Fifteen formins for an actin filament: a molecular view on the regulation of human formins." *Biochimica et Biophysica Acta (BBA)-Molecular Cell Research* 1803.2 (2010): 152-163.

Takeya, Ryu et al. “The Mammalian Formin FHOD1 Is Activated through Phosphorylation by ROCK and Mediates Thrombin-Induced Stress Fibre Formation in Endothelial Cells.” *The EMBO Journal* 27.4 (2008): 618–628.

Tan, L., *et al.* "Rapid vinculin exchange dynamics at focal adhesions in primary osteoblasts following shear flow stimulation." J Musculoskelet Neuronal Interact 10.1 (2010): 92-99.

Tanaka Y, Nakanishi H, Kakunaga S, *et al.* Role of Nectin in Formation of E-Cadherin–based Adherens Junctions in Keratinocytes: Analysis with the N-Cadherin Dominant Negative Mutant. Pfeffer SR, ed. *Molecular Biology of the Cell*. 2003;14(4):1597-1609. doi:10.1091/mbc.E02-10-0632.

Tzima, E. *et al.* A mechanosensory complex that mediates the endothelial cell response to fluid shear stress. Nature 437, 426-31 (2005).

van Buul, Jaap D., Floris P. van Alphen, and Peter L. Hordijk. "The presence of alpha-catenin in the VE-cadherin complex is required for efficient transendothelial migration of leukocytes." *International journal of biological sciences* 5.7 (2009): 695.

Van Tam, Janice Kal, *et al.* "Mesenchymal stem cell adhesion but not plasticity is affected by high substrate stiffness." *Science and Technology of Advanced Materials* 13.6 (2012): 064205.

Wilson, Christopher W., and Weilan Ye. "Regulation of vascular endothelial junction stability and remodeling through Rap1-Rasip1 signaling." *Cell adhesion & migration* 8.2 (2014): 76-83.

Xiao, Kanyan, *et al.* "p120-Catenin regulates clathrin-dependent endocytosis of VE-cadherin." *Molecular biology of the cell* 16.11 (2005): 5141-5151.

Yoon M, Spear PG. Disruption of Adherens Junctions Liberates Nectin-1 To Serve as Receptor for Herpes Simplex Virus and PseudoRabies Virus Entry.*Journal of Virology*. 2002;76(14):7203-7208. doi:10.1128/JVI.76.14.7203-7208.2002.

Zhang, Ye, *et al.* "Different contributions of clathrin-and caveolae-mediated endocytosis of vascular endothelial cadherin to lipopolysaccharide-induced vascular hyperpermeability." (2014): e106328.

Zigmond, Sally. "Formin'adherens junctions." *Nature cell biology* 6.1 (2004): 12-14.